KTH Aeronautical
and Vehicle Engineering

METHODS FOR MODELLING AND CHARACTERIZATION OF IN-DUCT SOURCES

Hans Rämmal

Stockholm 2005

Licentiate Thesis

The Marcus Wallenberg Laboratory for Sound and Vibration Research
Department of Aeronautical and Vehicle Engineering
The Royal Institute of Technology (KTH)

Akademisk avhandling som med tillstånd av Kungliga Tekniska Högskolan framläggs till offentlig granskning för avläggande av teknologie licentiatexamen torsdagen den 8 december 2005, kl 10:15 i sal MWL74, Teknikringen 8, KTH, Stockholm.

TRITA-AVE-2005:38
ISSN-1651-7660

Abstract

Methods to characterize acoustic sources in flow ducts have been investigated.

In the first part of this thesis a measurement procedure to characterize an air terminal device using an acoustic one-port source model based on the two microphone technique has been tested and validated. In order to provide a prediction of flow noise generation at different operating points for the device a scaling law was derived. Successful validation experiments were performed.

In the second part a new method based on the multi-load technique was developed and used to characterise the source data of various piston-engines with non-linear behaviour. The source characterisation results were compared to results obtained using the well-known linear two-load technique. It was shown that the new non-linear multi-load technique gave improved results when the source was slightly non-linear.

In the third part an improved method to characterize noise sources in high temperature flow-ducts has been suggested. As a test environment for the standard two microphone technique a helium-air mixture has been used to simulate acoustical conditions similar to hot exhaust gas systems. In order to test the method the passive acoustic properties of automotive diesel engine and an unflanged flow duct termination have been experimentally determined. The experimental results for duct termination have been compared to theoretical predictions.

Keywords:

Acoustic source, one–port, source model, duct termination, source impedance, reflection coefficient, source strength, IC-engine, flow duct, multi-load method, non-linear

This thesis consists of the following papers:

Paper I

Characterization of Air Terminal Device Noise Using Acoustic 1-Port Source Models.
Hans Rämmal, Mats Åbom (2003)

Paper II

Modified Multi-Load Method for Non-Linear IC-Engine Source Characterization.
Manuscript submitted to Journal of Sound and Vibration.
Hans Rämmal, Hans Bodén (2004)

Paper III

A Method for Experimental Determination of In-duct Acoustic Source Passive Properties in Simulated Hot Conditions.
Hans Rämmal, Jüri Lavrentjev (2005)

Division of work between authors:

The theoretical and experimental work presented in this thesis was done by Hans Rämmal under the supervision of Hans Bodén. Paper I was supervised by Mats Åbom and Paper III by Jüri Lavrentjev.

The content of this thesis has been presented at the following conferences:

1. 10th International Congress on Sound and Vibration (ICSV 10), Stockholm, Sweden, 7-10 July, 2003. "Characterization of Air Terminal Device Noise Using Acoustic 1-Port Source Models".
2. 11th International Congress on Sound and Vibration (ICSV 11), St. Petersburg, Russia, 5-8 July, 2004. "Modified Multi-Load Method for Non-Linear Source Characterization".
3. 33th International Congress on Sound and Vibration (INTER-NOISE 2004), Praque, Czech Republic, 22-25 August, 2004. "A Method for Experimental Determination of Source Impedance in Helium-Air Mixture".
4. 34th International Congress on Sound and Vibration (INTER-NOISE 2005), Rio de Janeiro, Brazil, 7-10 August, 2005. "Experimental Determination of Acoustic Reflection Coefficient of Duct Openings in Simulated Hot Conditions".

The work in this thesis was partly performed within the following project:

1. ARTEMIS: funded by EC (European Commission), contract number G3RD-CT-2001-0511. (Paper II and Paper III)

Acknowledgements

This work has mainly been carried out at the Department of Aeronautical and Vehicle Engineering, the Royal Institute of Technology (KTH) and partly at the Department of Automotive Engineering, the Tallinn University of Technology. The work has been financially supported by European Commission funded project ARTEMIS (Aerodynamic research on Turbocharged Engine Inlet and Exhaust Systems), contract number G3RD-CT-2001-0511 and the Development Foundation of Tallinn University of Technology.

I am very grateful to my supervisors Mats Åbom and Hans Bodén at MWL (KTH) who opened the gates of a new area for me – Acoustics.

Special thanks go to Jüri Lavrentjev (TUT), for his supervision and for always providing me motivation throughout my academic career.

Table of contents

I. Introduction

In this thesis techniques for characterizing in-duct aero-acoustic and fluid machine sources are treated. A complete source model gives information about how much sound the source delivers into any receiving system. The source data is defined via the physical quantities by which the source interacts with the receiving system.

In developing source models one is looking for the most simple model that is able to provide acceptable results. For the low frequency (plane wave) region cases studied in this thesis, an acoustic one-port source model is applicable. The one-port model is a linear time-invariant model. More complicated models include linear time-varying, hybrid and non-linear models, in order of increasing complexity.

1 Acoustic source models

1.1 Linear time-invariant source model

If only plane waves are considered in the duct system the most simple model that can be used to describe the source is the linear time-invariant frequency domain one-port model. If there is only one degree of freedom at the interface between the source and the system the one-port source models can be used. For in-duct fluid-borne sound sources this corresponds to cases where there is a plane wave state in the connected duct. In-duct sources normally have at least two openings which means that it further requires that the external acoustic load only can vary at one of the openings, or the openings are acoustically uncoupled from each other so that they can be treated separately.

In the frequency domain an acoustic one-port can be completely described by two complex parameters: the source strength (p_+^S) and the source reflection coefficient (R_S) (or alternatively the source impedance). The behavior of the one-port (see Fig. 1) can in the frequency domain, be described by [1]:

$$p_+ = R_S p_- + p_+^S, \tag{1}$$

where (p_-, p_+) are traveling acoustic pressure amplitudes, (R_S) is the source reflection coefficient at cross-section, where *x=0* (see Fig. 1), and (p_+^S) is the source strength. The

source strength (p_+^S) can be interpreted as the pressure generated by the source-side when the system is reflection free.

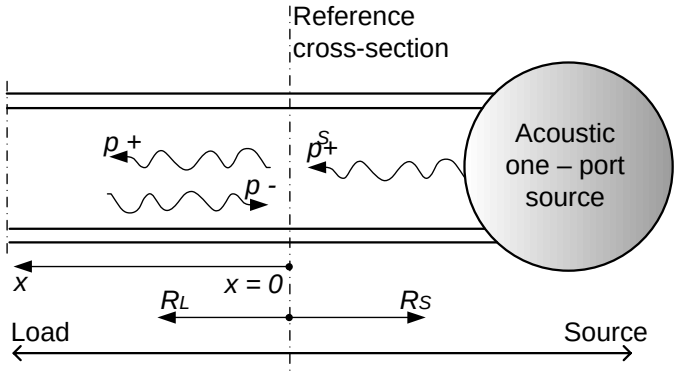

Figure 1. An in-duct source modeled as an acoustic 1-port

In the literature the source model for one-ports is often expressed in terms of source strength (p_S) and normalized source impedance (Z_S).

$$p = p_S - Z_0 \cdot Z_S \cdot q\,, \tag{2}$$

Where (p_S) is the source pressure, (p_S) and (q) are acoustic pressure and volume velocity, respectively, and (Z_0) is the characteristic impedance of the fluid. The source impedance (Z_S) represents the acoustic impedance seen from the reference cross-section towards the source.

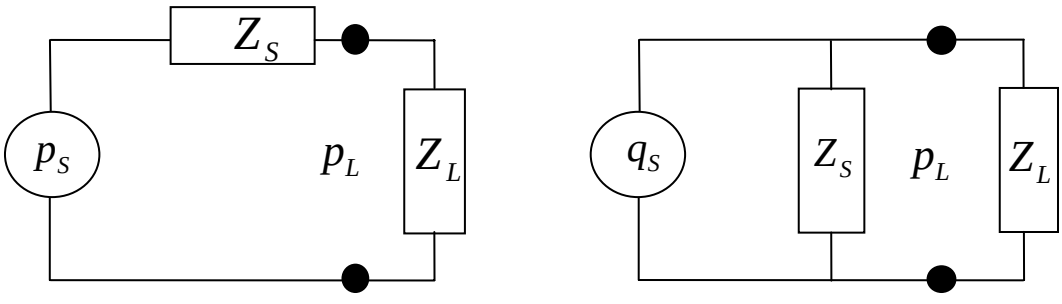

a) Pressure source b) Volume velocity source

Figure 2. Equivalent acoustic circuits for linear time invariant source

Fig. 2 shows the equivalent acoustic circuit for a linear time invariant source. In this figure (p_L) and (Z_L) denote the acoustic load data (the load pressure and the load impedance), while (p_S), (q_S) and (Z_S) denote the source data respectively. Theoretically the two representations of the source shown in Fig. 2 are equivalent and it is possible to go from one representation to the other by using the relationship $q = p_S / Z_S$. If there are errors in the experimental data or deviations from system linearity it can be expected that the error propagation is different for the two representations leading to different results when source data is extracted using over-determination. In addition to other techniques for testing system linearity discussed in section 3.3. Extracting source data using both formulations and comparing the resulting source impedance is a possibility to see if experimental data are in agreement with linear time-invariant source model. It can also be expected that if the source is close to a constant velocity source this model will give smaller errors than if a pressure source model is applied and vice versa.

The linear time-invariant equivalent source model will strictly be applicable only in situations where the pressure-fluctuations are small. Several authors however have found the linear time-invariant model to give reasonable results for modeling the systems with relatively large pressure fluctuations, i.e., slightly non-linear systems.

1.2 Linear time-varying model

When determining the passive acoustic data, i.e., the source impedance (Z_S) of a fluid machine it is assumed that it does not change with time. If the operating machine is studied it is observed that various parts, such as pistons, valves, or fan blades move. Therefore it can be expected that even the passive acoustic properties should be time-varying. In mathematical terms this means that the source is described by linear differential equations with time-varying coefficients. The time variation in the coefficients is normally caused by the periodic motion of the machine and will therefore be periodic [1].

A frequency domain linear time-varying source model was developed by Wang [2-3] for an internal combustion engine inlet system. By assuming that the variables and the coefficients have periodic time dependence, so that they can be expanded in Fourier series, a frequency domain model for the source can be deduced. Here the source strength is replaced by a vector containing the data for each frequency component, and the source impedance is replaced by a matrix which also describes the coupling between different frequency components which can occur at the source. Bodén [4] presented a measurement method for determining the source

data for such a model. The method used is similar to the multi-load methods used for time-invariant one-port sources.

In [2] it was found when comparing the experimental sound pressure levels with analytical ones that time-varying model gave better prediction than time-invariant for automobile 4-stroke engine inlet system.

1.3 Hybrid models

The hybrid linear/non-linear method, where a non-linear time domain model is used for the source and a linear frequency domain model is used for the receiving system, was introduced for in-duct sources in [5].

Generally one can say that the hybrid approach is the attempt to combine the linear and the non-linear techniques. The main idea is to retrieve the advantages of both types of methods.

The harmonic balance technique [6] is an alternative frequency domain technique with better convergence properties. The main conclusions, after implementing it on simple 1-cylinder "cold" engine model, were that the harmonic balance method was preferable for harmonic steady state simulations where parametric studies are performed. As the HBM method is a steady state method, true transient behavior cannot be modeled correctly.

The hybrid methods can be divided into a number of main groups. One group is the iterative techniques which can be further subdivided into frequency domain iterative techniques [5, 6] and time domain iterative techniques [7] depending on in which domain the convergence check and the coupling is performed. For applications to IC-engine exhaust systems the frequency domain iterative method was suggested by Jones [8] and tested by Bodén [4] for a modified compressor with unstable results.

Another group is the convolution techniques where the frequency domain boundary condition for impedance is transformed into the time domain. There are works on IC-engines exhaust and inlet systems where the convolution technique using the reflection function [9] or scattering matrix [10] has been used.

1.4 Non-linear model

Many fluid machines such as compressors and IC-engines generate high sound pressure levels or high flow velocities and are therefore considered as high level acoustic sources. The validity of modeling them as linear time-invariant systems may therefore decrease accuracy of the results. It has been noted [11] that a linear time-invariant source model when experimentally determining the source data of high level sources frequently gives unphysical

negative source resistance values. For a linear time-invariant passive system the real part of the impedance must be positive since this shows the direction of energy. Energy can only be lost into the system – it cannot be created since the system is passive. For a non-linear system energy can be transferred from one frequency to another. This could at certain frequencies, suggest that the system was no longer passive by giving a negative real part of the impedance. Linear time varying system can also produce this negative resistance as shown by Peat and Ih [12].

Therefore as an alternative to linear techniques, non-linear models can be used to describe the complete system, see, e.g., Jones [8]. Non-linear methods are often used for systems with high sound pressure levels or when clearly non-linear effects are present.

The non-linear time-domain methods are based on numerical simulations of the unsteady flow. The advantage, compared to the linear description, would be that the system is more correctly modeled. The results agree generally well with experimental results but the methods are time consuming. These methods also require a good knowledge of engine modeling, such as the combustion process, mechanics and timing of the valve movement, exact knowledge of the system geometry, temperature and so on.

2 Source characterization methods

A number of different methods exist for determining acoustic source data from experiments. An overview of the state of the art of experimental methods for determining the 1-port source data for in-duct fluid-borne sound sources was described in the review papers [1] and [13]. The measurement methods can be divided into direct (with an external source) [14] and indirect or multi-load methods (without an external source) [15].

2.1 Direct methods

The direct methods are two-step methods. First, the passive source data e.g., source reflection coefficient, is determined using the external source and the two-microphone technique [16] (see Fig. 3). Then with the external source off or removed a known acoustic load is applied to the source and the source strength is obtained.

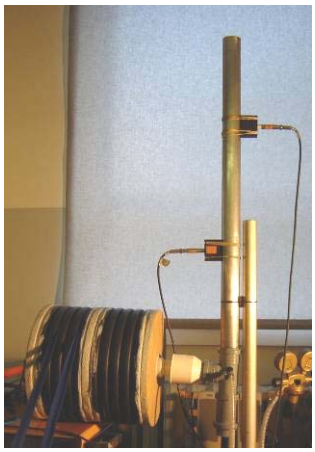

Figure 3. Application of direct method during duct termination characterization experiments using two microphone technique

One problem with this method is that in the first step when the external source is used only the signal from this source and not the signal from the source under test must be picked up by the transducers.

Increasing the level of the external source can in principle solve the problem. This has been attempted for IC-engines [14], [17] but did not succeed completely and good results could not be obtained in the low frequency region, where the engine produced the highest sound levels. Another possibility is to use a reference signal correlated with the sound field from the external source, e.g., an electric signal exciting a loudspeaker, but not correlated with the sound field from the machine under test [18] and by signal processing methods extracting the signal from the external source. Still there are sometimes difficulties to find an external source that produces sufficiently high sound levels. There may also be practical problems in mounting the external source in, e.g., hot and "hostile" environments. This makes the indirect methods attractive in many applications.

2.2 Indirect methods

When using the indirect methods the two unknowns, the source strength and the source impedance, are determined via a multi-load procedure, i.e., by applying known loads (Z_L) and measuring the acoustic pressure at the source receiver interface (p_L).

Since there are two unknowns, two loads should be sufficient to obtain the source data (p_S) and (Z_S), which leads to the two-load method [19].

In case of linear time-invariant one-port model the pressure at the source cross-section can be expressed by the equation:

$$p_L = p_S \frac{Z_S}{Z_S + Z_L} \tag{10}$$

or with the unknown source data on the left hand side,

$$p_S \cdot Z_S - p_L \cdot Z_S = p_L \cdot Z_L . \tag{11}$$

Equation (11) has got two complex unknowns, which means that it can be solved if we have two complex equations. The two equations can be obtained if we use two acoustic loads,

$$\begin{aligned} p_S Z_{L1} - p_{L1} Z_S &= p_{L1} Z_{L1} \\ p_S Z_{L2} - p_{L2} Z_S &= p_{L2} Z_{L2} \end{aligned}, \tag{12}$$

or we can also use more acoustic loads than we need, in order to get an over-determined system, which can be useful for improving the measurement results [4,20], and for checking if the source behaves as a linear system [11,18].

In order to determine the normalized impedances of the acoustic loads (Z_{Li}), used for experiments, a number of pressure transducers are usually mounted in the exhaust pipe (see Fig. 4).

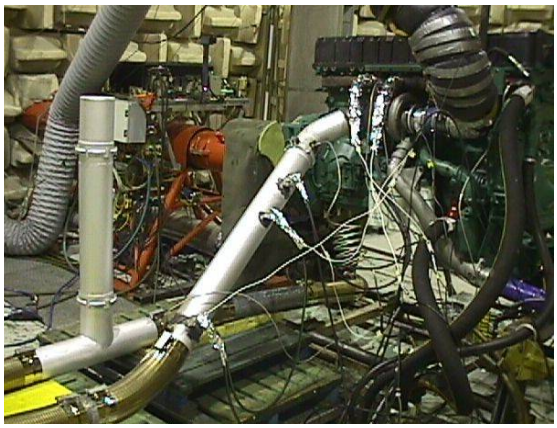

Figure 4. Pressure transducers mounted in an exhaust system of a 6 cylinder turbocharged diesel engine during source characterization experiments using the indirect approach

In the plane wave range we can use this information to perform wave decomposition and to determine the reflection coefficient looking into the acoustic load, which in turn gives the normalized load impedance.

To determine the complex load pressures (p_{Li}) we need a reference signal to ensure that the pressure time histories for the different acoustic loads start at the same point in the engine cycle. The pressure time histories are then Fourier transformed and used to calculate the load pressures and load impedances and subsequently the source data.

As described above the two-load method requires complex pressure measurements and a reference signal unaffected by acoustic load variations, which is related to the sound generating mechanism of the source. For fluid machines with periodic operation cycle the normal solution is to try to obtain a trig signal for each period [4]. This procedure can catch harmonic part of the spectrum generated by machine but not the broad band part. It can also be noted that a trig signal can be used to remove the flow noise disturbances from measured pressure signals. An alternative method, used for flow noise suppression, is to create a "noise-free" acoustic reference signal, by using one or several reference microphones [18].

Although the two-load method is strictly valid for linear time-invariant equivalent source characterization, several authors have reported that it gives useful results also in situations that are not exactly time-invariant or linear, if applied by using a number of extra loads to average out the modeling errors in the least squares sense.

For situations where no suitable source reference is available alternative methods have been developed, where the auto-spectra of the pressures are measured instead of the complex pressures. The first such method was the three-load method [21].

By taking the squared magnitude of the equation (2), describing the one-port source, one gets, after substituting: $q = p / Z_o \cdot Z_S$, a real-valued equation with three unknowns, i.e., $G^s = \left| p^s \right|^2$ and the real and imaginary parts of (Z_S), ($\mathrm{Re}(Z_S)$) and ($\mathrm{Im}(Z_S)$). To determine the unknowns measurements using three different loads are needed. The resulting system of equations is non-linear and can have more than one real-valued solution. This method is quite impractical to use and has also been reported to give large measurement errors. A four-load method for evaluation of source impedance in ducts was introduced by Prasad [22]. Following this method, the magnitudes of sound pressures in terms of sound pressure level, and measured with single channel instrumentation, were used to obtain the source data. In the four-load method a fourth measurement is used to eliminate the non-linear term containing

($|Z_S|^2$). This method has also been reported to be very sensitive to errors in the input data and can therefore sometimes give erroneous results. Bodén [23] showed that the four-load method can be formulated as a linear system of equations, if the non-linear term is interpreted as an independent unknown. By analyzing this formulation it was concluded that the main reason for previously reported is the choice of loads. A new improved method for analyzing the same experimental data used for the four-load method was also presented [23]. This method is based on a direct numerical fit of the data to the non-linear model using least squares methods. A comparison between the results, obtained when applying the described measurement methods to various sources, was also made. It was concluded that generally the direct methods give better results than the indirect methods in situations where it is suitable to use them. A further improvement of the technique of [23] has been presented by Jang and Ih [24].

An extension of the conventional two-load method, to characterize the linear time-variant sources, was presented by Boden [4]. This method is called the multiple-load method and it requires (1+2N) loads, where (N) denotes the number of harmonics to be included in the source spectrum.

The multiple load method was derived assuming that the time variance was caused by parametric excitation. In deriving the expressions a second order differential equation was used as an example [13]:

$$A(t)\cdot\ddot{Q}(t)+B(t)\cdot\dot{Q}(t)+C(t)\cdot Q(t)=P_S(t)-P_L(t)\,, \tag{19}$$

where ($Q(t)$) is the volume velocity, ($P_L(t)$) is the pressure at the outlet of the source and ($P_S(t)$) is the source pressure. The time variation in coefficients ($A(t)$), ($B(t)$) and ($C(t)$) represent for instance time varying volumes in a cylinder or time varying cross sectional areas in valves, giving a parametric excitation of the system.

For a typical fluid machines all time varying quantities in (19) are periodic and can be expanded in complex Fourier series,

$$Q(t)=\sum_{n=-\infty}^{\infty}q_n\exp(jn\omega_0 t)\,,\qquad P_L(t)=\sum_{n=-\infty}^{\infty}p_n\exp(jn\omega_0 t)\,,\qquad A(t)=\sum_{n=-\infty}^{\infty}a_n\exp(jn\omega_0 t)$$

$$B(t) = \sum_{n=-\infty}^{\infty} b_n \exp(jn\omega_0 t), \qquad C(t) = \sum_{n=-\infty}^{\infty} c_n \exp(jn\omega_0 t). \tag{20}$$

Inserting (20) in (19) and identifying terms with the same time variation gives, e.g., for the term with time variation ($\exp(jnw_0 t)$),

$$\sum_{k=-\infty}^{\infty} \left(-\omega_0^2 k^2 a_{n-k} + j\omega_0 k b_{n-k} + c_{n-k} \right) \cdot q_k = p_{sn} - p_n . \tag{21}$$

The result can also be expressed in matrix form,

$$[Z_S] \cdot (q) + (p_L) = (p_S), \tag{22}$$

where $[Z_S]$ is the source impedance matrix, and (q), (P_L) and (P_S) are vectors. The matrix and vectors will have infinite dimension, but in practice only a limited number of terms can be included. The number of terms, i.e. frequency components included, must be chosen so that sufficiently good description of the main characteristics of the studied source is given.

II. Summary of the papers

A. Paper I: Characterization of Air Terminal Device Noise Using Acoustic 1-Port Source Models

A measurement method to characterize a standard air terminal device as an acoustic one-port source has been tested and validated. The low frequency noise generated by flow separation in the device and radiated to a reverberation room has been measured, together with pressure auto- and cross-spectra inside the connected duct. A one-port source model, with parameters derived from the experiments, was then created. For the source strength part a scaling law was derived showing dipole dependence for the velocity exponent. To validate the one-port model and to prove its ability to predict flow noise generation measurements were performed on a modified duct system.

B. Paper II: Modified Multi-Load Method for Non-Linear IC-Engine Source Characterization

Linear frequency domain prediction codes are used for calculation of low frequency sound transmission in and sound radiation from IC-engine exhaust systems. To calculate insertion loss of mufflers or the level of radiated sound information about the engine as an acoustic source is needed. The source model used in the low frequency plane wave range is the linear time invariant 1-port model. The acoustic source data is usually obtained from experimental tests where multi-load methods and especially the two-load method are most commonly used. The exhaust pulsations of an IC-engine are of high level, which means that the engine is not a perfectly linear and time invariant source. It is therefore of interest to develop source models and experimental techniques that try to take this non-linearity into account. In this paper a modified version of the two-load method to improve the characterization of the non-linear acoustic 1-port sources has been developed and tested. Simulation results from various source configurations of a simplified IC-engine model were used to validate the method. The influence of parameters controlling the linearity of the system was investigated. The time-variance of the source model was varied and the source characterization quality using the two-load method and the modified two-load method was evaluated.

C. Paper III: A Method for Experimental Determination of In-Duct Acoustic Source Passive Properties in Simulated Hot Conditions

Acoustic properties of in-duct noise sources under high temperature conditions (for instance in IC engine exhausts) are best determined under real working conditions. However, the hot pulsating exhaust gas flow causes experimental problems: need for transducer cooling, pipe vibration etc. Therefore from a practical point of view in many cases experiments are made in cold conditions (room temperature). Due to the difference in speed of sound in the environments this can lead to incorrect measurement results.

In this paper a new measurement method to characterize in-duct noise systems is suggested and preliminary tests are made. In order to simulate the acoustical conditions of the hot gases, a helium-air mixture is used as the testing environment. Since the speed of sound in helium is close to that in the hot exhaust gases, the cold exhaust system filled with helium simulates the hot system.

As a test of the method experiments to determine the reflection coefficient of the exhaust port of an automotive IC-engine were performed in the first part of the paper. The measured reflection coefficients at the IC engine exhaust port were compared with the experimental data determined using the classical cold airflow technique.

In the second part of the paper the reflection coefficient of an unflanged circular duct termination has been experimentally determined in simulated hot conditions. To investigate the flow profile of the gases close to the duct termination flow visualization experiments were performed and the results studied. The measured reflection coefficients of the duct opening were compared with simulation results obtained from the well-known theory according to Munt.

III. Future research

An interesting continuation of the work done in the first part of the thesis would be to try to establish methods to estimate one- and two-port source data directly from CFD calculations. Since the passive part of the source data is often weakly affected by the flow it could be sufficient “only” to estimate the active part (source strength).

In order to prove the new simulation technique presented in the third part of the thesis for characterization of the exhaust duct components at any temperature in the temperature range a number of experiments could be performed with varied helium – air proportion in the test medium. Accordingly the comparison experiments with “real” hot flow could be of interest to validate the existing theory for circular unflanged duct terminations.

References

1. H. Bodén and M. Åbom 1995 *Acta Acoustica* **3**, 549-560. Modelling of Fluid Machines as sources of sound in duct and pipe systems.

2. W.M. Wang 1967 *Journal of the Acoustical Society of America*, **41**, 1418-1423. Matrix formulation in acoustic analysis of mechanically driven fluid systems.

3. W.M. Wang 1967 *Journal of the Acoustical Society of America*, **42**, 1244-1249. Acoustical analysis of a multicylinder engine air induction system.

4. H. Bodén 1991 *Journal of Sound and Vibration* **148**, 437-453. The multiple load method for measuring the source characteristics of time-variant sources.

5. R. Singh and W. Soedel 1979 *Journal of Sound and Vibration*, **63**, 124-143. Mathematical modeling of multicylinder compressor discharge system interactions.

6. F. Albertson and J. Gilbert 2001 *Journal of Sound and Vibration* **241**, 541 – 565. Harmonic Balance Method used for calculating the steady state oscillations of a simple one-cylinder cold engine.

7. V. H. Gupta 1991 *Doctoral thesis from the Indian Institute of Science*, Bangalore, India. On the flow-acoustic modeling of the exhaust system of a reciprocating internal combustion engine.

8. A.D. Jones 1984 *Noise Control Engineering*, **23**, 12-31. Modelling the exhaust noise radiated from reciprocating internal combustion engines - A literature review.

9. P.O.A.L. Davies and M.F. Harrison 1993 *Proceedings of the Institute of Acoustics* **15**, 369-374. Hybrid systems for IC engine breathing noise synthesis.

10. F. Payri, J.M. Desantes and A.J. Torregrosa 1995 *Journal of Sound and Vibration* **188**(1), 85-110. Acoustic boundary condition for unsteady one-dimensional flow calculations.

11. H Bodén and F Albertson 2000 *Journal of Sound and Vibration*, **237**(1), 45-65. Linearity tests for in-duct acoustic one-port sources.

12. K. S. Peat and J.-G. Ih 2001 *Journal of Sound and Vibration*, **244**, 821-835. An analytical investigation of the indirect measurement method of estimating the acoustic impedance of a time-varying source.

13. H. Bodén 2002 *Proceedings of the 9th International Congress on Sound and Vibration*. Characterization of fluid-borne sound sources and structure-borne sound sources.

14. D. F. Ross and M. J. Crocker 1983 *Journal of the Acoustical Society of America, **74,*** 18-27. Measurement of the acoustic internal impedance of an internal combustion engine.

15. M. L. Munjal 1998 *Journal of Sound and Vibration* **211**, 425-433. Analysis and design of mufflers –an overview of research at the Indian Institute of Science.

16. A. F. Seybert and D. F. Ross 1977 *Journal of Acoustical Society of America,* **61**, 1362-1370. Experimental determination of acoustic properties using a two-microphone random excitation technique.

17. M. G. Prasad and M. J. Crocker 1983 *Journal of Sound and Vibration, **90,*** 491-508. Studies of acoustical performance of a multi-cylinder engine exhaust muffler.

18. J. Lavrentjev, H. Bodén and M. Åbom 1992 *Journal of Sound and Vibration*, **155**, 534-539. A linearity test for acoustic one-port sources.

19. D. P. Egolf and R. G. Leonard 1977 *Journal of the Acoustical Society of America, **62,*** 1013-1023. Experimental scheme for analyzing the dynamic behavior of electro-acoustic transducers.

20. H. Bodén 1988 *Journal of Sound and Vibration* **126**, 173-177. Error analysis for the two-load method.

21. H.S. Alves and A.G. Doige 1987 *Proceedings of NOISE-CON* **87**, 329-334. A three-load method for noise source characterization in ducts.

22. M. G. Prasad 1987 *Journal of Sound and Vibration*, **114**, 347-356. A four-load method for evaluation of acoustical source impedance in a duct.

23. H. Bodén 1995 *Journal of Sound and Vibration*, **180**, 725-743. On multi-load methods for determination of the source data of acoustic one-port sources.

24. S-H. Jang and J.G. Ih 2003 *Proceedings of the 10th International Congress on Sound and Vibration*. A measurement method for the nonlinear time-variant source characteristics of intake and exhaust systems in fluid machines.

Paper A

CHARACTERIZATION OF AIR TERMINAL DEVICE NOISE USING ACOUSTIC 1-PORT SOURCE MODELS

H. Rämmal and M. Åbom

Abstract A measurement method to characterize a standard air terminal device as an acoustic one-port source has been tested and validated. The low frequency noise generated by flow separation in the device and radiated to a reverberation room has been measured, together with pressure auto- and cross-spectra inside the connected duct. A one-port source model, with parameters derived from the experiments, was then created. For the source strength part a scaling law was derived showing dipole dependence for the velocity exponent. To validate the one-port model and to prove its ability to predict flow noise generation measurements were performed on a modified duct system.

1. INTRODUCTION

As a result of interaction between the air flow and duct discontinuities flow-induced noise can reach significant levels in duct systems and become a limiting factor determining the minimum sound level. The sound field in a duct system depends on both the passive and active properties of the system. The passive properties are controlled by the duct geometry and speed of sound and determine the sound propagation through the system, while the active properties define the acoustic sources in the system and describe how sound energy is generated [1]. To solve problems of noise reduction and to understand aerodynamic noise generation mechanisms, it is necessary to characterize noise sources. A source is commonly described by the physical quantities via which it interacts with the outside world. In the simplest case where an infinite space around the source can be assumed, the source can be characterized by its radiated acoustic power. This sound power based description is the basis of most standards for the analysis of sound in ducts, e.g., see ASHRAE [2], and is valid in the high frequency range. In general more complex source descriptions such as multi-port models are needed [1], to correctly describe the interaction between a source and a duct system. For instance the case studied here, an air terminal device in the low frequency (plane wave) region, can be modeled as an acoustic one-port source.

The air terminal device (ATD) investigated in this paper is a standard device typically mounted to the ventilation duct openings in buildings. Its purpose is to regulate and distribute the air flow in a room. Although the air terminal device studied here is designed for the ventilation systems used in buildings the modeling approach suggested is applicable for air terminal devices in general, e.g., for the ventilation system in vehicles.

Following the investigations of Lavrentjev [3] the source data of an acoustic one-port, as a linear and time invariant system, can in the frequency domain be completely described by source impedance and source strength. In the present paper, the source impedance is determined using the two microphone method [4]. As a second step, the source strength is determined by measuring the acoustic pressure spectrum with a known acoustic load connected to the duct inlet. In addition the sound power level, emitted from the sound source to a reverberant room, was determined using a standard measurement method (ISO 3747).

All the experimental data obtained were at low Mach numbers ($M<0.05$). In duct systems with low Mach numbers the dominating mechanism for flow generated sound is aero-acoustic dipoles created by fluctuating pressures in regions of flow separation [5].

In order to provide a prediction of a flow noise generation at different operating points, a scaling law based on earlier investigations, e.g., Nelson & Morfey [5] and Nygård [6], is derived. In the last part of the paper a new duct system connected to the given air terminal device is studied to validate the one-port model and to prove its ability to predict flow noise generation.

2. THEORY

For fluid machines with two openings, where the external acoustic load only can vary at one of the openings, or the openings are acoustically uncoupled from each other so that they can be treated separately, the one-port model can be used if there is a plane wave state in the connected duct. The behavior of the one-port (see Fig. 1) can in the frequency domain, be described by [1]

$$p_+ = R_S p_- + p_+^S , \tag{1}$$

where p_-, p_+ are traveling acoustic pressure amplitudes, R_S is the source reflection coefficient and p_+^S is the source strength.

The one-port model can be used as long as the studied source process is linear, time invariant and the source term can be regarded as independent of the acoustic field. Following Bodén and Åbom [1] two basic approaches exist for the determination of the source data; methods *with* and *without* an external source. When possible to apply the methods with an external source are preferred and normally give a better result. Such a method will be applied here and is based on a two step procedure. First, the source reflection coefficient is determined using the external source and the two-microphone technique [4]. Then with the external source turned off or removed a known acoustic load is applied to determine the source strength.

2.1 Determination of the passive source data

Using the pressure signals from microphones 1 and 2 (Fig. 2) it is possible to separate left- and right-going waves and then to calculate the reflection coefficients and the source impedance. The plane wave acoustic pressures at microphones 1 and 2 can be written as [4]

$$p_1(f) = p_{1+}(f) + p_{1-}(f), \tag{2}$$

$$p_2(f) = p_{1+}(f)\exp(ik_+ s) + p_{1-}(f)\exp(-ik_- s), \tag{3}$$

where p is the acoustic pressure, f is the frequency, $k = 2\pi f / c$ is the wave number, c is the speed of sound, s is the microphone separation, - and + denote the pressure waves propagating in neg. and pos. direction relative to the x-axis, $k_- = k/(1-M)$, $k_+ = k/(1+M)$ and M is the Mach number. Using the transfer function between the microphones 1 and 2 the acoustic reflection coefficient can be obtained [4]. The measurements of the transfer functions were done at different flow speeds both with the ATD and with a free termination (ATD valve removed). The reflection coefficient at the ATD cross – section is defined as

$$R_S^r(f) = \frac{p_-^e(f)}{p_+^e(f)}, \tag{4}$$

where r denotes values measured at a reference point (microphone 1 cross-section) and p_-^e, p_+^e is the acoustic field generated by the external (loudspeaker) source. From equations (2) – (4) it can be shown that [4]

$$R_S^r(f) = \frac{H_{12}^e - \exp(-ik_- s)}{\exp(ik_+ s) - H_{12}^e}, \tag{5}$$

where $H_{12}^e = h_2 / h_1$ is the transfer function from microphone 1 to 2 and $h_1 = p_1 / e$ and $h_2 = p_2 / e$ are the transfer functions between the microphone signals p_1, p_2, and the reference signal (here the electrical signal e driving the loudspeaker), respectively. A “single” microphone approach was used to avoid the phase calibration needed when two different microphones are used. Likewise, the load reflection coefficient (loudspeaker mounted instead of the ATD, see Fig. 3) can be obtained from

$$R_L^r(f) = \frac{p_+^e(f)}{p_-^e(f)} = \frac{H_{12}^e - \exp(ik_+ s)}{\exp(-ik_- s) - H_{12}^e}. \tag{6}$$

In order to determine the acoustic properties of the air terminal device (at the outlet cross-section of the ATD, see Fig. 2), it is necessary to move all measured quantities, i.e., R_S^r, R_L^r to this location. This can be done by using the following equations

$$R_S = R_S^r \exp\left(i \cdot \left(k_+ + k_-\right) \cdot l\right) , \tag{7}$$

$$R_L = R_L^r \exp\left(-i \cdot \left(k_+ + k_-\right) \cdot l\right), \tag{8}$$

where l is the distance from the reference position (microphone 1 cross-section) to the desired cross-section (ATD).

When the source reflection coefficient is known the normalized acoustic impedance of the source Z_S is given by the equation

$$Z_S = \left(\frac{\rho c}{S}\right) \cdot \frac{1 + R_S}{1 - R_S} , \tag{9}$$

where ρ is the density of the fluid and S is the cross-sectional area of the duct.

2.2 Determination of the active source data

As the second step, after the modifications of the test-rig used for impedance measurements, the source strength was determined. During the source strength measurements the external source was not in use and the ATD was acting like a source for the different flow speeds (see section 3). To avoid additional flow noise creation, the loudspeaker unit was removed from the duct system.

In order to suppress effects of turbulence noise in the acoustic measurements, which can be a large problem especially for measurements on weak sources as in this case, two different microphone cross-sections were used. The source auto-spectrum was obtained from a measured sound pressure cross-spectrum G_{13} between microphones 1 and 3 (see Fig. 4). The microphones were flush mounted at the inner duct wall and microphone 3 was positioned to the opposite side of the pipe. Assuming that the two cross-sections, say *x1* and *x3*, are sufficiently separated so that local turbulent pressure fluctuations are uncorrelated, this approach will improve the measurement quality.

To derive the equation for the source strength, the equation for the load reflection coefficient at the source cross-section $R_L = \frac{p_-}{p_+}$, and equation (1) are combined. As a result the following equation for the source strength is obtained

$$p_+^S = p_+(1 - R_S R_L). \tag{10}$$

The pressure wave propagating in positive direction, at microphone 1 is given by

$$p_{1+} = \frac{p_1}{(1 + R_L^r)}. \tag{11}$$

To move the pressure p_{1+} to the assumed ATD source cross–section, the following equation is used

$$p_{1+} = p_+ \exp(-ik_+ l_1), \tag{12}$$

where l_1 is the distance between microphone 1 and the source cross-section (see Fig. 4). Using the equations (10) and (12) gives

$$p_+^S = p_{1+} \exp(ik_+ l_1) \cdot (1 - R_S R_L), \tag{13}$$

and if equation (13) is combined with equation (11), we obtain

$$p_+^S = \frac{p_1 \exp(ik_+ l_1) \cdot (1 - R_S R_L)}{(1 + R_L^r)}, \tag{14}$$

where the load reflection coefficient at the microphone 1 cross-section is $R_L^r = R_L \exp(i(k_+ + k_-) l_1)$. Now the source strength can be written in the following form

$$p_+^S = \frac{p_1 \exp(ik_+ l_1) \cdot (1 - R_s R_L)}{(1 + R_L \exp(i(k_+ + k_-) l_1))}. \tag{15}$$

Equation (15) could be used directly for the source strength measurements, but for turbulence noise suppression, the second microphone (mic. 3), where the flow noise is assumed to be uncorrelated with the noise at microphone 1, is additionally used and a cross-spectrum measurement is performed. To make a correction of the phase error between the microphones, the cross-spectrum G_{13} between the microphones 1 and 3 was measured twice, by switching microphone positions. The corrected cross-spectrum was then obtained from

$$G_{13cor} = \sqrt{G_{13} \cdot G_{31}} \ . \tag{16}$$

The source auto-spectrum $G_{SS} = p_+^S \cdot (p_+^S)^C$ is finally obtained by using equation (14), and the cross-spectrum definition $G_{13} = p_1 \cdot p_3^C$,

$$G_{SS} = \frac{G_{13cor} \exp(ik(l_1 - l_3)) \cdot \left|1 - R_S R_L\right|^2}{(1 + R_L \exp(i(k_+ + k_-) l_1)) \cdot (1 + R_L \exp(i(k_+ + k_-) l_3))^C}, \tag{17}$$

where the superscript c denotes a complex conjugated quantity.

2.3 Sound power radiated

Of interest in practice is the determination of the sound power radiated from an ATD unit. When the 1-port source data is known the resulting volume flow *q* in the opening will create a monopole type of source. The volume flow in the opening can be written as: $q = S \cdot (u_+ + u_-)$, where *u* is the acoustic velocity in the +/- *x*-direction (see Fig. 4) and *S* is the cross-sectional area of the duct. It is known that: $u_+ = \frac{p_+}{\rho \cdot c}, u_- = -\frac{p_-}{\rho \cdot c}$, using equation (10) this implies

$$q = \frac{p_+^S \cdot S \cdot \left(1 - R_L\right)}{\rho \cdot c \cdot \left(1 - R_S R_L\right)}. \tag{18}$$

For sufficiently low frequencies and small Mach-numbers the radiation resistance of the ATD can be approximated by that of a monopole [7]. This implies that if the acoustic volume flow q at the ATD is known then the radiated power is

$$W_{rad} = \frac{\rho \cdot c \cdot k^2 \cdot |q|^2}{4\pi}. \tag{19}$$

Combining this with equation (18) leads to

$$W_{rad} = \frac{\pi^3 \cdot f^2 \cdot d^4 \cdot \left|1 - R_L\right|^2 \cdot G_{SS}}{16 \cdot c^3 \cdot \rho \cdot \left|1 - R_s \cdot R_L\right|^2}, \tag{20}$$

where $S = \pi d^2 / 4$ and d is the duct diameter has been inserted. Expressing this as levels using the normal reference values gives

$$L_W = L_S + 10 \cdot \log_{10}\left(\frac{\pi^3 \cdot f^2 \cdot d^4 \cdot \left|1 - R_L\right|^2}{16 \cdot c^3 \cdot \rho \cdot \left|1 - R_S \cdot R_L\right|^2}\right) + 26, \tag{21}$$

where $L_S = 10 \cdot \log_{10}\left(G_{SS} / p_{ref}^2\right)$.

2.4 A scaling law for the source strength

To enable source data measured at one operating condition to be used at other operating points (flow speeds) a scaling law is necessary. As observed in earlier investigations, e.g. [3], the passive part of the source data is often weakly dependent on the flow speed. Therefore it is mainly of interest to find a scaling law for the source strength. Based on earlier works, e.g., Nelson & Morfey [5] and Nygård [6], the in-duct plane wave sound power produced by flow separation from a compact source region will scale as

$$\frac{G_{SS}}{\rho \cdot c} = \rho \cdot U^3 \cdot M^{\alpha} \cdot F(St) \,. \tag{22}$$

Where U is the mean flow speed, α depends on the aero-acoustic source type, $F(St)$ is a dimensionless source-spectrum depending on a Strouhal number, $St = f \cdot d / U$, f is the frequency and d is the duct diameter. Note, when writing down the power in the plane wave in equation (22), the effect of the mean flow has been omitted. For the air terminal device studied the experiments show that the best collapse is obtained with $\alpha=0$. Integrating (22) over all frequencies will then produce a velocity exponent dependence of 4, corresponding to a dipole in the plane wave range [5].

3. MEASUREMENTS

Measurements were performed on a standard rectangular air terminal device (ATD) shown in Fig. 5 and on a circular orifice (with inner diameter of 73mm) (see Fig. 6) mounted to the end of the test duct. Three different measurement set-ups were used in the experiments. First in duct measurements were performed with external sound source (loudspeaker) for source impedance determination, using the two-microphone technique, see Figs. 7 and 8. Secondly, the source strength was measured using the same rig but with the loudspeaker section removed, see Figs. 9 and 10. Thirdly, measurements were performed, according to the ISO 3747 standard, for radiated sound power emitted from the ATD to a reverberant room, see Figs. 11 and 12.

Using the two-microphone method, the total error in calculated quantities from all disturbances will be smallest in a region around $ks = \pi / 2$, where k is the wave-number, and s is the separation of microphones 1 and 2 (see Fig. 2). If we restrict the two-microphone method to the region around $0.1\pi < ks < 0.8\pi$, the total error in the calculated quantities will at the most be a factor 10 times the error around $ks = \pi / 2$ [4]. For the impedance measurements two different microphone separations were chosen: $s1 = 0.1$ m for frequencies from 175 Hz to the first cut-on frequency, and $s2 = 0.5$ m to cover a frequency region from 33 to 270 Hz. The first cut-on frequency of the duct with an inner diameter d=0.146 m was around 1400 Hz (c = 343 m/s). For the source strength measurements a microphone separation $s2 = 0.5$ m between microphone 1 and 3 (see Fig. 4) was used. A frequency resolution for the FFT – system of 1.25 Hz was chosen for the measurements. A relatively

large number of averages (400 for the source and load impedance or alternatively the reflection coefficient measurements and for the source strength measurements, 250 for emitted sound power measurements) were used to achieve a good suppression of flow noise and to reduce the random error in the measurements.

At the real operating conditions the flow speed in the duct before the ATD is typically around 5 m/s. At this low speed the flow noise production is relatively small making an accurate measurement difficult. One alternative is then to measure with higher flow velocities and use a scaling law to calculate the source data at the appropriate speed. In order to obtain data to derive a scaling law acoustic measurements were done for three different flow speeds: $U_1 = 8.2m/s$, $U_2 = 12.3m/s$ and $U_3 = 16.4m/s$.

The pressure drop Δp across the air terminal device was measured for all the three flow speeds. The aim of this experiment was to determine a pressure loss coefficient C_L for the ATD. Using the following equation

$$\Delta p = \frac{1}{2}\rho U^2 C_L, \tag{23}$$

the pressure loss coefficient can be derived. A value close to 0.42 was found from these tests, see table 1.

For validation of the source model additional measurements were done with a modified duct system, having the same inner diameter but no conical inlet part (see Figs. 13 and 14). The validation ducts were used for both in-duct (cross-spectra) and reverberant room measurements (sound power). Two different flow velocities were chosen for the validation measurements; $U_1 = 7.0m/s$, and $U_2 = 12.0m/s$. The reflection coefficients R_L for the conical inlet of the duct system and for the flanged inlet of the validation duct were determined experimentally following the procedure described earlier.

To create a flow in the duct, having an inlet in anechoic room and outlet connected to the air terminal device under study in a reverberation room, an axial fan was used to pressurize the anechoic room. The return flow of the air was through a third room with a system of silencers. The test duct consisted of a glass fiber conical inlet pipe and of PVC test pipes with circular cross-section area. The flanged inlet section used for the validation measurements was made of an aluminum plate with a thickness of 15 mm. For the in-duct acoustic pressure measurements ¼-inch condenser microphones (Brüel & Kjaer 2670 and Norsonic 1245) were

used. In order to determine the flow velocity in the duct system a Pitot-tube connected to an electronic micro-manometer was mounted in the duct, see e.g. Figs. 7-8. The static air pressure close to the ATD was also measured using the same micro-manometer. As an external noise source for the impedance measurements, a loudspeaker positioned in the duct, was used. The loudspeaker was driven by a sound generator through a power amplifier and an equalizer. The signal acquisition was performed by a four-channel digital Fourier analyzer (Siglab 20-42) connected to a PC. The sound power measurements (according to ISO 3747) in the reverberation room (see Figs. 11, 12, 13) were performed using a ½-inch microphone fixed to a rotating microphone support. The reference sound power was created by a calibrated fan type sound source (Brüel & Kjaer 4204) positioned at the location of the air terminal device in the reverberation room.

4. RESULTS AND DISCUSSION

The measured (normalized) source impedances for the air terminal device (Figs. 15-18) show only a small dependence on flow velocity up to 500-600 Hz ($d/\lambda < 0.25$). For low frequencies the main effect of the flow will be related to dissipation [8] of acoustic energy, which can be related to the pressure drop over the ATD. From [8] it follows that the flow induced (normalized) acoustic resistance is given by

$$R_{flow} = M \cdot C_L \,. \tag{24}$$

This can be compared with the (normalized) radiation resistance which, assuming a monopole type of radiation, is given by

$$R_{rad} = \frac{(k \cdot d)^2}{16} \,. \tag{25}$$

For the case studied here with a Mach number less than 0.05 and C_L=0.42, we then have $R_{flow} \leq 0.025$, so the radiation resistance will dominate for frequencies above 200-300 Hz.

Results for the source strength auto-spectrum are shown in Fig. 19. Fig. 20 shows the coherence between the microphones 1 and 3, used for the in-duct cross-spectrum

measurements to determine the source strength according to equation (17). In Fig. 21 the collapse of all the source strength data is shown, based on the scaling law in equation (22) with $\alpha=0$.

To validate the source model, including the scaling law for the source strength, the modified duct described above was used. In Figs. 22 and 23 examples for the prediction of the pressure cross-spectrum (G_{13}) are shown. As can be seen the agreement for the in-duct case is good with a deviation of typically less than 2 dB up to about 1000 Hz. In Figs. 24-27 examples for the prediction of the sound power auto-spectrum radiated are shown in narrow and 1/3-octave band. Here the agreement is not as good as for the in-duct case. The peaks occurring in the spectra are related to the low frequency resonances occurring in the validation ducts used.

In order to investigate the reason for the less good agreement for the radiated sound power tests with a simplified ATD, a plate with a hole Fig. 6, were performed. An example of the results is shown in Figs. 28-29. As can be seen the agreement is better for this case than for the ATD unit. This and other tests led to the conclusion that the resulting dipole source generated by an obstruction at the duct opening often has more than one component. When the source data is determined inside the duct only the axial (along x) component of the dipole will excite a plane wave field. The source data determined inside the duct will therefore only contain information about this component. For the outside radiation all the dipole components can play a role. Therefore we will underestimate the radiated field if we use the in-duct source data to also determine the radiation. For a proper description of the radiated power a more complex source model is needed, which can include all the components of the dipole source.

5. CONCLUDING REMARKS

This paper represents an effort to use 1-port models to characterize flow generated sound which works as long as the source process is unaffected by the acoustic field. This kind of assumption is consistent with the basic assumption used when writing down the source term in Lighthills famous equation. Therefore it holds in many cases with the exception of situations where strong flow-acoustic feedback occurs, e.g., whistles. In the paper the use of this approach has been tested and proven for a flow constriction mounted at a duct opening. In the experimentally derived scaling law a velocity dependence of 3 was found for the narrow band spectra, corresponding to a dipole-like behavior of the source in the plane wave

range. In earlier works done at MWL the approach has also been successfully applied to in-duct elements that can be described as active 2-ports such as bends [6, 8]. The use of 1- and 2-port models is of importance for modeling the low frequency plane wave range in duct systems. This range is of particular interest to study resonance and standing wave effects that significantly can affect the acoustic output. An interesting future continuation of this work would be to try to establish methods to estimate 1- and 2-port source data directly from CFD calculations. Since the passive part of the source data often is weakly affected by the flow it could be sufficient “only” to estimate the (active) source strength part.

REFERENCES

1. H. BODÉN and M. ÅBOM 1995 *Acta Acustica* 3, p. 1-12. Modeling of fluid machines as sources of sound in duct and pipe systems.

2. ASHRAE, 2003 ASHRAE Applications Handbook, chap. 47: "Sound and Vibration Control", ASHRAE Inc., Atlanta, 2003.

3. J. LAVRENTJEV 1998 *Doctoral Thesis* TRITA-FKT-9828. Issn: 1103-470X. The Marcus Wallenberg Laboratory, KTH. Multi-port models for source characterization of fluid machines.

4. M. ÅBOM and H. BODÉN 1988 *Journal of Acoustical Society of America* **83**, p. 2429-2438. Error analysis of two-microphone measurements in ducts with flow.

5. P. A. NELSON and C. L. MORFEY 1981 *Journal of Sound and Vibration* **79,** p. 263-286. Aerodynamic sound production in low speed flow ducts.

6. S. NYGÅRD 2000 *Lic. Tech Thesis* TRITA-FKT-0057, ISSN 1103-470X, The Marcus Wallenberg Laboratory, KTH. Low frequency sound in duct systems.

7. M. S. HOWE 1980 *Journal of Sound and Vibration* **70**, p. 407-411. The dissipation of sound at an edge.

8. H. GIJRATH, S. NYGÅRD and M. ÅBOM 2001 *ICSV 8*, Hong Kong, paper no. 578. Modeling of flow generated sound in ducts.

FIGURES

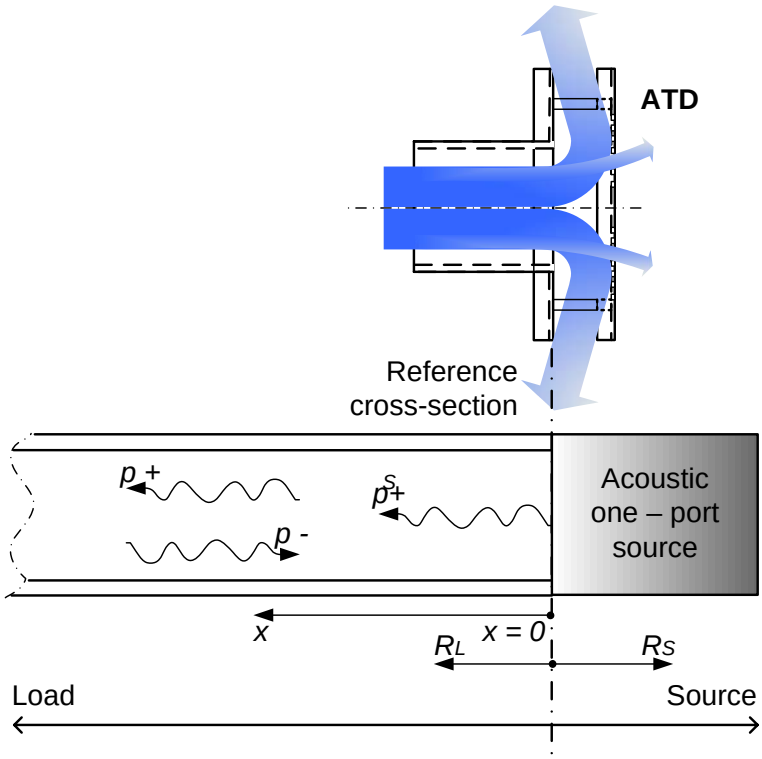

Fig. 1. Representation of an ATD, a device regulating the air flow at the end of a duct system as an acoustic one-port source.

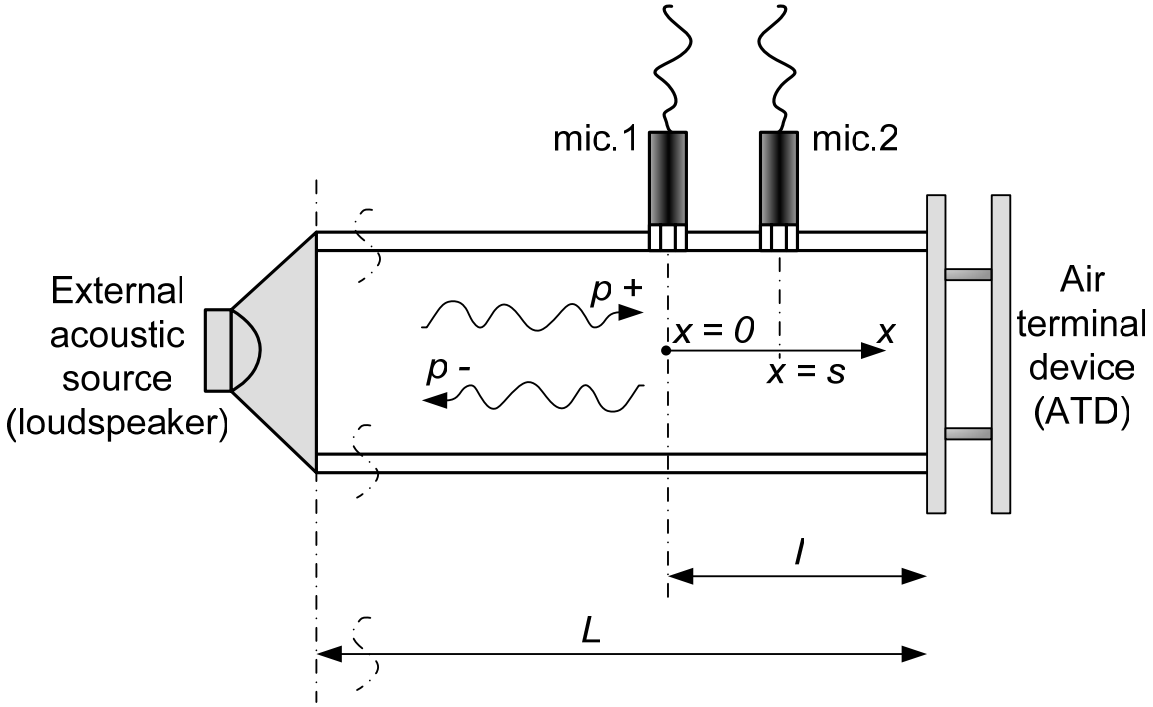

Fig. 2. Basic measurement configuration for the two-microphone method for impedance measurements. Determination of the source impedance.

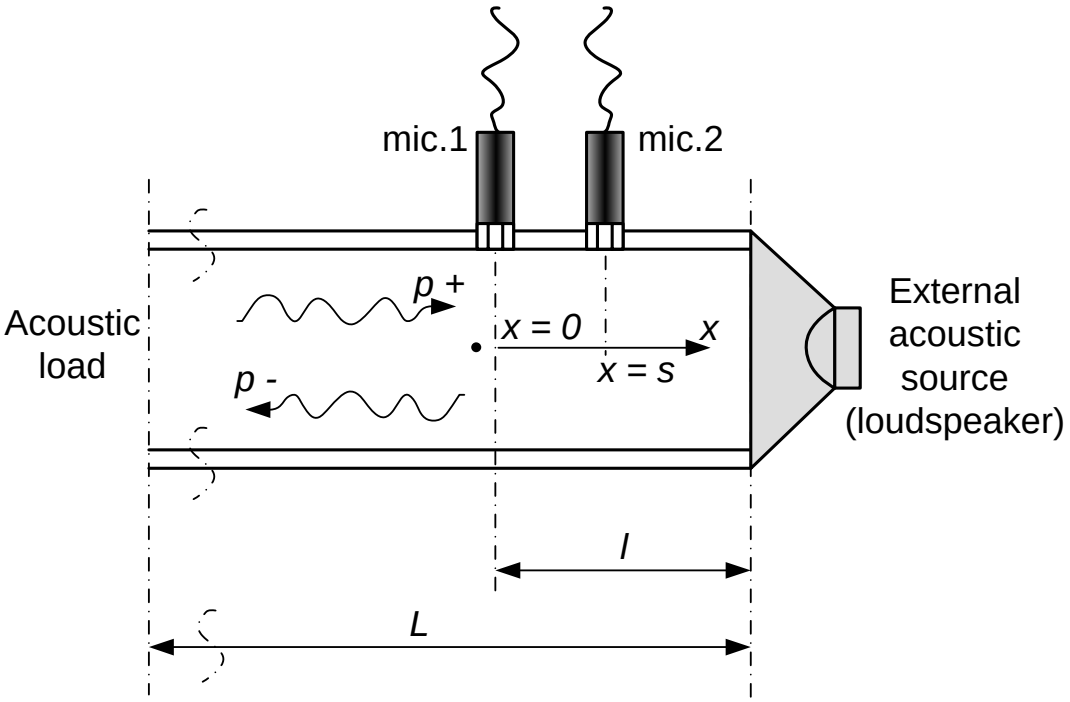

Fig. 3. Basic measurement configuration for the two-microphone method for impedance measurements. Determination of the acoustic load.

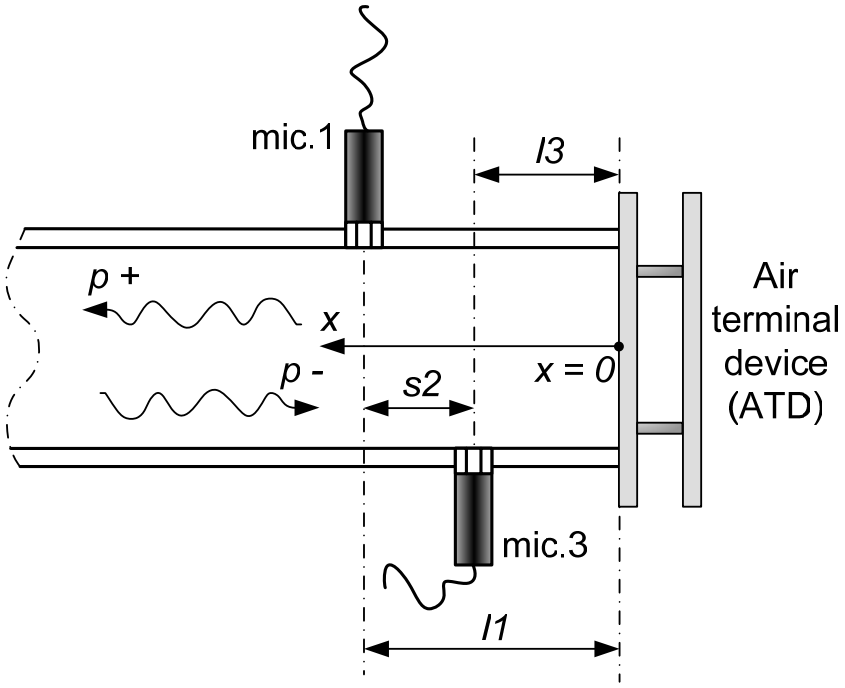

Fig. 4. Basic measurement configuration for source strength measurements.

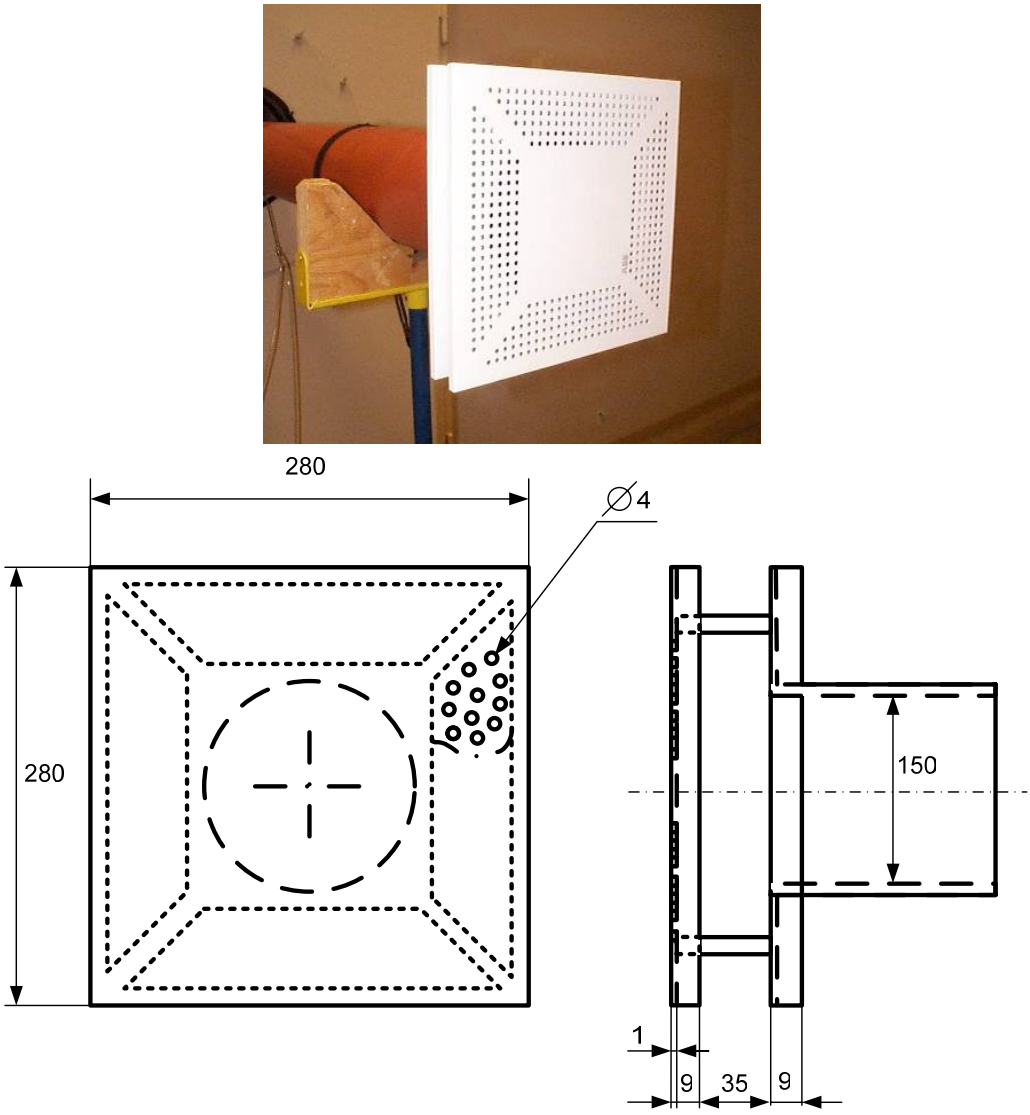

Fig. 5. Photo and drawing (units in mm) of the standard air terminal device used in the experiments.

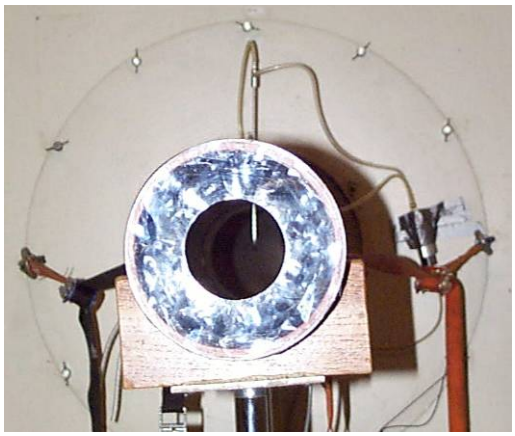

Fig. 6. Photo of the circular orifice used in the experiments.

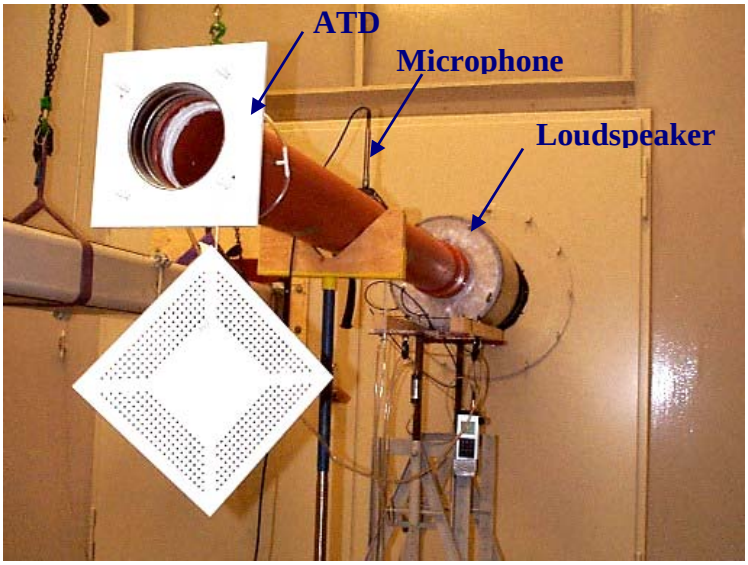

Fig. 7. Photo of the experimental set-up for source impedance measurements.

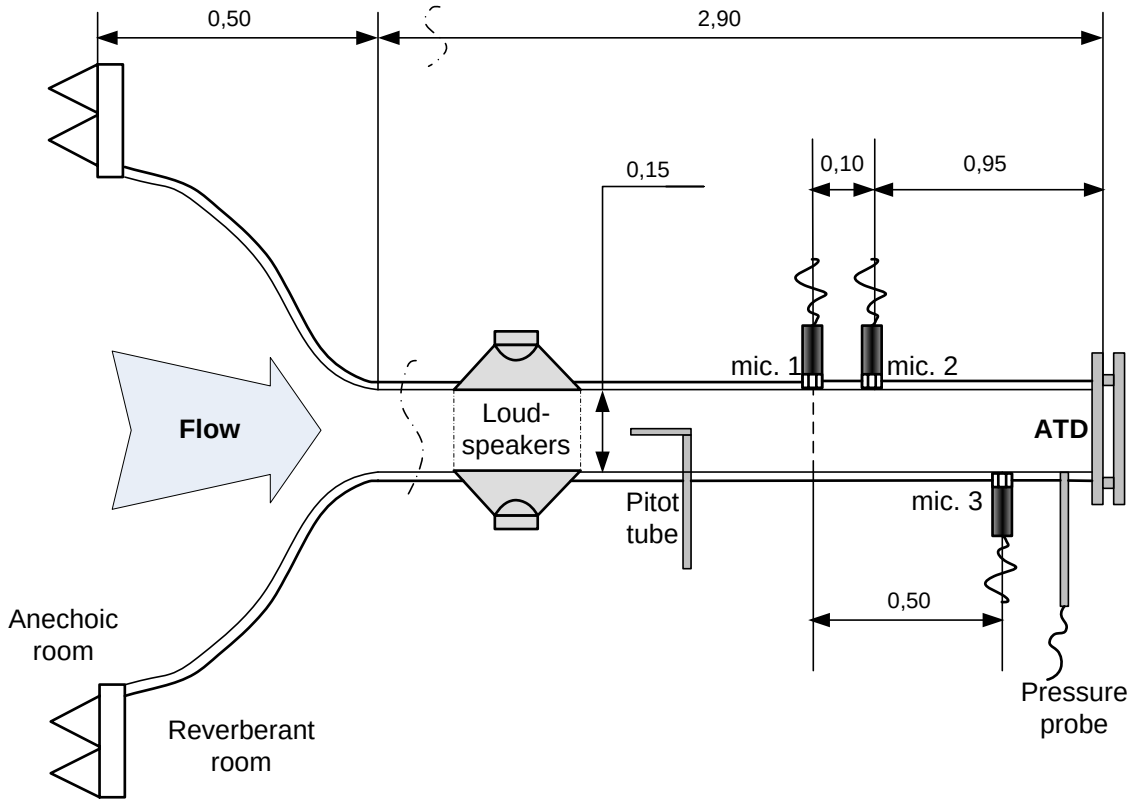

Fig. 8. Layout of the rig for source impedance measurements. All units are in [m]

Fig. 9. Photo of the experimental set-up for source strength measurements

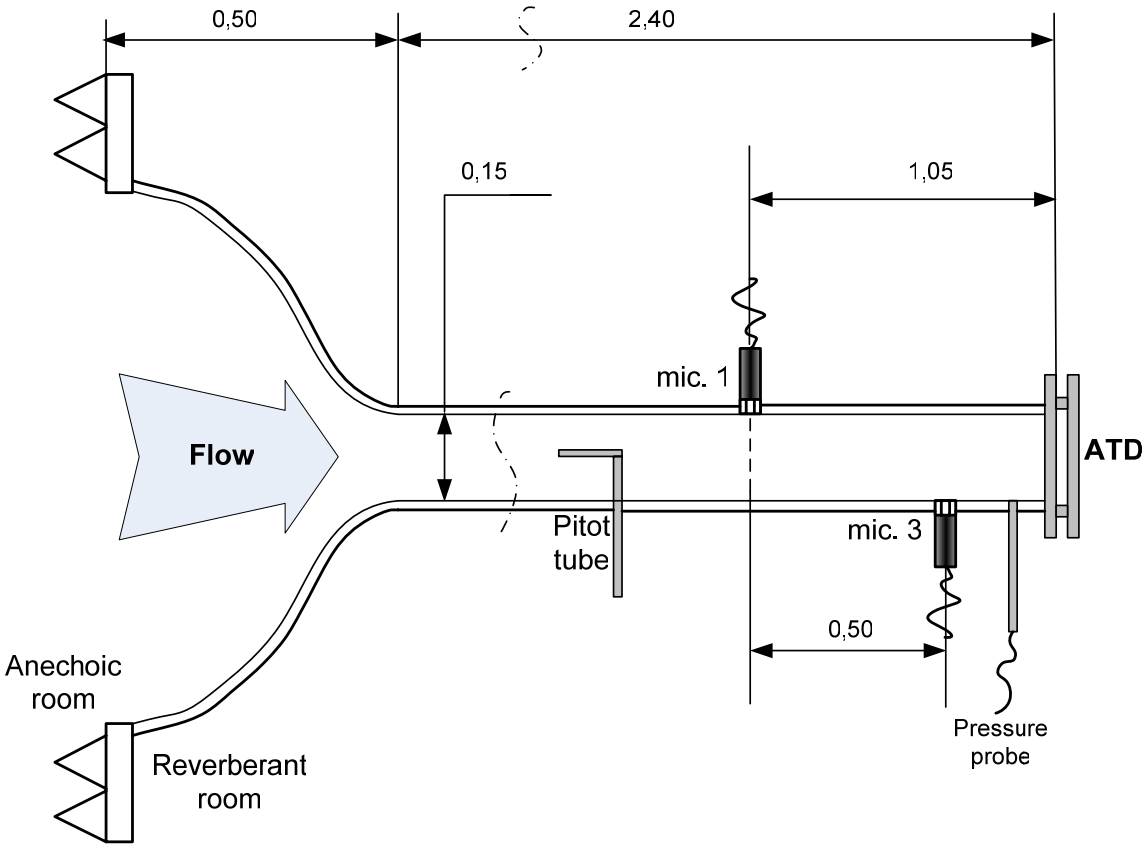

Fig. 10. Layout of the rig for source strength measurements. All units are in [m]

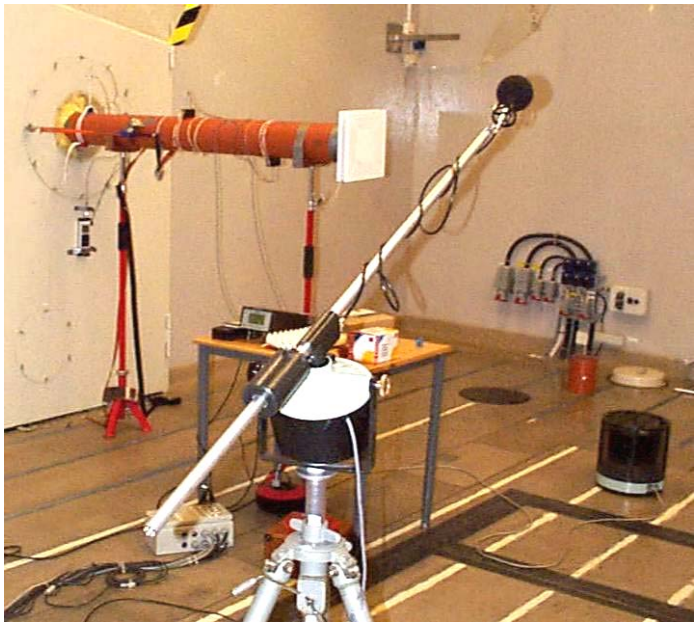

Figure 11. Photo of the experimental set-up for the radiated sound power measurements

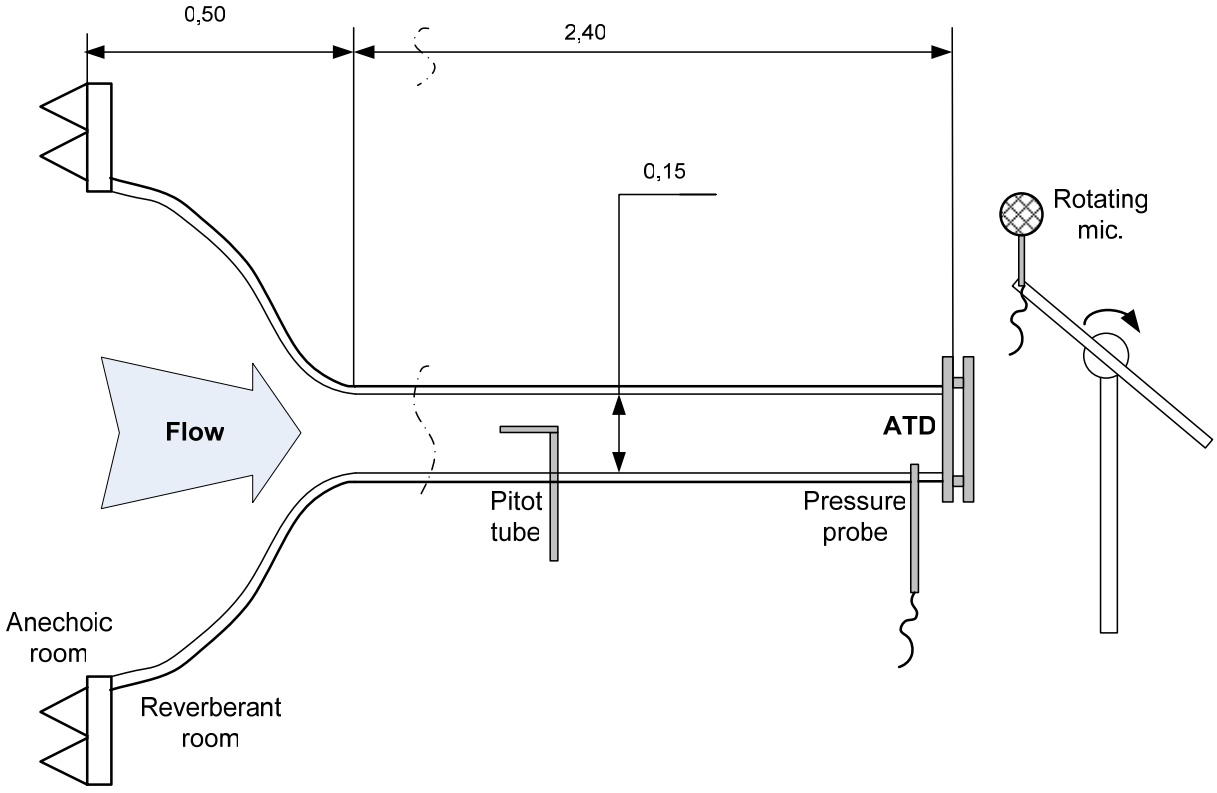

Fig. 12. Layout of the rig for the radiated sound power measurements. All units are in [m]

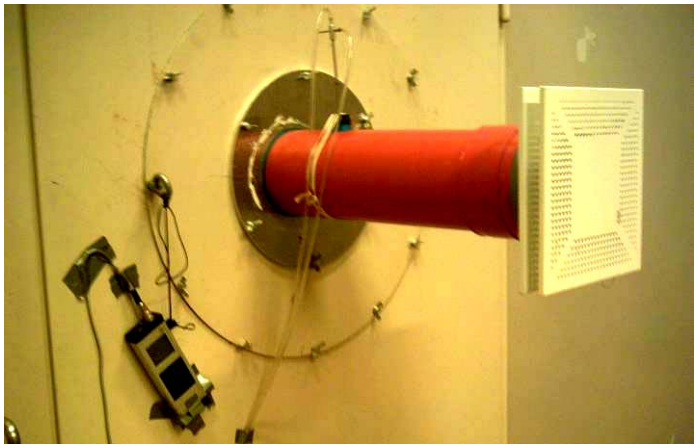

Fig. 13. Photo of the experimental set-up for the radiated sound power measurements using a validation duct system.

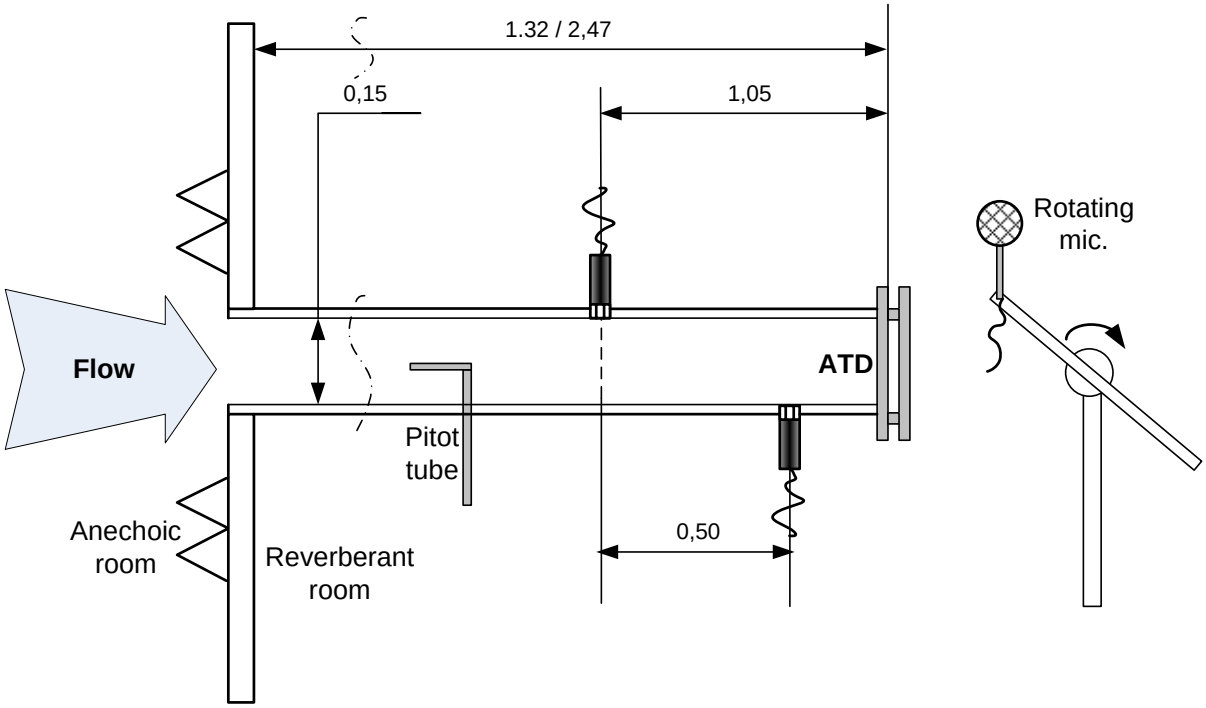

Fig. 14. Layout of the rig for the validation measurements. All units are in [m]. Note, that two different lengths were used 1.32 and 2.47 m.

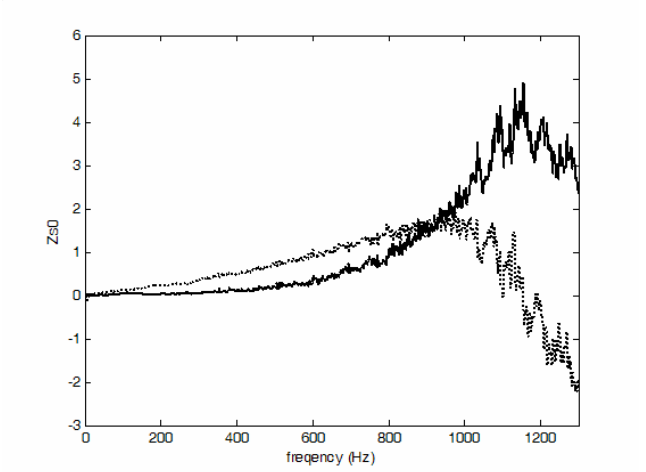

Fig. 15. The real and the imaginary part of the source impedance of the ATD; v=0 m/s; real part (full-line), imaginary part (dotted-line);

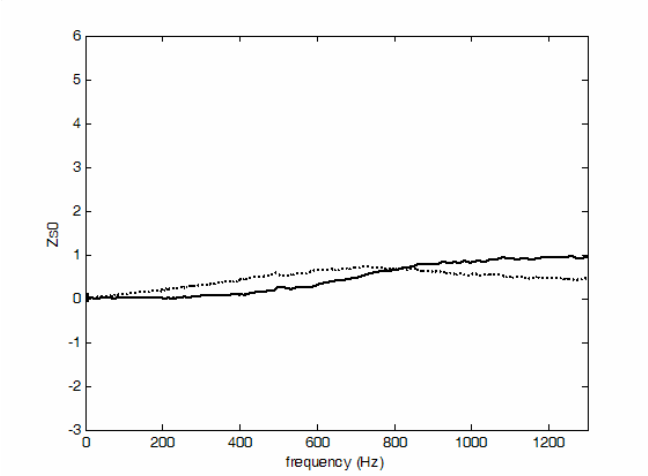

Fig. 16. The real and the imaginary part of the source impedance of the open termination (the ATD removed); v=0 m/s; real part (full-line), imaginary part (dotted-line);

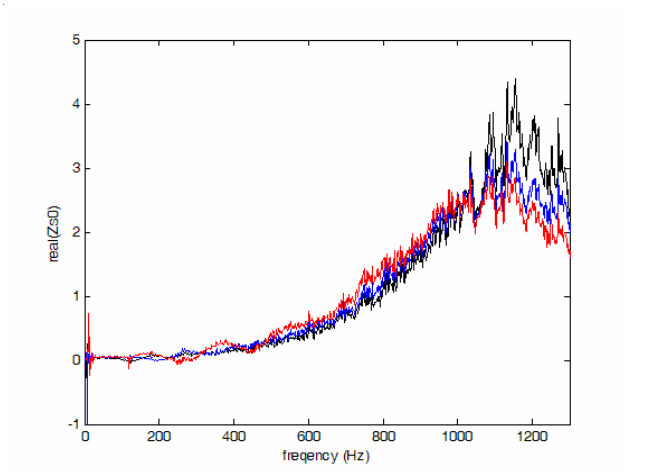

Fig. 17. The real parts of the source impedance of the ATD; v=8.2 m/s (black line), v=12.3 m/s (blue line), v=16.4 m/s (red line);

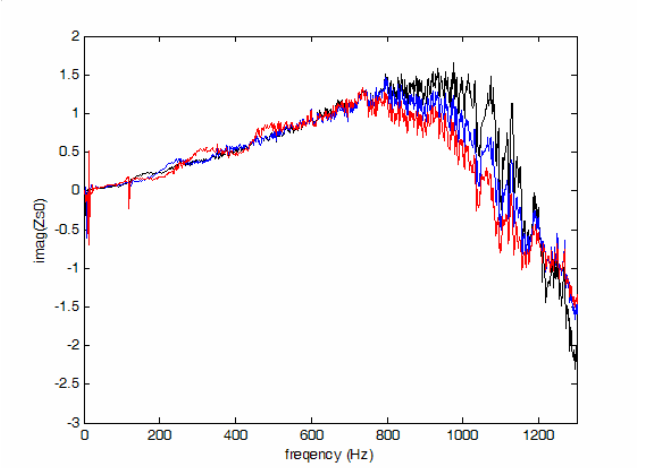

Fig. 18. The imaginary parts of the source impedance of the ATD; v=8.2 m/s (black line), v=12.3 m/s (blue line), v=16.4 m/s (re);

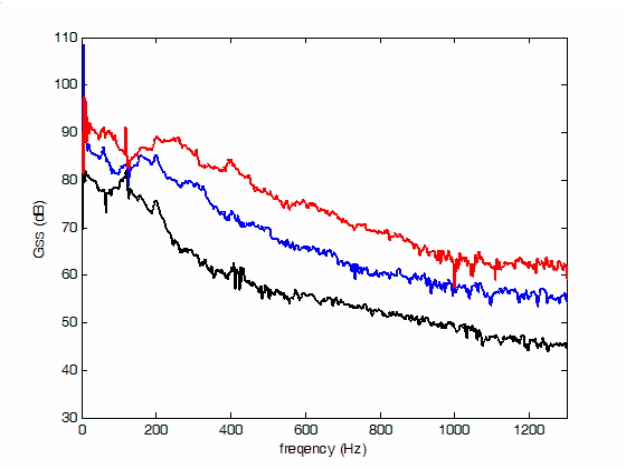

Fig. 19. The source strength of the air terminal device from in-duct measurements; v=8.2 m/s (black line), v=12.3 m/s (blue line), v=16.4 m/s (red line);

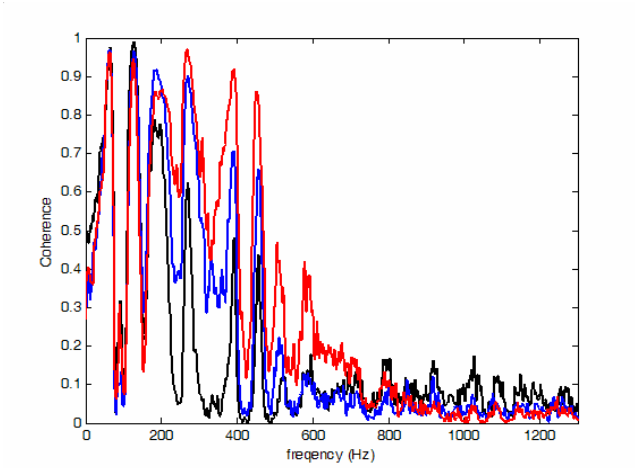

Fig. 20. The coherence between two-microphones; source strength measurements of the ATD; v=8.2 m/s (black line), v=12.3 m/s (blue line), v=16.4 m/s (red line);

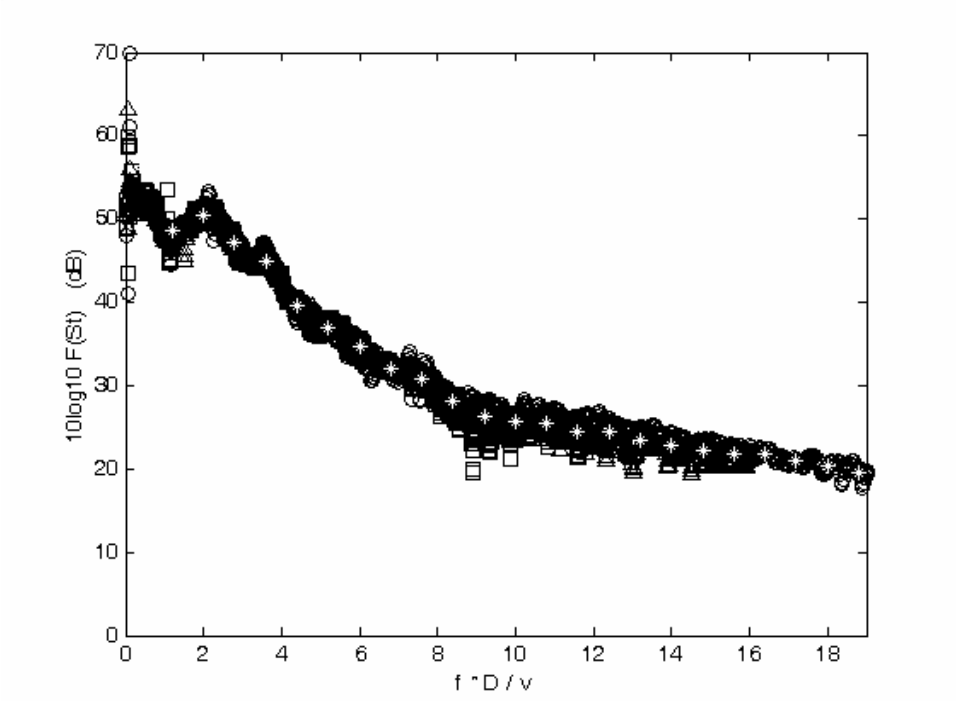

Fig. 21. The Strouhal number dependent source spectrum;
o the source strength based on in-duct measurements,
* the polynomial source model used in the validation.

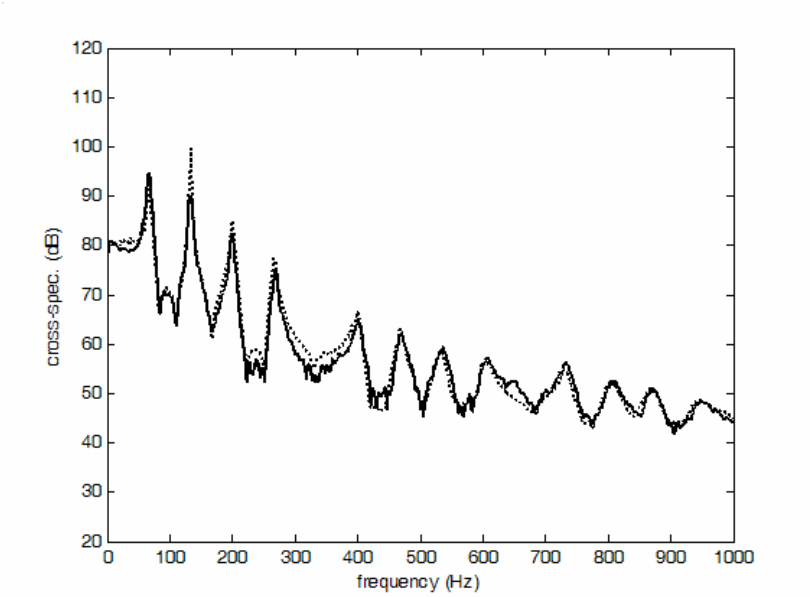

Fig. 22. The cross-spectrum of the air terminal device with 7.0 m/s flow velocity in validation duct system;
measurements (full-line),
prediction (dotted-line).

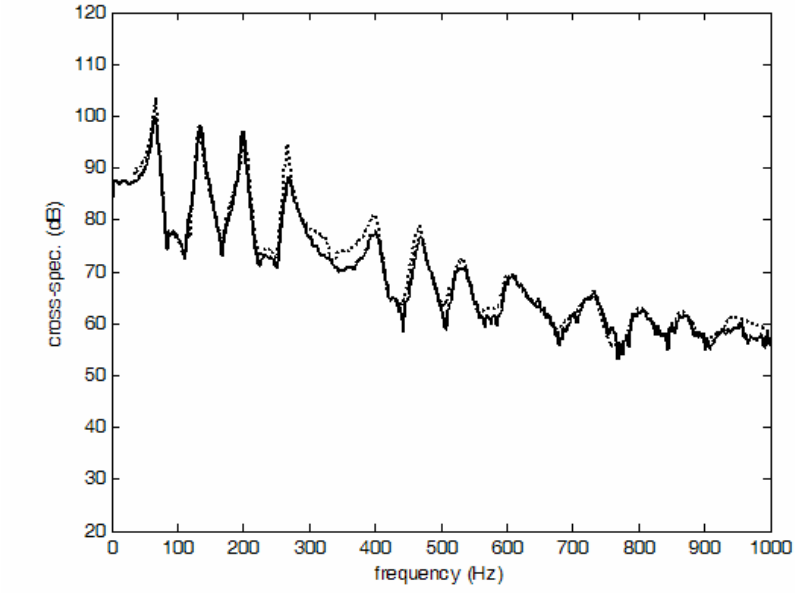

Fig. 23. The cross-spectrum of the air-terminal device with 12.0 m/s flow velocity in validation duct system;
measurements (full-line),
prediction (dotted-line).

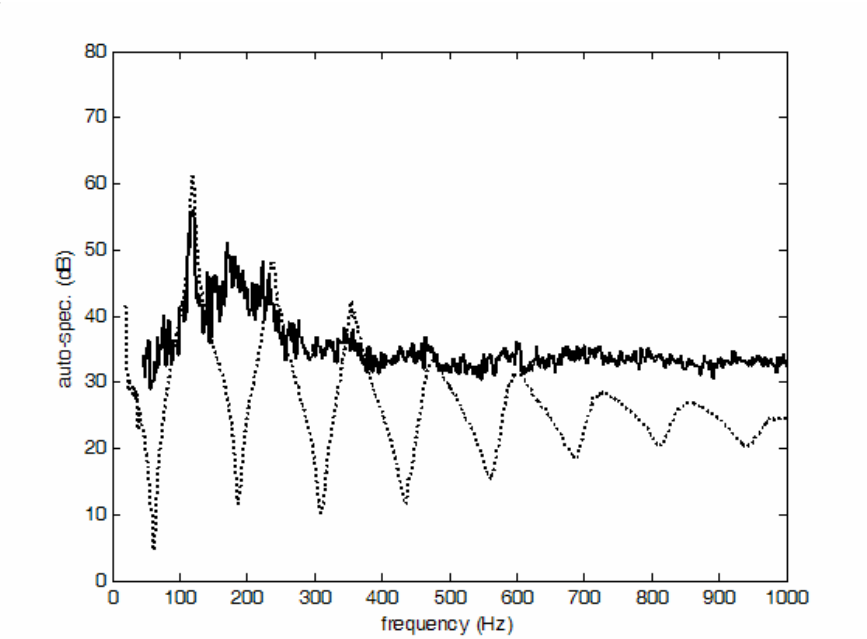

Fig. 24. Sound power spectrum in the reverberation room from the air terminal device with 7.0 m/s flow velocity in validation duct system; measurements (full-line), prediction (dotted-line).

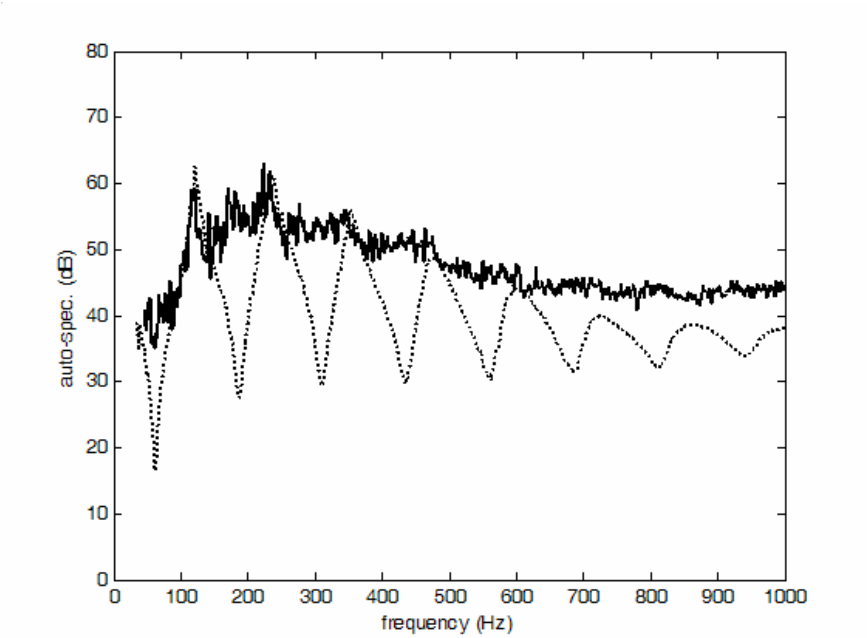

Fig. 25. Sound power spectrum in the reverberation room from the air terminal device with 12.0 m/s flow velocity in validation duct system; measurements (full-line), prediction (dotted-line).

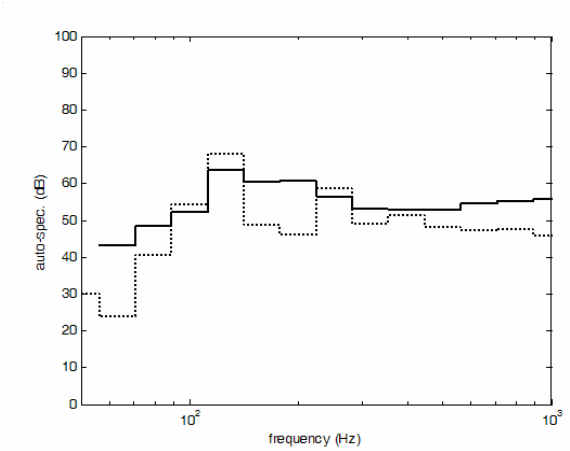

Fig. 26. Same as Fig. 24 but in 1/3-octave band.

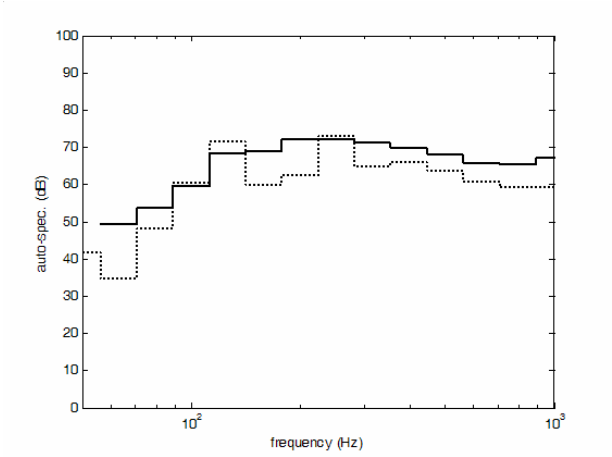

Fig. 27. Same as Fig. 25 but in 1/3-octave band.

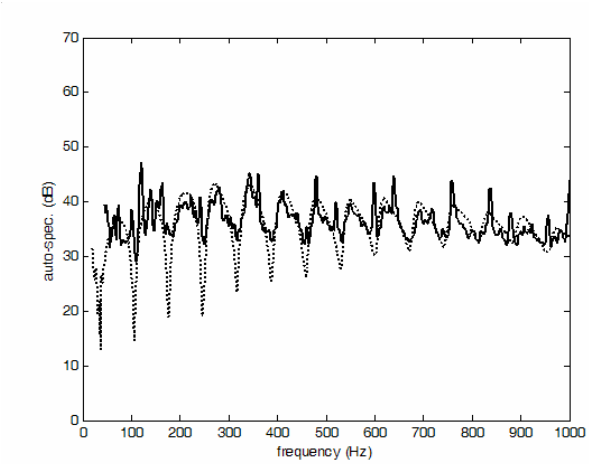

Fig. 28. Sound power spectrum in the reverberation room from the circular constriction; 7.0m/s flow velocity.

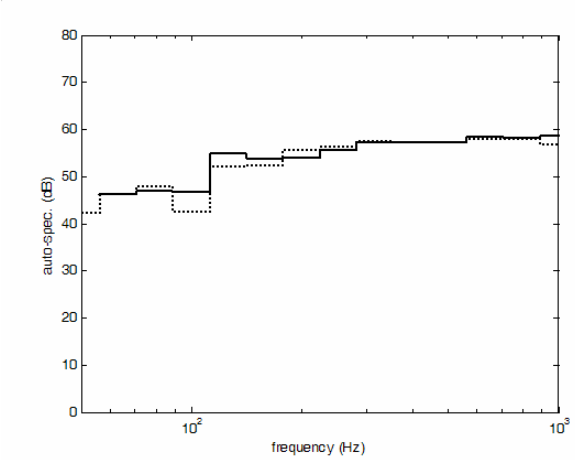

Fig. 29. Same as in Fig. 28 but in 1/3-octave bands.

TABLES

Flow velocity v [m/s]	Pressure difference Δp [Pa]	Pressure loss coefficient CL
8.2	42,1	0,42100
12.3	94,8	0,42133
16.4	165,5	0,41375
		Average CL 0,41869

Table 1. The pressure loss coefficient of the air terminal device

Paper B

MODIFIED MULTI-LOAD METHOD FOR NON-LINEAR IC-ENGINE SOURCE CHARACTERIZATION

H. Rämmal and H. Bodén

Abstract Linear frequency domain prediction codes are used for calculation of low frequency sound transmission in and sound radiation from IC-engine exhaust systems. To calculate insertion loss of mufflers or the level of radiated sound information about the engine as an acoustic source is needed. The source model used in the low frequency plane wave range is the linear time invariant 1-port model. The acoustic source data is usually obtained from experimental tests where multi-load methods and especially the two-load method are most commonly used. The exhaust pulsations of an IC-engine are of high level, which means that the engine is not a perfectly linear and time invariant source. It is therefore of interest to develop source models and experimental techniques that try to take this non-linearity into account. In this paper a modified version of the two-load method to improve the characterization of the non-linear acoustic 1-port sources has been developed and tested. Simulation results from various source configurations of a simplified IC-engine model were used to validate the method. The influence of parameters controlling the linearity of the system was investigated. The time-variance of the source model was varied and the source characterization quality using the two-load method and the modified two-load method was evaluated.

1. INTRODUCTION

Noise and vibration are usually most efficiently reduced at the source. It is therefore important to be able to characterise noise sources by their source strength and also to know how they interact with their surroundings. The goal of source characterisation is to provide a complete and independent source model, which fully describes how the source interacts with the receiving system and does not depend on the properties of the receiver. An acoustic source model can be used for calculation of the acoustic field generated in duct systems coupled to fluid machines: e.g., pumps, fans, internal combustion engines, for source modifications, for evaluation of noise sources and for appropriate source and receiver design.

The types of source models can first be divided into linear and non-linear models. The linear models can further be subdivided into time-invariant models and time-varying models which means that the parameters (or boundary conditions) in the governing equations are either independent of or dependent on time.

The methods used for experimental source characterisation can be classified as direct methods (with external sound source) and indirect methods or multi-load methods (without external sound source).

An overview on previous studies and the measurement methods available for determination of the source data can be found in [1] and [2].

Regarding linear and time-invariant one- and two-port sources, the measurement techniques for obtaining source data are quite well developed but regarding time-varying and non-linear source models there is still a lack of complete models, e.g., for the intake and exhaust noise of IC-engines [3]. In the conclusions of [3] it is stated that one of the areas where considerable research input is needed is the frequency domain characterisation of the engine exhaust source. Due to the simplicity of existing characterisation models the fluid machines connected to a duct system are quite commonly modelled as linear and time-invariant sources. In [4] a method was proposed by Bodén to characterize linear time-variant sources and Jang and Ih [5] have proposed a method for including non-linearity in direct source characterization technique.

Many fluid machines such as compressors and IC-engines are high level acoustic sources where clearly non-linear processes take place, for example, combustion, critical flow through the valve openings and large temperature fluctuations. As these processes,

generated by the source, may violate the linearity assumption, non-linear effects included in the models could improve the source characterisation results.

In this paper the source data from the experimental and simulated data is determined using indirect characterisation methods and the focus will be on characterisation of fluid borne sources with non-linear behaviour, using a refined version of the well-known two-load method in which non-linear effects are included. The new method is developed and used to characterise the source data of various acoustic sources. The source characterisation results are then evaluated and the results are compared to the "classical" two-load method.

Knowledge about systems linearity and time-variance is often needed to be able to make decisions when choosing a method for source modelling and characterisation. Using a one-cylinder "cold" engine simulation model [6] the linearity and time-variance of this simplified IC-engine as acoustic one-port source, are investigated in this paper in order to study the influence of geometric and dynamic parameters on the system behaviour. The developed methods have also been tested on the experimental data. Linearity tests [7], [8] are used on simulated and experimental data, obtained from several engine model parametric configurations and IC-engine operating points.

2. SOURCE MODELS

In developing source models one is looking for the most simple model that is able to provide an acceptable results. The models can be classified as linear time-invariant, linear time varying, hybrid and non-linear models, in order of increasing complexity.

The source is described by the physical quantities via which it interactions with the outside world. In the simplest case where an infinite space around the source can be assumed, the source can be characterized by its radiated acoustic power. For low frequencies in-duct more complex descriptions such as multi-port models are often needed [1].

2.1 Linear time-invariant source model

If only plane waves are considered in the duct system the simplest model that can be used to describe the source is the linear time-invariant frequency domain one-port

model. If there is only one degree of freedom at the interface between the source and the system the one-port source models can be used. For in-duct fluid-borne sound sources this corresponds to cases where there is a plane wave state in the connected duct. In-duct sources normally have at least two openings which means that it further requires that the external acoustic load only can vary at one of the openings, or the openings are acoustically uncoupled from each other so that they can be treated separately.

In the frequency domain an acoustic one-port can be completely described by two complex parameters: the source strength (p_+^S) and the source reflection coefficient (R_S) (or alternatively the source impedance). The behavior of the one-port (see Fig. 1) can in the frequency domain, be described by [1]:

$$p_+ = R_S\, p_- + p_+^S\,, \tag{1}$$

where (p_-, p_+) are traveling acoustic pressure amplitudes, (R_S) is the source reflection coefficient at cross-section, where x=0 (see Fig. 1), and (p_+^S) is the source strength. The source strength (p_+^S) can be interpreted as the pressure generated by the source-side when the system is reflection free.

In the literature the source model for one-ports is often expressed in terms of source strength (p^S) and normalized source impedance (Z_S).

$$p = p^S - Z_0 \cdot Z_S \cdot q\,, \tag{2}$$

Where (p^S) is the source pressure, (p) and (q) are acoustic pressure and volume velocity, respectively, and (Z_0) is the characteristic impedance of the fluid. The source impedance (Z_S) represents the acoustic impedance seen from the reference cross-section towards the source.

Fig. 2 shows the equivalent acoustic circuit for a linear and time invariant source. In this figure (p_L) and (Z_L) denote the acoustic load data (the load pressure and the load impedance), while (p_S), (q) and (Z_S) denote the source data respectively.

Theoretically the two representations of the source shown in Fig. 2 are equivalent and it is possible to go from one representation to the other by using the relationship $q = p^S / Z_S$. If there are errors in the experimental data or deviations from system linearity it can be expected that the error propagation is different for the two representations leading to different results when source data is extracted using over-determination. In addition to other techniques for testing system linearity discussed in section 3.3. Extracting source data using both formulations and comparing the resulting source impedance is a possibility to see if experimental data are in agreement with linear time-invariant source model. It can also be expected that if the source is close to a velocity source this model will give smaller errors than if a pressure source model is applied and vice versa.

The linear time-invariant equivalent source model will strictly be applicable only in situations where the pressure-fluctuations are small. Several authors however have found the linear time-invariant model to give reasonable results for modeling the systems with relatively large pressure fluctuations, i.e., slightly non-linear systems.

2.2 Non-linear source model

To improve the described source characterization methods, especially for applications where clearly non-linear effects are expected, such as for IC-engines, a technique was suggested by Jang and Ih [5]. The idea was to include non-linear effects in the direct methods for source impedance determination.

In this paper the method has been modified for applications with indirect or multi-load methods. The time domain representation of the source model with non-linear term is described by

$$\int Z_S(\tau)Q(t-\tau)d\tau + \int h_S(\tau)b(t-\tau)d\tau = P_S(t) - P_L(t)\,, \qquad (3)$$

where ($P_L(t)$) and ($Q(t)$) denote the pressure and volume velocity, ($Z_S(t)$) is the time domain representation of the source impedance, ($P_S(t)$) is the source strength, (*b(t)*) is the non-linear input and ($H_S(t)$) is the source data coefficient for the non-linear part. When applying this technique in section 5 and 6 it has been assumed that $b(t) = Q^3(t)$

which is the first higher order series expansion term obtained for the pressure drop over an orifice. It can be expected that the main type of non-linearity for many applications will be caused by the flow through a constriction characterized by the pressure difference over the constriction being equal to $\Delta p = \left(\frac{\rho_0}{2S^2} \right) \cdot Q(t) \cdot |Q(t)|$. It is shown in [9] that, under the assumption that ($Q(t)$) follows a zero mean Gaussian distribution, the third-order polynomial least-squares approximation to $\left(\frac{\rho_0}{2S^2} \right) \cdot Q(t) \cdot |Q(t)|$ is

$$P(t) = \frac{\rho_0}{2 \cdot S^2} \cdot \left[\left(\sigma_q \cdot \sqrt{2/\pi} \right) \cdot Q(t) + \left(\frac{\sqrt{2/\pi}}{3 \cdot \sigma_q} \right) \cdot Q^3(t) \right], \tag{4}$$

where σ_q is the standard deviation of ($q(t)$). Taking the Fourier transform of (4) gives

$$p(f) = \frac{\rho_0}{2 \cdot S^2} \cdot \left[\left(\sigma_q \cdot \sqrt{2/\pi} \right) \cdot q(f) + \left(\frac{\sqrt{2/\pi}}{3 \cdot \sigma_q} \right) \cdot q_3(f) \right], \tag{5}$$

where ($p(f)$),($q(f)$) and ($q_3(f)$) are the Fourier transforms of ($P(t)$), ($Q(t)$) and ($Q^3(t)$). The original "square-law system with sign" $\left(\frac{\rho_0}{2S^2} \right) \cdot Q(t) \cdot |Q(t)|$ can therefore to the third order be replaced by a linear system in parallel with a cubic system.
In the frequency domain Eq. (3) can be formulated as

$$p_S Z_L - p_L Z_S - H_S B = p_L Z_L \tag{6}$$

where (H_S) and (B) are the Fourier transforms of ($h_S(t)$) and ($b(t)$). This equation has compared to Eq. (7) a third complex unknown (H_S), which means that now at least three acoustic loads will have to be used in order to solve the equation and to obtain the source data.

3. EXPERIMENTAL SOURCE CHARACTERIZATION

A number of different methods exist for determining acoustic source data from experiments. An overview of the state of the art of experimental methods for determining the 1-port source data for in-duct fluid-borne sound sources was described in the review papers [1] and [2].

The measurement methods can be divided into direct (with an external source) [10] and indirect or multi-load methods (without an external source) [11].

3. 1 The two-load method

If the source is time-invariant, the one-port source characteristics can be determined by using only two external loads. This method is known as the two-load method.

$$p_S \cdot Z_L - p_L \cdot Z_S = p_L \cdot Z_L \tag{7}$$

Eq. (7) has got two complex unknowns, which means that it can be solved if we have at least two complex equations. If we use n acoustic loads we get

$$\begin{bmatrix} Z_{L1} & p_{L1} \\ Z_{L2} & p_{L2} \\ \vdots & \vdots \\ Z_{Ln} & p_{Ln} \end{bmatrix} \cdot \begin{pmatrix} p_S \\ Z_S \end{pmatrix} = \begin{pmatrix} p_{L1} \cdot Z_{L1} \\ p_{L2} \cdot Z_{L2} \\ \vdots \\ p_{Ln} \cdot Z_{Ln} \end{pmatrix}, \tag{8}$$

where we have included more acoustic loads than we need, in order to get an over-determined system, which can be useful for improving the measurement results [4,12], and for checking if the source behaves as a linear system [7,8].

Alternatively the one-port model for the volume velocity source (see Fig. 2) can be expressed as:

$$q - p_L \cdot \frac{1}{Z_S} = \frac{p_L}{Z_L}, \tag{9}$$

or with *n* loads:

$$\begin{bmatrix} 1 & -p_{L1} \\ 1 & -p_{L2} \\ \vdots & \vdots \\ 1 & -p_{Ln} \end{bmatrix} \cdot \begin{pmatrix} q \\ 1/Z_S \end{pmatrix} = \begin{pmatrix} p_{L1}/Z_{L1} \\ p_{L2}/Z_{L2} \\ \vdots \\ p_{Ln}/Z_{Ln} \end{pmatrix}, \tag{10}$$

where we now solve for (q) and ($1/Z_S$). In order to determine the normalized impedances of the acoustic loads (Z_{Li}), used for experiments, a number of pressure transducers are usually mounted in the exhaust pipe. In the plane wave range we can use this information to perform wave decomposition and to determine the reflection coefficient looking into the acoustic load, which in turn gives the normalized load impedance.

To determine the complex load pressures (p_{Li}) we need a reference signal to ensure that the pressure time histories for the different acoustic loads start at the same point in the engine cycle. The pressure time histories are then Fourier transformed and used to calculate the load pressures and load impedances and subsequently the source data.

For a linear source it can be expected that the source impedance results from both the source formulations (see Fig. 2) should converge towards the same results when a large degree of over-determination is used. Any discrepancy between the results can therefore be an indication of a non-linear source behavior.

As described above the two-load method requires complex pressure measurements and a reference signal unaffected by acoustic load variations, which is related to the sound generating mechanism of the source. For fluid machines with periodic operation cycle the normal solution is to try to obtain a trig signal for instance giving one pulse per revolution [4]. This procedure can catch harmonic part of the spectrum generated by machine but not the broad band part. It can also be noted that a trig signal can also be used to reduce flow noise disturbances from measured pressure signals. An alternative method, used for flow noise suppression, is to create a “noise-free” acoustic reference signal, by using one or several microphones with turbulence screens [7].

Although the two-load method is strictly valid only for linear time-invariant source model, several authors have reported that it gives useful results also in situations that are

not exactly time-invariant or linear. By using a number of extra loads, a solution which is the best fit in least squares sense, can be obtained.

3. 2 The non-linear multiple-load method

The procedure for obtaining (6) is that ($P(t)$) and ($Q(t)$) are first determined from measurements or simulations. The nonlinear function ($b(t)$) is then calculated followed by the Fourier transform of these quantities. It should be noted that an anti aliasing filter should be applied on ($b(t)$) to avoid aliasing problems caused by the presence of frequency components higher than half the sampling frequency. The load impedance (Z_L) is obtained from the ratio of the Fourier transform of ($P(t)$) and ($Q(t)$) ($Z_L = p_L / Q_L$). By using n acoustic loads (6) gives

$$\begin{bmatrix} Z_{L1} & -p_{L1} & -B_1 \\ Z_{L2} & -p_{L2} & -B_2 \\ \vdots & \vdots & \vdots \\ Z_{Ln} & -p_{Ln} & -B_n \end{bmatrix} \cdot \begin{pmatrix} P_S \\ Z_S \\ H_S \end{pmatrix} = \begin{pmatrix} p_{L1} \cdot Z_{L1} \\ p_{L2} \cdot Z_{L2} \\ \vdots \\ p_{Ln} \cdot Z_{Ln} \end{pmatrix}. \tag{11}$$

A minimum of three loads is required to solve for the source data while over-determination is used to reduce effects of measurement errors and deviations from the model just as for the two-load method. It should be noted that one difference between the method proposed here and the method of Jang and Ih [5] is that in the method proposed here the non-linear term is expressed using boundary conditions seen from the source side towards the load while situation is reverted for method of Jang and Ih [5]. This makes the method of Jang and Ih [5] potentially more relevant for characterization of non-linear source behavior. It is however possible that the extra non-linear term will anyway give an improved result compared to the linear time-invariant model for non-linear sources. This will be tested in the subsequent sections.

3.3 Linearity tests

To treat the problem of source characterization in an efficient way an appropriate source model should be chosen. It is therefore important to apply linearity tests to assess

whether a linear model is sufficient. If the linearity test indicates non-linear behavior, the use of non-linear or hybrid methods is a natural step.

For the 1-port sources a linearity test for direct methods has been proposed by Lavrentjev et al. [7]. Further linearity tests for in-direct or multi-load methods were proposed by Bodén and Albertsson [8]. The idea behind the tests is to verify that the source data (p_S, Z_S) are unchanged under acoustic load variations.

If we assume that we have a problem with m complex unknowns and make (n) measurements the over-determined equation system for determining the unknowns (x) can be written in the following way

$$\mathbf{A} \cdot \mathbf{x} = \mathbf{b} \tag{12}$$

where (*A*) is a ($n \times m$) matrix, (*x*) is a ($m \times 1$) vector and (*b*) is a ($n \times 1$) vector. The idea is now to formulate tests, i.e. linearity coefficients, which can tell us if the measured data in (*A*) and (*b*) are consistent with the linear relationship (12). The number of measurements, (*n*) in (12), has to be larger than (*m*) for the linearity coefficients to be meaningful. If (*n*) equals (*m*) the linearity coefficients will always indicate a linear relationship. A linearity coefficient, which is similar to the coherence function, can then be defined as

$$\gamma = \mathbf{x}^{-1} \cdot \mathbf{x} = \mathbf{b}^{-1} \cdot \mathbf{A} \cdot \mathbf{A}^{-1} \cdot \mathbf{b}\,, \tag{13}$$

where x^{-1} is interpreted as the pseudo-inverse of (x). This linearity coefficient will have a value in the interval $0 \le \gamma \le 1$, where the upper limit represents a perfect linear relationship. A drawback with such a test is that it is also sensitive to random errors. In [8] techniques to determine if a value lower than 1 is caused by non-linearities or random noise are discussed.

To increase the sensitivity of the linearity test, the right hand side in the equation $\mathbf{A} \cdot \mathbf{x} = \mathbf{b}$ can be normalized to a unity vector, which means that every row in the equation system $\mathbf{A} \cdot \mathbf{x} = \mathbf{b}$ is divided by the corresponding right hand side.

4. TEST CASES

A theoretical model of a simple piston-restriction system, according to Fig. 3, was developed in [4, 6] and analyzed with forced oscillations. The solutions were obtained using the Harmonic balance method [4]. The duct system connected to the 1-cylinder engine was modeled in the frequency domain, assuming that linear acoustic theory holds, while for the source part – a non-linear time-domain model was used. The purpose of using this model is to be able to vary the degree of time-variation and non-linearity. As the first part of the present study the influence of geometric parameters on the linearity of the source was studied. It was initially assumed that the flow velocity through the constriction would be the main factor determining the linearity. In order to investigate if this was true, linearity tests as described in section 3.3, were first applied to various system configurations. Since it was reasonably easy to perform a parametric study using the computational H.B.M. code, a relatively large number of different parametric settings of the system were studied.

The results for a number of geometrically different configurations giving approximately the same velocity variation were compared. Fig. 4 shows an example of the flow velocity obtained for the three different configurations giving approximately the same flow velocity in the constriction. The three parameters varied (see Fig. 3) were: the piston amplitude (A), the piston diameter (d_1), and the diameter of the constriction (d_2). Only one of the parameters was varied at a time. Another parameter that was varied was the geometric compression ratio (ε) of the cold engine model, the distance (L_V) between TDC (top dead centre) of the piston and the constriction was decreased compared to the original value in the simulations.

In the second part of the study a new indirect source characterisation method was introduced and implemented for various source configurations. In order to evaluate the new non-linear multi-load technique and to compare the results with the conventional two-load technique the simulated system configurations with varied linearity and time-variance were used. The test configurations were at first studied to investigate the linearity of the system.

In order to test the new source characterization technique on experimental data the results from 1-cylinder valve-less compressor measurements [13] and a 6-cylinder

turbocharged truck diesel engine exhaust were used. During the truck diesel engine measurements 12 different acoustic loads (10 side-branches with lengths from 0 to 3130 mm and one muffler with and without particulate trap) were used as acoustic loads. Measurements were made for various engine operating points: 4 different engine speeds (1200, 1400, 1600, and 1800 rpm) and 3 engine loads (25%, 50%, and 100%).

5. RESULTS FROM NUMERICAL SIMULATIONS

5.1 Source linearity study

The acoustic impedance of the loads and the pressure, for the piston-constriction system shown in Fig. 3, at a cross-section just outside the constriction were extracted from the simulations. These data were then analyzed using the linearity tests described in section 3.3. It was concluded that the linearity of the studied system was not totally controlled by the flow velocity through the constriction, although this parameter was of high importance. The linearity of the "cold" engine model was found to be significantly influenced by its main geometrical parameters, described in section 4.

Fig. 5 shows the linearity coefficient (γ) according to (13) for three different geometric configurations giving the same constriction velocity. The discrepancy of the data, for the six first harmonics studied, was typically less than 10%. The dependence on constriction velocity was rather strong. The normalized linearity coefficient (γ_n) was on the other hand found to have a relatively weak dependence on flow velocity in the constriction, but it was strongly influenced by the changes in the main geometric parameters determining the flow velocity, see Fig. 6. It should be noticed that the velocity profile in the constriction was reasonably comparable for the different parametric configurations, but the shape of the curves was somewhat different, see e.g. Fig. 4.

It was also found that the linearity coefficients (γ) and (γ_n), are relatively dependent on constriction diameter (d_2), and have a tendency to increase gradually when (d_2) is decreased.

Additionally the effect on the normalized linearity factor of a variation of the piston diameter (d_1) was studied. Both linearity coefficients (γ) and (γ_n) had a relatively

weak sensitivity to variation in (d_1). A relatively large increase in piston amplitude (A) caused relatively small changes in both the linearity coefficients. Notable changes in the normalized linearity coefficient data caused by variations in piston amplitude value (A) were found only at the fourth harmonic.

The linearity coefficients showed a considerable sensitivity to the variation of the geometric compression ratio (ε), depending on the distance (L_V) between piston TDC and the constriction, see Fig. 7. The changes in normalized linearity coefficient value were notable at most of the harmonics studied. The results of these studies of the dependence of system linearity on geometrical parameters were used in the next section to see if there is a correlation between linearity according to the linearity tests and improvement in results obtained using the new non-linear source model.

5.2 Results from source data extraction

In the simulations, 10 load ducts with a stepwise increased length (l_3) (l_3 = 0.3…2.1 m), with a step of 0.2 m, were used as the acoustic loads connected to the source. Based on acoustic load impedances and pressures obtained from the simulations the source data was extracted using the two-load technique and the new non-linear multi-load method. In order to have a sufficient over-determination, the data from eight acoustic loads out of the ten were included in the calculations of the source data following the procedures given in section 3. Different combinations of loads were used to investigate the influence of the choice of loads on the results. The pressure in the load duct for a load not included in the calculations of the source data was predicted. The procedure was repeated until the pressure predictions were performed for all the described loads and for all the 16 system configurations, altogether for 160 different cases. The prediction quality was evaluated by comparing the results obtained by using the new non-linear multi-load method and the conventional two-load method with direct simulated results. The prediction quality was classified into five categories, described in Table 3. Using Table 1 an attempt was made to statistically analyze the influence of linearity and time-invariance.

The non-linear multi-load method gave better prediction results for 71 different system configurations, while the two-load method was better in 43 cases. In 46 investigated cases the prediction quality was considered to be equal for both the tested methods. A

better agreement between predicted and directly simulated data was noticeable when the linearity coefficients (γ) and (γ_n) indicated more linear system behavior.

Some examples of the source data extraction results are presented in Figs. 8 to 12. Fig. 8 shows an example of good prediction of the sound pressure level in a load duct, achieved by both techniques. In this case the piston amplitude had been decreased to an extremely low value which should give a linear result. Fig. 9 presents an example of typical prediction of sound pressure level in a system with high compression ratio, were the new non-linear multi-load method normally gave better results. In Figs. 10 to 12 results from configurations where the flow velocity in the constriction is kept almost constant is shown. The agreement between predicted and simulated results differs substantially and it can be related to the varying linearity (see Figs. 5 and 6) of the system.

The evaluation of the influence of time-variance on the source characterization results obtained from the simulations of the system configurations with varied piston amplitude (*A*) showed that both the two-load and the non-linear multi-load method gave better prediction results when the system was more time-invariant. It was also noticed that the conventional two-load method showed a higher sensitivity to the time-variance than the non-linear multi-load method. An example of the results, obtained for model configuration with high time-variance, is shown in Fig. 13. These curves should be compared to the results shown in Fig. 8 for a case with low time variation.

In Figs. 14 to 16 the new method has been validated using a model configuration in geometrical parameters similar to that existing in the diesel powered IC-engines with a tendency to higher non-linearities. The linearity coefficient of the system with higher compression ratio is shown in Fig. 17. It can be seen from Fig. 14 that the non-linear multi-load technique gives a better result for this non-linear case. In Figs. 15 and 16 the resulting source impedance when a pressure source and a volume velocity source model have been used in the two-load method is compared. Rather big differences can be seen especially at frequencies where the linearity coefficient indicates non-linearities.

The source data obtained from the simulations using the conventional two-load method with 10 loads included in calculations were finally compared to the source strength and source impedance based on the measurements performed by Bodén [4], [13], see Fig. 18. Fig. 18 shows the imaginary part of the source impedance and it can be seen that

there is a similarity in frequency dependence except for the first harmonic where the simulation, obtained using two-load technique gives a result not consistent with the Helmholtz resonator like result expected for low frequencies. However the source impedance extracted from the simulated data using the new multi-load technique gives considerably better agreement with the measured results. The latter could indicate that the unexpected behavior of the model at the first harmonic is caused by the system non-linearities. The agreement between simulated and measured real part of impedance and source strength are also far from perfect. It can also be noted that the measurements give unphysical negative resistance values at the same frequencies where the imaginary part gives an unexpected result. This could be caused by non-linear or time-variation effects not fully accounted for in the simulation model.

6. RESULTS FROM EXPERIMENTAL TESTS ON VALVE-LESS ONE-CYLINDER COLD ENGINE

An example of sound pressure prediction in a load duct obtained from the source data from the 1-cylinder compressor measurements [4], [13] is presented in Fig. 19. The agreement between predicted and measured sound pressure levels was reasonable for both the two-load method and the non-linear multi-load method for most of the tested crankshaft rotation speeds and system configurations. From the Figs. 20 and 21, where the real and imaginary part of the source impedance is calculated using the constant pressure source model and the volume velocity based source model, it can be noticed that except at 1 or 2 harmonics the source exhibited a relatively linear behavior. The linearity coefficient of the cold engine is presented in Fig. 22. It should be highlighted that at most of the harmonics where the source behaved linearly the difference between the results obtained from modified multi-load method calculation and the two-load method calculation was marginal. The advantage of the new method can be seen at the harmonics where the non-linearities of the system occurred.

7. RESULTS FROM EXPERIMENTAL TESTS ON IC-ENGINES

An example of source data extraction results for a truck diesel engine is presented in Fig. 23. The agreement between predicted and measured sound pressure levels was good for both the two-load method and the non-linear multi-load method for most of the tested engine loads and speeds. This engine exhibited a relatively linear behavior. The linear behavior of the engine can also be seen from the Figs. 24 and 25, where the real and imaginary part of the source impedance calculated using the constant pressure source model are compared to the source data obtained using the volume velocity based source model. The linearity coefficient of the engine is presented in Fig. 26.

8. CONCLUSIONS

A new non-linear source model and a multi-load technique for extracting the source data has been proposed. The new method has been tested using numerical simulations for a cold one-cylinder valve-less engine. A study was made on a number of geometrical configurations that were non-linear and time-varying. This information was used to try to correlate the outcome of the new method with the non-linearity and time variance.

A general tendency for better source characterization results was noticed when the linearity coefficients indicated more linear system behavior.

The non-linear multi-load technique gave better results for more non-linear sources, compared to the conventional two-load technique.

Both the source data extraction techniques gave better source characterization results when the system was more time-invariant. The non-linear multi-load method gave better results when the source was more time-varying, even though the model used is time-invariant.

The method has also been tested on experimental data from a 1-cylinder valve-less compressor and from 6-cylinder turbocharged truck diesel engine. According to the source characterization results a noticeable advantage over the two-load technique was exhibited by the new non-linear multi-load method.

The new non-linear indirect source characterization technique proposed requires one additional acoustic load compared to the two-load technique. Since over-determination is anyway used in many cases the additional data would often be available. It has been shown that the new technique gives improved results compared to the two-load technique if the source is non-linear or time-varying. For cases when the source is linear and time-invariant the new technique gives the same result as the two-load technique. This means that there is not a risk for increased errors when the source is linear and time-invariant which can happen if a linear time-varying source model is used [4]. It can therefore be recommended that the new technique proposed is used whenever sufficient data is available.

REFERENCES

1. H. Bodén ,M. Åbom, Modelling of Fluid Machines as sources of sound in duct and pipe systems. *Acta Acoustica* **3** (1995) 549-560.

2. H. Bodén, Characterization of fluid-borne sound sources and structure-borne sound sources, *Proceedings of the 9th International Congress on Sound and Vibration*, 2002.

3. M. L. Munjal, Analysis and design of mufflers –an overview of research at the Indian Institute of Science. *Journal of Sound and Vibration* **211** (1998) 425-433.

4. H. Bodén, The multiple load method for measuring the source characteristics of time-variant sources. *Journal of Sound and Vibration* **148** (1991) 437-453.

5. S-H. Jang, J.G. Ih, A measurement method for the nonlinear time-variant source characteristics of intake and exhaust systems in fluid machines, *Proceedings of the 10th International Congress on Sound and Vibration*, 2003.

6. F. Albertson, J. Gilbert, Harmonic Balance Method used for calculating the steady state oscillations of a simple one-cylinder cold engine. *Journal of Sound and Vibration* **241 (**2001) 541 – 565.

7. J. Lavrentjev, H. Bodén, M. Åbom, A linearity test for acoustic one-port sources. *Journal of Sound and Vibration* **155 (**1992) 534-539.

8. H Bodén, F Albertson, Linearity tests for in-duct acoustic one-port sources. Journal of Sound and Vibration **237** (2000) 45-65.

9. J. S. Bendat, Nonlinear System Analysis and Identification, John Wiley & Sons Inc., 1990.

10. D. F. Ross, M. J. Crocker, Measurement of the acoustic internal impedance of an internal combustion engine. *Journal of the Acoustical Society of America* **74** (1983) 18-27.

11. D. P. Egolf, R. G. Leonard, Experimental scheme for analyzing the dynamic behavior of electro-acoustic transducers. *Journal of the Acoustical Society of America* **62** (1977) 1013-1023.

12. H. Bodén, Error analysis for the two-load method. *Journal of Sound and Vibration* **126** (1988) 173-177.

13. H. Bodén, The Multiple Load Method for Measuring the Source Characteristics of Time Variant Sources. Report Trita-Tak-8802, Royal Institute of Technology, Stockholm, 1988.

FIGURES

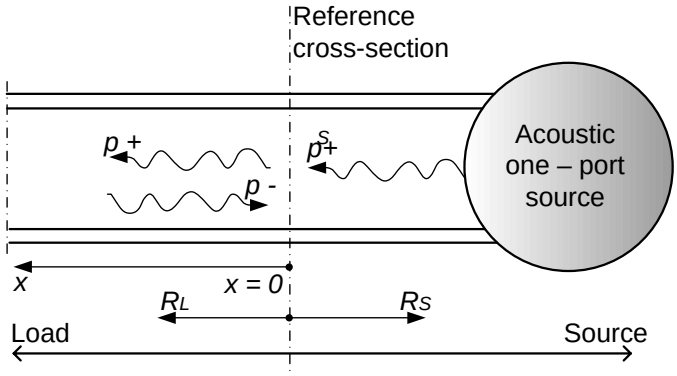

Figure 1. An in-duct source modeled as an acoustic 1-port

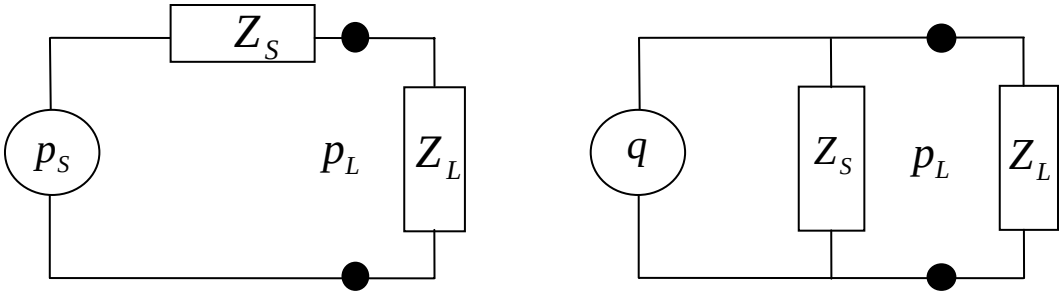

a) Pressure source

b) Volume velocity source

Fig. 2. Equivalent acoustic circuits for linear time invariant source

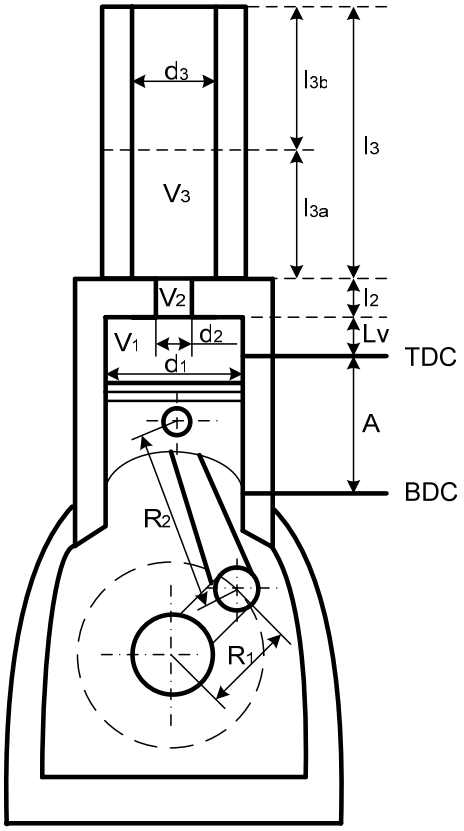

Fig. 3. Piston-constriction system studied

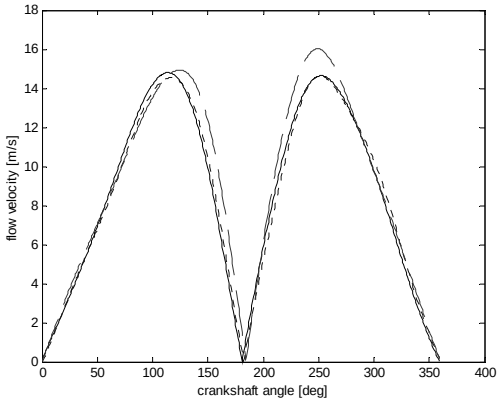

Fig. 4. Flow velocity in the constriction for three geometric configurations:
A=0.160m, d_2=0.030m, d_1 =0.070m (full-line);
A=0.080m, d_2=0.021m, d_1=0.070m (dotted line);
A =0.080m, d_2=0.030m, d_1=0.099m (dashed line)

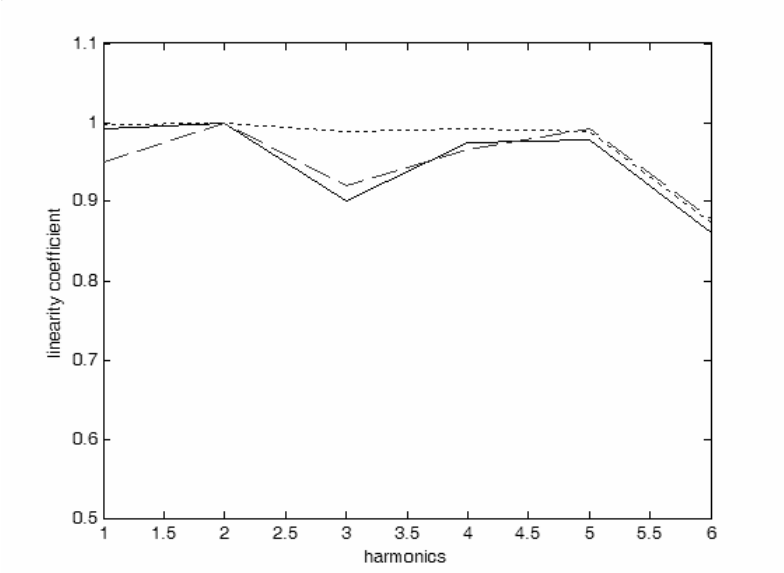

Fig. 5. Linearity coefficient γ;
Variation of piston amplitude A=0.16m (full-line),
variation of diameter of constriction d_2=0.0212m (dotted line),
variation of piston diameter d_1=0.09899m (dashed line);

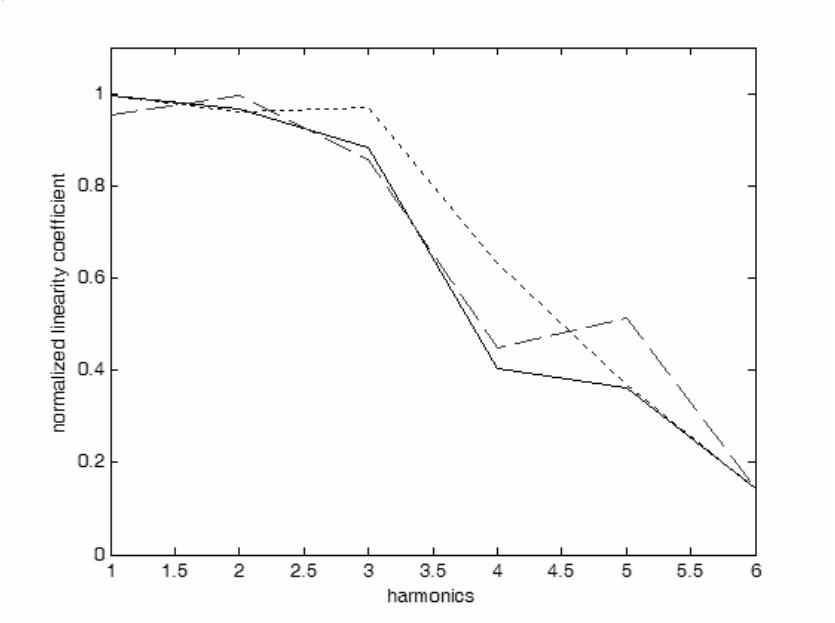

Fig. 6. Normalized lin. coefficient. γ_n ;
Variation of piston amplitude A=0.16m (full-line),
variation of diameter of constriction
d_2=0.0212m (dotted line),
variation of piston diameter
d_1=0.09899m (dashed line);

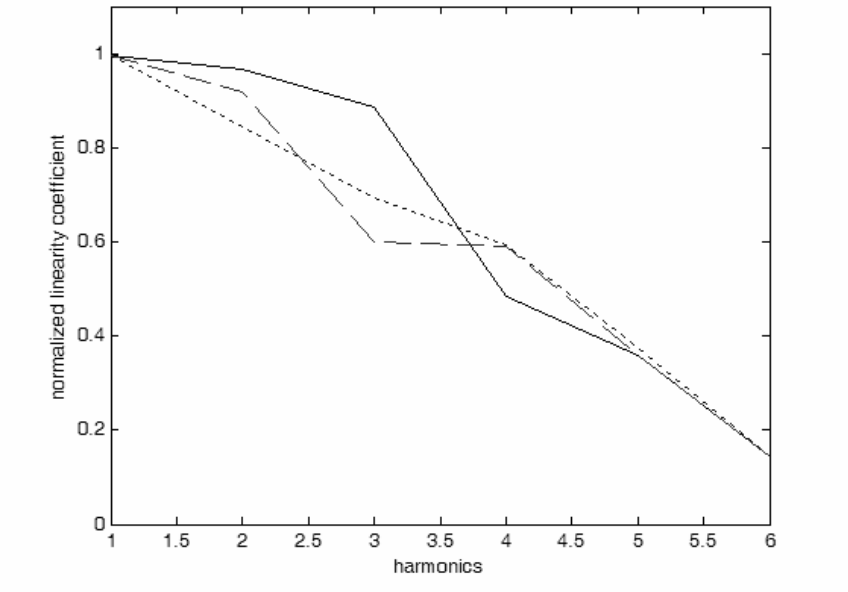

Fig. 7. Normalized linearity coefficient γ_n ;
L_V =0.36m (full-line), L_V =0.18m (dotted line),
L_V =0.12m (dashed line)

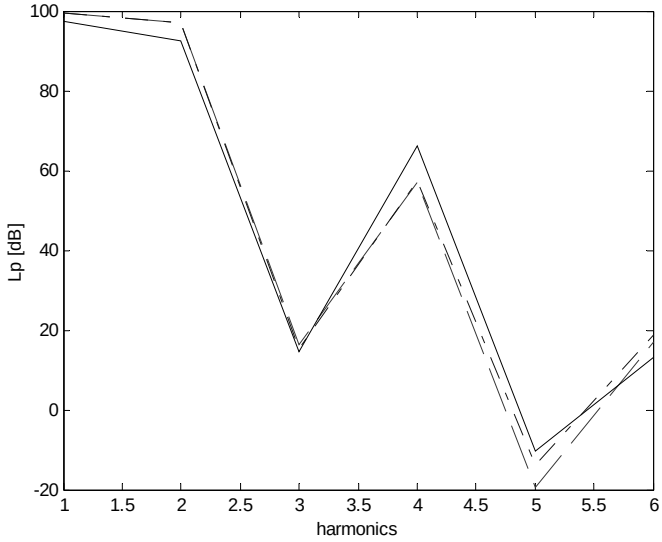

Fig. 8. The sound pressure in a load duct with length 1.3m;
Two-load technique (dashed line),
Non-linear multi-load technique (dash-dotted line),
Direct simulation (full-line); A=0.0008m

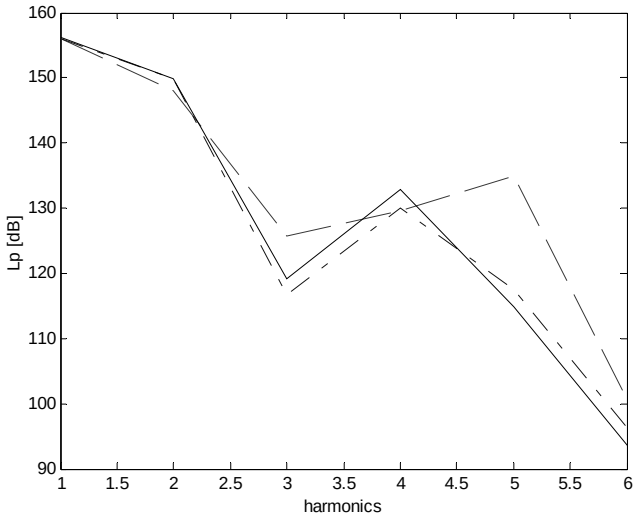

Fig. 9. The sound pressure in a load duct with length 0.5m for a source configuration with high compression ratio, L_V =0.12m;
Two-load technique (dashed line),
Non-linear multi-load technique (dash-dotted line),
Direct simulation (full-line)

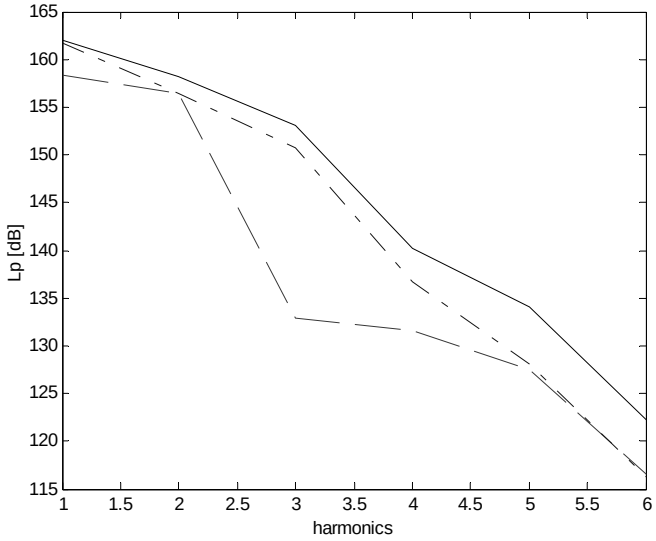

Fig. 10. The sound pressure in a load duct with length 0.3m for d_1 =0.0989m;
Two-load technique (dashed line),
Non-linear multi-load technique (dash-dotted line),
Direct simulation (full-line)

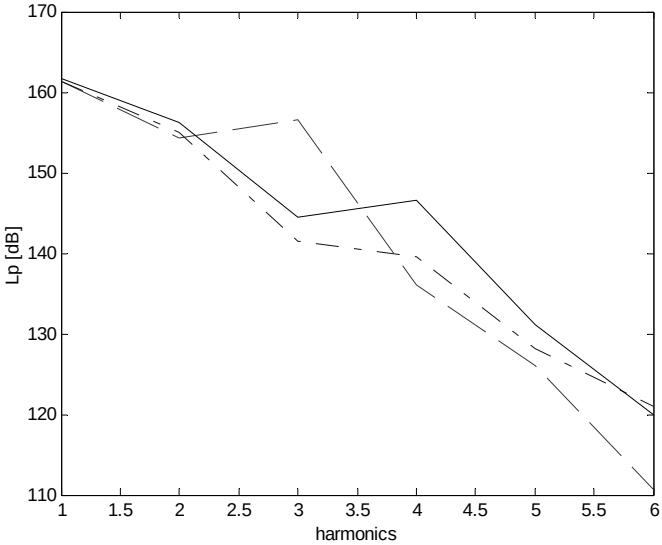

Fig. 11. The sound pressure in a load duct with length 0.3m for A=0.16m;
Two-load technique (dashed line),
Non-linear multi-load technique (dash-dotted line),
Direct simulation (full-line)

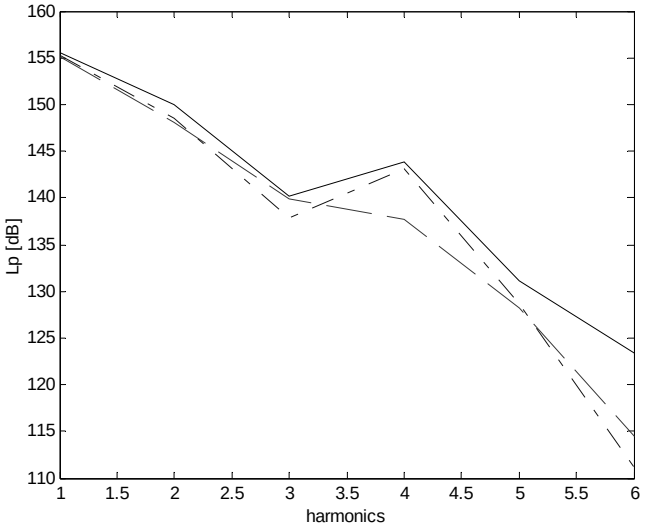

Fig. 12. The sound pressure in a load duct with length 0.3m for d_1=0.0212m; Two-load technique (dashed line), Non-linear multi-load technique (dash-dotted line), Direct simulation (full-line)

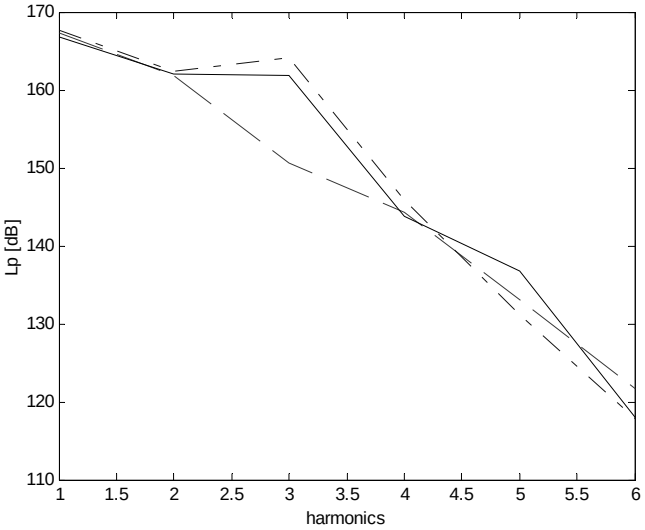

Fig. 13. The sound pressure in a load duct with length 0.7m for A=0.24m; Two-load technique (dashed line), Non-linear multi-load technique (dash-dotted line), Direct simulation (full-line)

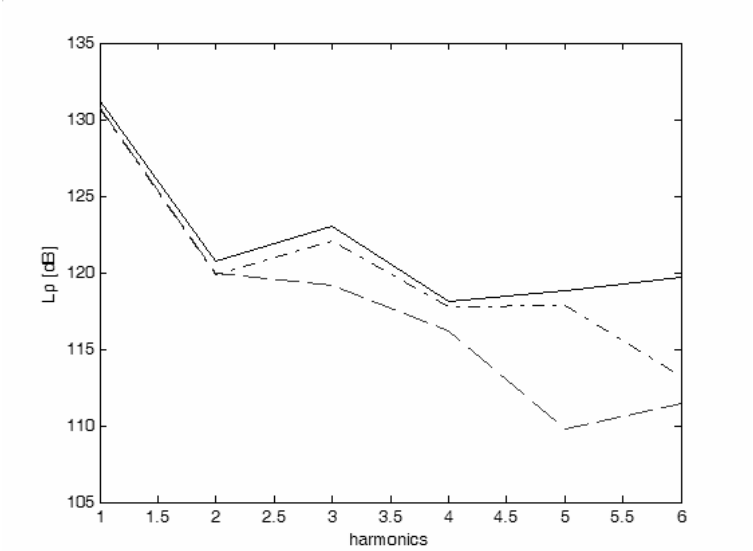

Fig. 14. The sound pressure in a load duct with length 0.3m;
Highly non-linear model configuration:
d_2 =0.002m, L_V =0.1m, A=2.0;
Two-load technique (dashed line),
Non-linear multi-load technique (dash-dotted line),
Direct simulation (full-line)

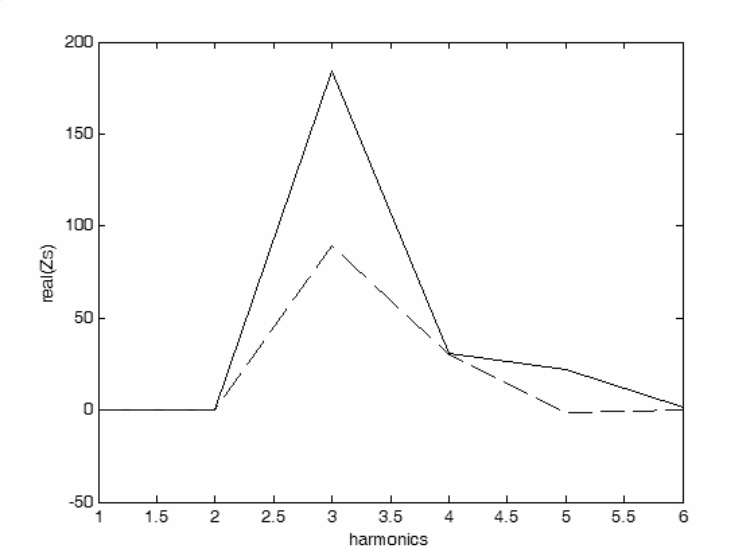

Fig. 15. The real part of the source impedance;
Highly non-linear model configuration:
d_2=0.002m, L_V =0.1m, A=2.0m;
Constant pressure source model (full-line),
Constant volume velocity source model (dashed line);

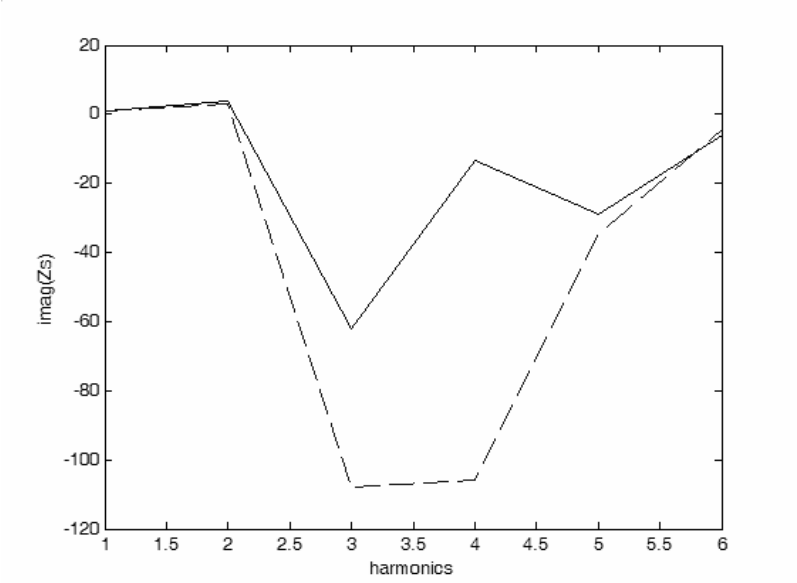

Fig. 16. The imaginary part of the measured source impedance;
Highly non-linear model configuration:
d_2=0.002m, L_V =0.1m, A=2.0m;
Constant pressure source model (full-line),
Constant volume velocity source model (dashed line);

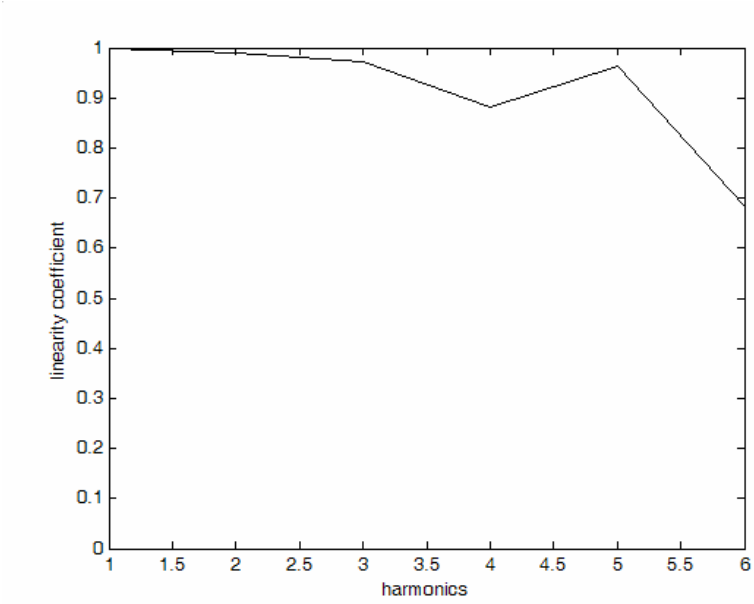

Fig. 17. Linearity coefficient γ;
Highly non-linear model configuration:
d_2=0.002m, L_V =0.1m, A=2.0m;

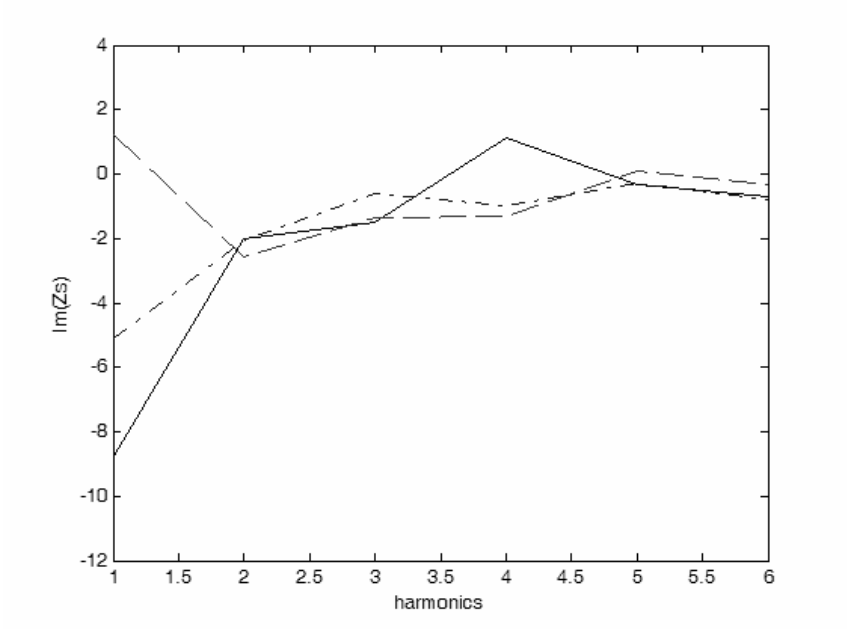

Fig. 18. The imaginary part of the source impedance;
Measurements (full-line), simulations using two-load technique (dashed line),
simulations using non-linear multi-load technique (dash-dotted line);

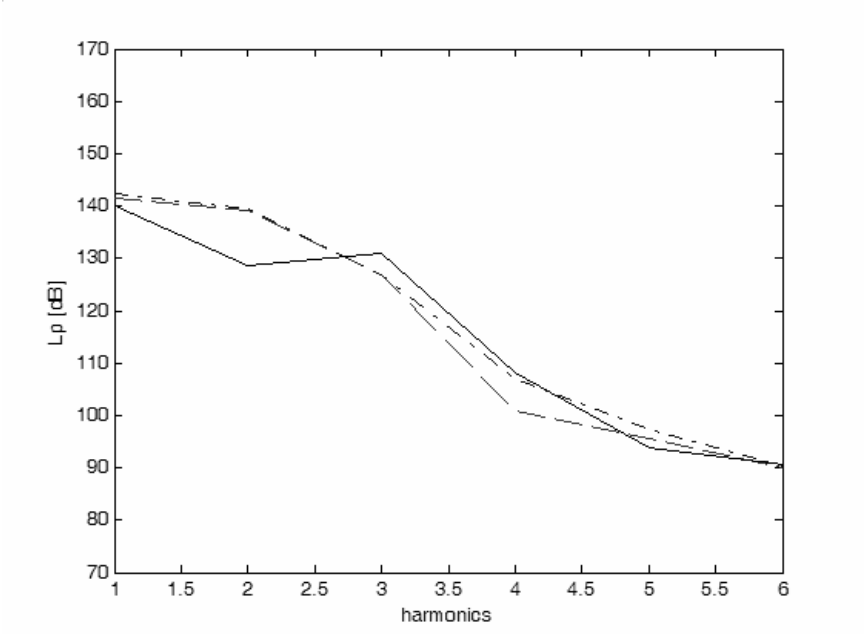

Fig. 19. Pressure in a load duct with length 1.5m;
Measurements – full-line,
Two-load method – dashed line,
Non-Linear method – dash-dotted line;

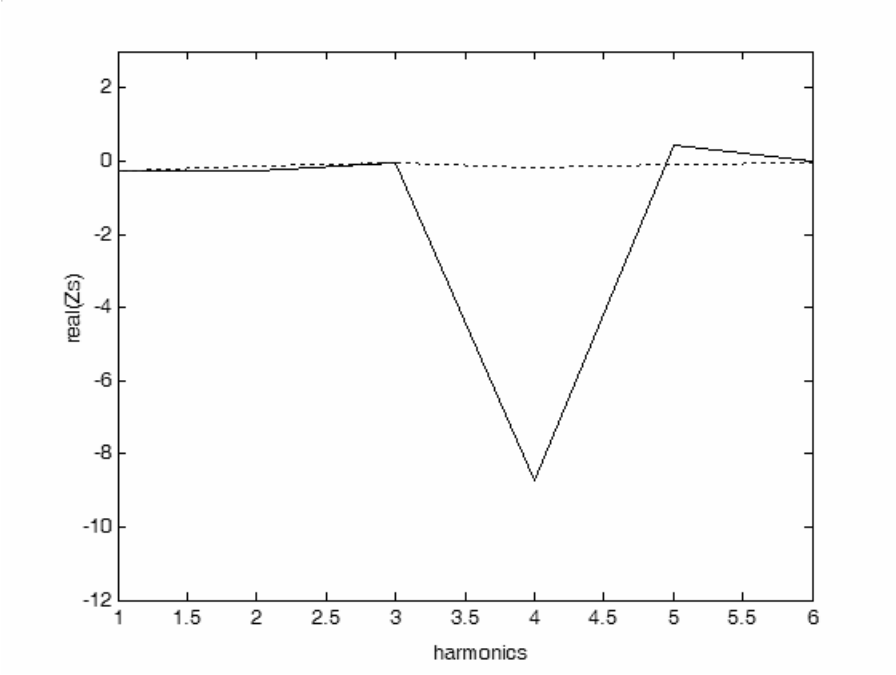

Fig. 20. The real part of the measured source impedance;
Constant pressure source model (full-line),
Constant volume velocity source model (dotted line);

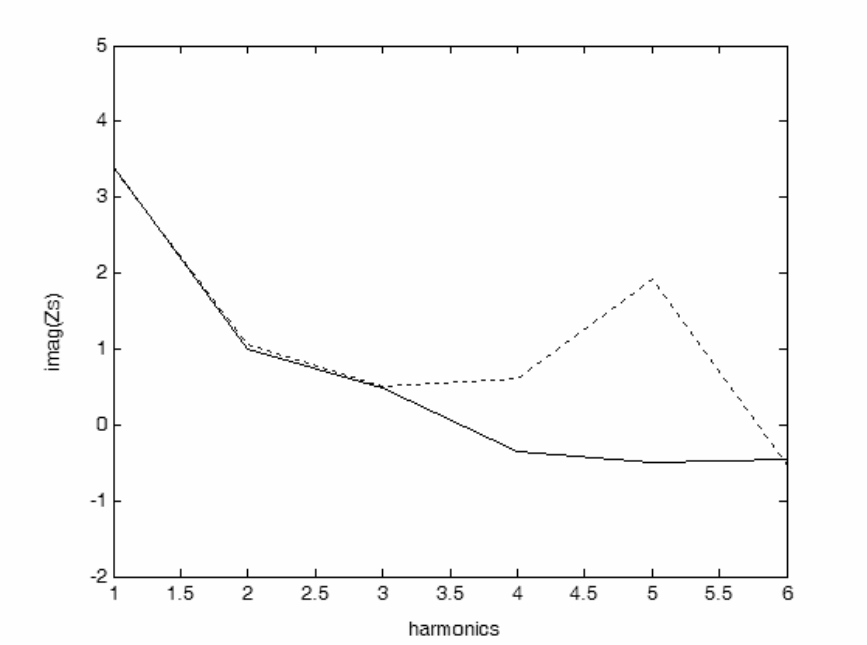

Fig. 21. The imaginary part of the measured source impedance;
Constant pressure source model (full-line),
Constant volume velocity source model (dotted line);

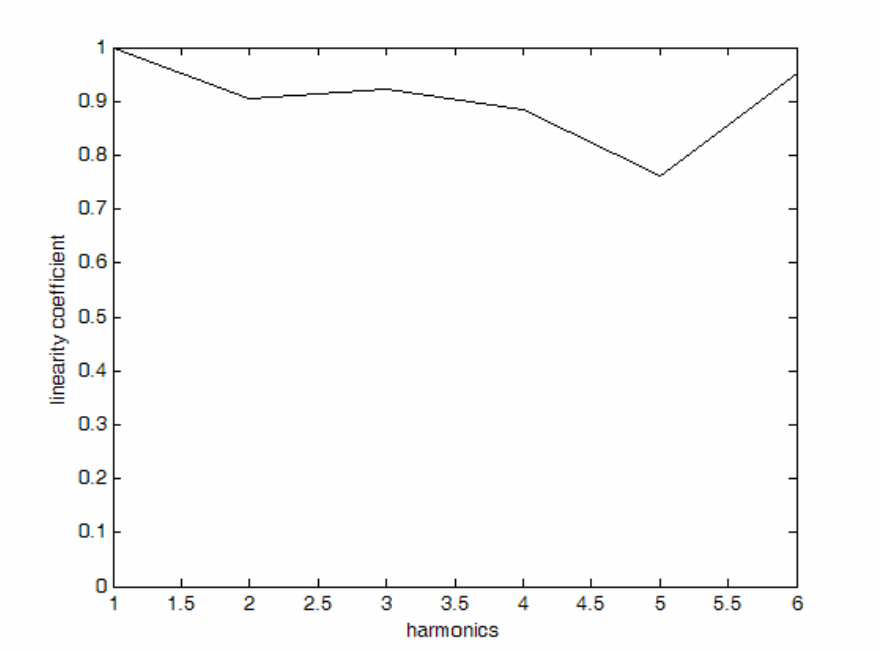

Fig. 22. Linearity coefficient γ; 1-cylinder valve-less cold engine;

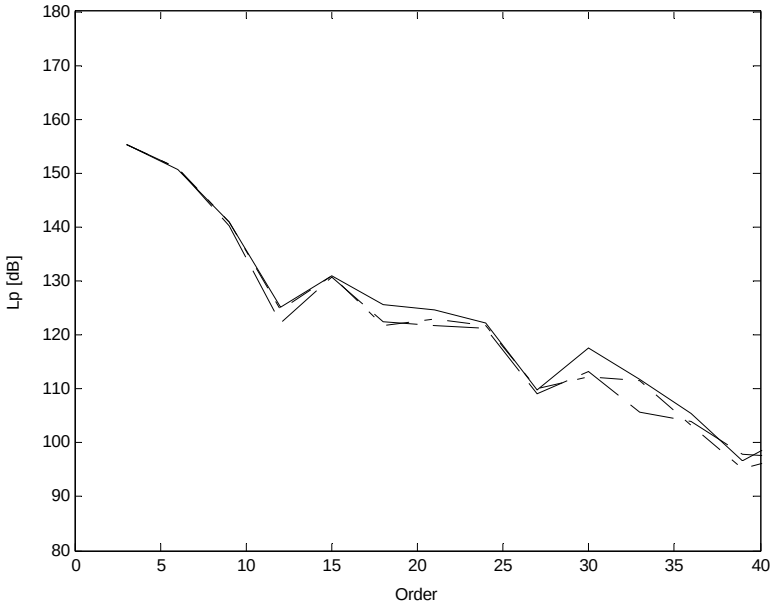

Fig. 23. The sound pressure in the exhaust system
for 50 % engine load and 1600 rpm;
Two-load technique (dashed line),
Non-linear multi-load technique (dash-dotted line),
Direct measurements (full-line)

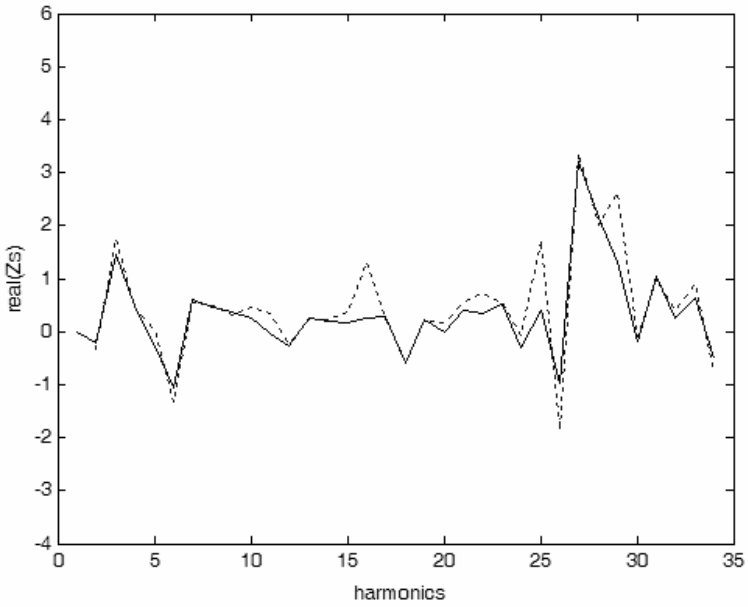

Fig. 24. The real part of the source impedance;
50 % engine load and 1600 rpm;
Constant pressure source (full line),
Constant volume velocity source (dotted-line)

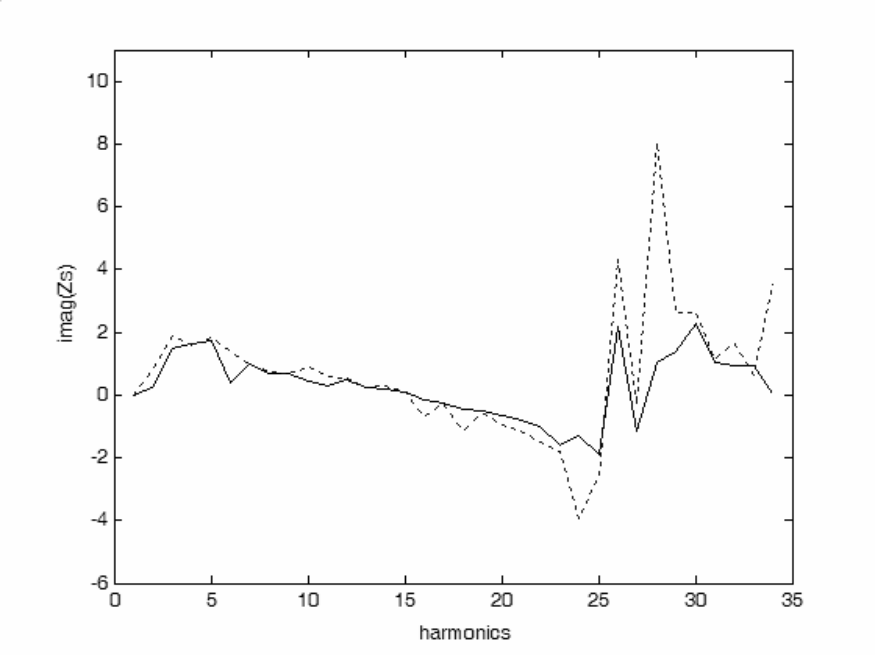

Fig. 25. The imaginary part of the source impedance;
50 % engine load and 1600 rpm;
Constant pressure source (full line),
Constant volume velocity source (dotted-line)

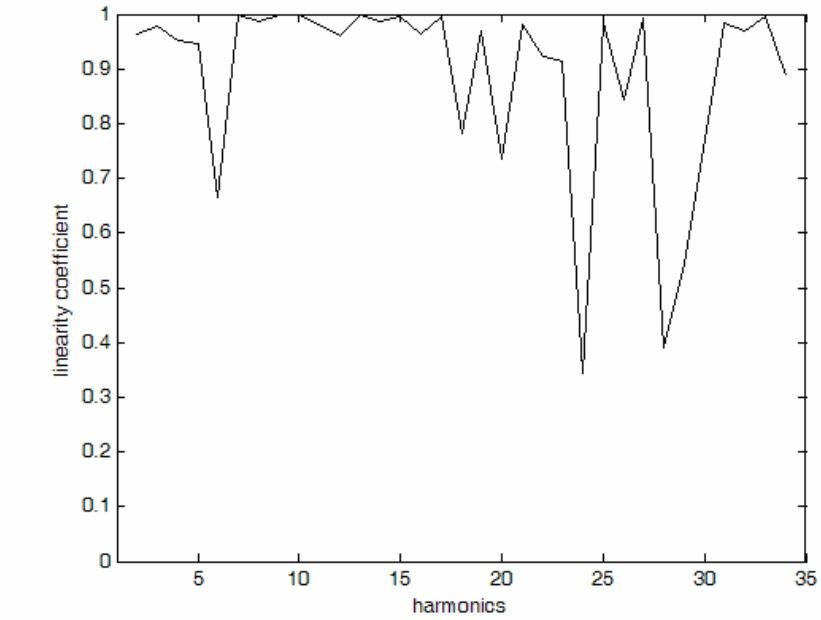

Fig. 26. Linearity coefficient γ;
6-cylinder turbocharged truck diesel engine;
50 % engine load and 1600 rpm;

TABLES

Load no.	1	2	3	4	5	6	7	8	9	10
A=0,0008m	E	TL	TL	TL	TL	E	E	E	NL	E
A=0,0400m	E	E	E	NL	TL	E	E	TL	NL	E
A=0,0800m	NL	NL	NL	NL	TL	TL	E	TL	E	E
A=0,1200m	NL	NL	NL	NL	TL	TL	E	TL	TL	NL
A=0,1600m	NL	NL	NL	NL	NL	TL	E	TL	E	E
A=0,2400m	TL	TL	NL	NL	TL	TL	E	NL	E	TL
d1=0,09899m	NL	NL	TL	NL	TL	NL	NL	NL	TL	NL
d1=0,12124m	NL	NL	TL	E	TL	TL	E	NL	NL	NL
d1=0,14000m	NL	TL	E	TL	TL	E	E	E	TL	NL
d1=0,21000m	NL	NL	TL	TL	TL	E	NL	NL	E	NL
d2=0,0212m	NL	E	NL	TL	TL	NL	E	NL	TL	NL
d2=0,0173m	NL	E	E	TL	TL	NL	NL	NL	NL	E
d2=0,0150m	NL	E	E	TL	TL	E	E	NL	NL	E
d2=0,0100m	NL	NL	TL	TL	TL	NL	NL	NL	NL	E
Lv=0,18m	E	NL	NL	TL	NL	NL	E	E	E	E
Lv=0,12m	NL	NL	NL	NL	NL	NL	NL	NL	E	NL

Table 1. The comparison of the two-load technique (TL)
and the non-linear multi-load technique (NL);
The indicated method gave better prediction results

Method	TL	NL	TL	NL	TL	NL	TL	NL	TL	NL	TL	NL	TL	NL	TL	NL	TL	NL	TL	NL	Average		Total
Load no.	**1**	**1**	**2**	**2**	**3**	**3**	**4**	**4**	**5**	**5**	**6**	**6**	**7**	**7**	**8**	**8**	**9**	**9**	**10**	**10**	TL	NL	Avg.
A=0,0008m	3	3	5	4	5	4	5	3	5	3	5	5	3	3	3	3	4	4	1	1	3,9	3,3	3,6
A=0,0400m	3	3	5	5	5	5	3	4	5	4	4	4	2	2	3	2	3	3	1	1	3,4	3,3	3,4
A=0,0800m	2	3	4	5	3	4	2	5	4	4	4	4	2	2	3	3	3	3	1	1	2,8	3,4	3,1
A=0,1200m	3	4	4	5	4	4	3	5	4	3	4	4	2	2	3	3	3	2	1	2	3,1	3,4	3,3
A=0,1600m	2	4	5	5	4	4	2	3	3	3	4	3	2	2	4	3	3	3	1	1	3,0	3,1	3,1
A=0,2400m	3	3	5	3	4	5	2	3	3	3	3	3	2	2	3	3	4	4	1	1	3,0	3,0	3,0
d1=0,09899m	3	4	4	5	4	4	4	4	4	4	3	3	3	3	3	3	3	3	2	2	3,3	3,5	3,4
d1=0,12124m	3	5	5	5	5	4	5	5	5	3	3	3	4	4	3	4	4	4	2	3	3,9	4,0	4,0
d1=0,14000m	3	5	5	4	4	4	5	3	3	2	3	3	4	4	3	3	4	3	2	2	3,6	3,3	3,5
d1=0,21000m	4	4	5	4	5	3	5	3	4	3	3	3	3	4	2	4	2	2	3	4	3,6	3,4	3,5
d2=0,0212m	4	5	5	5	4	5	5	4	5	5	4	4	4	4	3	3	3	3	2	2	3,9	4,0	4,0
d2=0,0173m	4	5	5	5	5	5	5	5	4	4	3	4	4	4	2	3	3	3	2	2	3,7	4,0	3,9
d2=0,0150m	4	4	5	5	5	4	5	5	5	4	3	3	3	3	2	3	3	3	2	2	3,7	3,6	3,7
d2=0,0100m	4	5	5	5	5	4	5	5	4	4	2	3	3	3	2	2	3	3	1	1	3,4	3,5	3,5
Lv=0,18m	3	3	4	5	3	5	5	3	4	4	2	3	3	3	2	2	3	4	2	2	3,1	3,4	3,3
Lv=0,12m	2	3	3	5	3	3	3	3	3	3	1	1	2	4	2	3	3	3	1	1	2,3	2,9	2,6
Average	3,1	3,9	4,6	4,7	4,3	4,2	4,0	3,9	4,1	3,5	3,2	3,3	2,9	3,1	2,7	2,9	3,2	3,1	1,6	1,8			
Total Avg.	3,5		4,7		4,2		4,0		3,8		3,3		3,0		2,8		3,2		1,7				

Table 2. The comparison of the two-load technique (TL)
and the non-linear multi-load technique (NL);
The numbers denote the quality classes of the prediction results

“5” - difference typically less then than 3 dB for at least 5 harmonics
“4” - difference typically less than 3-6 dB for at least 5 harmonics
“3” - difference typically less than 6-10 dB for at least 5 harmonics
“2” - difference typically less than 10-15 dB for at least 5 harmonics
“1” - difference typically more than 15 dB

Table 3. The classification of the prediction results

Paper C

A METHOD FOR EXPERIMENTAL DETERMINATION OF IN-DUCT ACOUSTIC SOURCE PASSIVE PROPERTIES IN SIMULATED HOT CONDITIONS

H. Rämmal and J. Lavrentjev

Abstract Acoustic properties of in-duct noise sources under high temperature conditions (for instance in IC engine exhausts) are best determined under real working conditions. However, the hot pulsating exhaust gas flow causes experimental problems: need for transducer cooling, pipe vibration etc. Therefore from a practical point of view in many cases experiments are made in cold conditions (room temperature). Due to the difference in speed of sound in the environments this can lead to incorrect measurement results.

In this paper a new measurement method to characterize in-duct noise systems is suggested and preliminary tests are made. In order to simulate the acoustical conditions of the hot gases, a helium-air mixture is used as the testing environment. Since the speed of sound in helium is close to that in the hot exhaust gases, the cold exhaust system filled with helium simulates the hot system.

As a test of the method experiments to determine the reflection coefficient of the exhaust port of an automotive IC-engine were performed in the first part of the paper. The measured reflection coefficients at the IC engine exhaust port were compared with the experimental data determined in air at ambient temperature.

For a number of practical applications knowledge about the radiation impedance, or alternatively the reflection coefficient, of duct opening exhausting hot gases is essential for effective design of a duct system. Despite several experimental and theoretical investigations in the field, there is still little experimental data available to validate the existing theory. This could be a possible application of the measurement technique if it can be validated.

In the second part of the paper the reflection coefficient of an unflanged circular duct termination has been experimentally determined in simulated hot conditions. To investigate the flow profile of the gases close to the duct termination flow visualization experiments were performed and the

results studied. The measured reflection coefficients of the duct opening were compared with simulation results obtained from the well-known theory according to Munt.

1. INTRODUCTION

Effective acoustic design of any system, for instance IC engine exhaust systems assumes knowledge of the acoustical behavior of the system elements as well as that of the acoustic source (i.e. the engine). The intention of this paper is to introduce a new experimental characterization method for in-duct acoustic experiments simulating hot exhaust system conditions. The idea of the presented method is to use helium as a test medium in a duct system in order to achieve an acoustic wavelength similar to that encountered in high temperature gas.

For silencer systems the acoustical source impedance (or alternatively the reflection coefficient) of the engine is essential for the evaluation of insertion loss and radiated sound pressure level. Acoustic engine data are most often determined experimentally. However, experimental determination of the acoustic data of IC engine can be a difficult task, because of high noise levels, high temperature, turbulence effects, vibrating structures and a corrosive atmosphere.

In the first part of the paper the implementation of the method will be tested on the exhaust system of an IC engine. The method can as well potentially be applicable for evaluation of the exhaust system elements, i.e. silencers, after treatment devices and duct terminations. These exhaust system components are usually tested at room temperature which can lead to incorrect interpretation of the results in terms of considerably shorter wavelength in the testing media compared to the actual conditions they are designed for. The noise radiation from a duct exhausting a hot gas to the atmosphere is a common problem in exhaust system design for IC-engines, burners and aeronautical application of jet engines. For predicting the sound pressure level in the far-field of the exhaust system and assessment the performance of the system components a knowledge of the acoustic reflection coefficient at the duct opening is essential. It is also well known that the exhaust gas temperature represents an important factor in realistic acoustic modeling since it has a significant influence on the acoustic wavelength.

In the second part of the paper the method is applied on an unflanged circular duct termination in order to experimentally determine the reflection coefficient in simulated hot conditions. The purpose of the investigation is to obtain experimental data for the reflection coefficient R for high temperature exhaust gas conditions and to test the new experimental technique on duct openings. The theory by Munt [1] can be used for prediction of the reflection coefficient in the presence of hot mean flow, including the full Kutta condition. In this investigation the reflection coefficient measured in acoustical conditions simulating the hot gases with high temperature is compared to the numerical results obtained from Munt´s theory.

2. ACOUSTIC 1-PORT SOURCE CHARACTERIZATION

It has been found in a number of studies (see e. g. [2]) that the IC engine can with reasonable accuracy be treated as an acoustic one-port source [2]. Further references on this subject are discussed in the introduction to this thesis.

In the frequency domain an acoustic one-port (see Fig. 1) can be completely described by the equation:

$$p_+ = R_S p_- + p_+^S, \tag{1}$$

where p_-, p_+ are traveling acoustic pressure amplitudes, R_S is the source reflection coefficient at cross-section and p_+^S is the source strength. The source reflection coefficient and the source strength p_+^S together are called acoustic source data, which describe the acoustic behavior of the source completely.

Generally the experimental methods for experimental determination of the one-port source data can be divided into direct (with external source) and indirect or multi-load methods (without an external source) [2]. The direct methods require a two-step procedure. First the reflection coefficient (passive source data) is determined by exciting the source from an external source. In the second step the external source is turned off and the source strength is determined by making a measurement when a known load is applied to the source [3-5]. When using the indirect methods the two unknowns, the source strength and the source impedance are determined via a multi-load procedure [6], i.e., by applying known loads and measuring the acoustic pressure at the source receiver interface. Based on a comparison between the results, obtained when applying the direct and the indirect measurement methods in [6], it was concluded that the direct methods generally give better results and are therefore preferred, if it is possible to use them. In the application studied in this paper a direct method was therefore used.

3. EXPERIMENTS

The gas temperature in the exhaust manifold of a 4-stroke engine can in case of high load and crankshaft speed conditions reach values around t=1000 °C. Consequently the value of the speed of sound will be around c=950 m/s. The equivalent acoustic condition can be simulated using an air-helium mixture with close to 100% of helium inside a duct system. By varying the ratio of air to

helium it is possible to simulate the desired temperature conditions for exhaust system components for all operating points. As Helium is odorless, non-toxic and noninflammable gas, it is safe to use it in test environment. Furthermore, pressurized technical helium is available at a relatively low cost.

3.1 Experiments on the IC-engine exhaust port

First experiments to demonstrate the new method were performed on a 5-cylinder 4-stroke passenger car diesel engine. The measurement system was mounted on the exhaust system of the IC-engine, see Figs. 2 and 3. The geometry of the engine exhaust port is shown in Fig. 4. In the current study on testing and developing of the technique, the measurements were carried out on a stationary engine. Different crankshaft positions of the engine were chosen to determine the passive source data of the exhaust port. For further studies on the subject it is possible to modify the test-rig so that the crankshaft is reciprocated by a variable speed electric motor, giving the additional time variance as encountered in operating IC-engines.

Two different transducer separations (*Pt.1* - *Pt.2*) were chosen: for helium $s_H = 0.35\,\mathrm{m}$ and $s_A = 0.13\,\mathrm{m}$ for air, covering a frequency range from 120 to 1000 Hz for both media [7].

The test duct was a standard PVC duct with circular cross-section area and inner diameter d=0.05 m. The test duct was connected to one of the exhaust ports of the engine cylinder head (see Fig. 3). The other end of the duct was filled with sound absorbing material to reduce the reflections. A bottle with pressurized helium was connected to the duct system via pressure control system and a flexible pipe.

For the in-duct acoustic pressure measurements two piezoelectric pressure transducers (Kistler 4045A) with signal conditioners were used in three different microphone positions in the test pipe. As an external noise source, a loudspeaker, positioned in a side-branch of the duct system, was used. The loudspeaker was driven by software-based tone generator (NCH) through a power amplifier. The signal acquisition was performed by a PC based four-channel Dynamic Signal Analyzer (National Instruments NI PCI-4552). Sufficient data was taken to perform 100 frequency domain averages.

The source reflection coefficient was determined at transducer *Pt.1* and then transferred to the exhaust port of the cylinder head.

3.2 Experiments on open duct termination

Experiments were performed on a duct termination using a standard steel automotive exhaust pipe with 2 m length and circular cross-section area. The inner diameter of the duct was d=47.0 mm and the wall thickness was Δ=1.8 mm. The experimental set-up used for the measurements is presented in Figs. 5 and 6. During the experiments the unflanged test duct termination was positioned vertically and directed upwards in order to achieve uniform helium out-flow to the surrounding air maintained at 20 °C temperature. The other end of the test-duct was filled with sound absorbing material to reduce the reflections.

Two different transducer separations were chosen: $s_{H1} = 0.13$ m, $s_{H2} = 0.34$ m for helium, and $s_{A1} = 0.05$ m, $s_{A2} = 0.13$ m for air, covering a frequency region from 130 to 2700 Hz for both media [7]. The first cut-on frequency of the duct with a diameter D=0.047m was around 12.6 kHz when filled with helium (c=*970 m/s*) and around 4.4 kHz when filled with air (c=*340 m/s*). In order to reduce the random error in the measurements 100 averages were made.

The flow velocity in the duct was too low (U<0.3 m/s, M<0.001) to significantly influence the reflection coefficient during the experiments with helium.

For the in-duct acoustic pressure measurements two ½" condenser microphones (IAAS MK224) with four-channel amplifier (MWL UNO-06) were used in three different microphone positions (*P1, P2, P3*) in the test pipe. The acoustic excitation was provided by a loudspeaker enclosed in a cylindrical box and mounted to a side-branch of the duct system. To avoid transfer of mechanical vibrations from the loudspeaker to the test section of the pipe a circular rubber damper was used in the side-branch and test duct connection flange. The signal generator, power amplifier and signal acquisition was the same used for the engine source data measurements described in section 3.1.

The source reflection coefficient was first determined at the microphone position *P1* cross-section and thereafter transferred to the duct termination cross-section.

In order to investigate the flow profile close to the duct termination and to compare the results obtained with Helium to the results of air exhausting from test-duct, a flow visualization experiment was performed. As a visualization method a smoke addition technique was found to be appropriate for this type of experiment. A photo of the experimental setup used during the flow visualization experiments is shown in Fig. 7. To visualize helium and air that are colorless gases a smoke generator was activated inside a mixing chamber, which can be seen as the white plastic reservoir under the test-duct in Fig. 7. During the experiments helium was inserted at the bottom of the mixing chamber from a pressurized storage bottle via a pressure control valve. During diffusion

with the smoke particles it continued to fill the chamber and spread into the duct section. Finally the visual helium flow was exhausting into a room-temperature air (t=20 ºC) through the studied duct termination. The same procedure was followed with air-flow which was created by an electrical fan. To improve the image quality the image plane was brightened using an intensive light-source projector, Sanyo Pro-Xtrax). The images of gas-flow were captured to APS film (Fujicolour Superia, ISO 200) using a photo camera (Nikon F80).

4. MEASUREMENT RESULTS AND DISCUSSION

4.1 Results from measurements on the IC-engine exhaust port

Measurement results from the IC-engine exhaust port tests are presented in Figs. 8-15. In Figs. 8-11 the measured reflection coefficient for the crankshaft at the top dead center (TDC) is presented for air and helium. The exhaust valve is closed at this position. In Fig. 9 the experimentally obtained phases of the reflection coefficient are compared to the analytical ones for both the testing media. A straight duct (with the length equal to that of a centerline of the real exhaust port, see Fig. 4) having a rigidly closed termination was assumed when the analytical results for the phase were determined. In Figs. 10-11 the experimental results of the reflection coefficient for helium and air are compared in Helmholz no. domain and a reasonable collapse of data was found. This is expectable in a case where the only parameter varied is the speed of sound c. As one can see, that the losses are very small measured in both environments. The phase shift in degrees (due to the distance from cylinder head opening to the valve) is larger due to shorter wavelength for air than for helium. This verifies that the measurement set-up and the technique performed as expected and the duct was completely filled with helium. Both for the air-filled duct and the helium-filled duct, reflection coefficient amplitudes larger than one are found at some frequency ranges. These results must be attributed to experimental errors since this is an unphysical result without flow.

In Figs. 12-13 the measured reflection coefficient for the crankshaft at the bottom dead center (BDC) is presented for air and helium. The exhaust valve of the cylinder is opened and the intake valve is closed at this piston position. As one can see, losses here depend on the chosen measurement environment. As expected, the phase shift for the air case is larger. The phase shift is determined by the engine stroke.

The phase shift dependence on the piston position is demonstrated in Figs. 14-15, where the determined reflection coefficients are presented for different crankshaft (and piston) positions. It is clearly seen that the reflection coefficient is determined mostly by the piston position.

4.2 Results from measurements on duct terminations

Measured reflection coefficient results presented as magnitude R and phase angle Φ are presented in Figs. 16-19.

The results of experimentally determined reflection coefficient for room temperature air (Figs. 16-17) showed a good agreement with theoretically predicted curves obtained by Munt´s theory. Similar experimental results have also been found by several other authors investigating the acoustic properties of duct terminations in cold conditions. A reasonable agreement in the low frequency region was found also between the experimental and theoretical pressure reflection coefficient of the duct termination in simulated hot flow conditions (Figs. 18-19).

The flow visualization results (Figs. 20 and 21) indicate that for the low exit flow velocity (U=0.3 m/s), used in the reflection coefficient experiments, a difference in flow profile can be observed when comparing helium and air flow. This can possibly be one of the reasons leading to the discrepancy found when comparing the high frequency region of experimental reflection coefficient results measured in helium environment to the ones obtained theoretically for hot air flow conditions. It should further be noticed that at the low flow speeds used in the experiments the Reynolds number based on the duct diameter will be around 1000. This means that the flow will be laminar while turbulent flow is assumed in the theory.

5. CONCLUSIONS

In this paper the idea of using helium as a measurement environment in the exhaust system of IC-engines to simulate high temperature conditions has been presented. The measurement procedure uses helium at normal room temperature and is potentially simpler than experiments with the actual running engine. The described technique could be implemented to study engine source data as well as exhaust system components and silencers.

Results for IC-engine source data showed reasonably consistent results. For the experiments on the open duct termination there are discrepancies between theoretical results and experimental which may have to do with the out-flow profile obtained in the helium experiments.

The amplitude of the experimentally determined reflection coefficient of the duct termination, measured in a simulated hot condition, shows a reasonably good agreement with theoretical results by Munt in a low frequency range. Flow visualization experiments have been performed and the flow profile close to the duct exit termination investigated showing a considerable difference for air and helium exhaust.

In order to prove the new simulation technique for characterization of the exhaust duct components at any temperature in the temperature range up to the limiting value for pure helium (1065 °C), a number of experiments should be performed with varied helium – air proportion in the measurement environment. Additionally, the effects of flow profile on the reflection coefficient results should be further investigated.

ACKNOWLEDGEMENTS

This work was done with financial support from the EU Commission (5FP Contract No G3RD-CT-2001-00511 ARTEMIS) and the Estonian Science Foundation (Grant 5622).

REFERENCES

1. R. M. Munt. Acoustic transmission properties of a jet pipe with subsonic jet flow: 1. The cold jet reflection coefficient, *Journal of Sound and Vibration*, **142**, pp. 413-436, 1990

2. H. Bodén and M. Åbom. Modeling of fluid machines as sources of sound in duct and pipe systems, *Acta Acustica* **3**, pp. 1-12, 1995.

3. J. Lavrentjev, M. Abom and H. Boden. A measurement method for determining the source data of acoustic two-port sources, *Journal of Sound and Vibration*, **183**, pp. 517-531, 1995.

4. D. F. Ross and M. J. Crocker. Measurement of the acoustic internal impedance of an internal combustion engine. *Journal of the Acoustical Society of America,* **74***, 18-27*, 1983

5. M. G. Prasad and M. J. Crocker. Acoustical source characterization studies on a multi-cylinder engine exhaust system, *Journal of Sound and Vibration*, **90**(4), pp. 479-490, 1983.

6. H. Bodén. On multi-load methods for determination of the source data of acoustic one-port sources, *Journal of Sound and Vibration*, **180**, pp. 725-743, 1995.

7. M. Åbom and H. Bodén. Error analysis of two-microphone measurements in ducts with flow. *Journal of Acoustical Society of America,* **83**, pp. 2429-2438, 1988

FIGURES

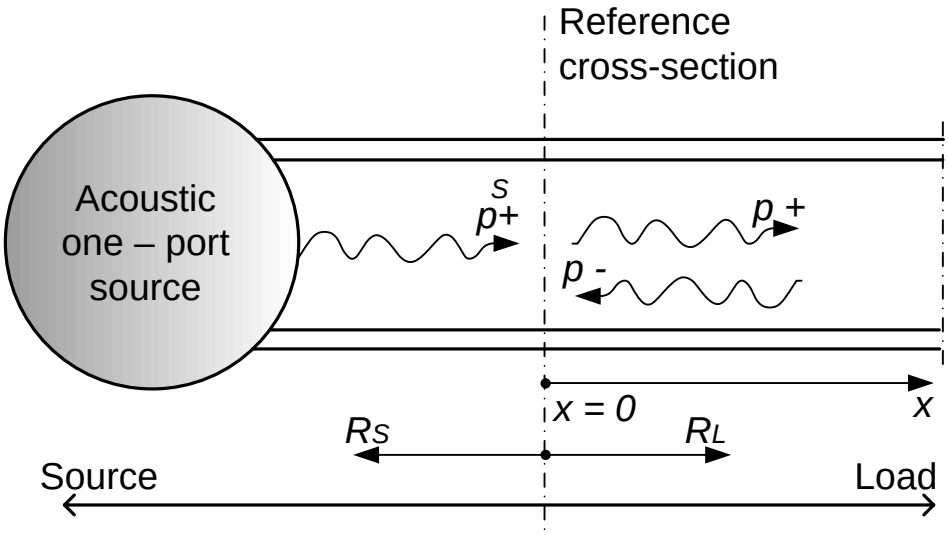

Fig. 1. An acoustic 1-port

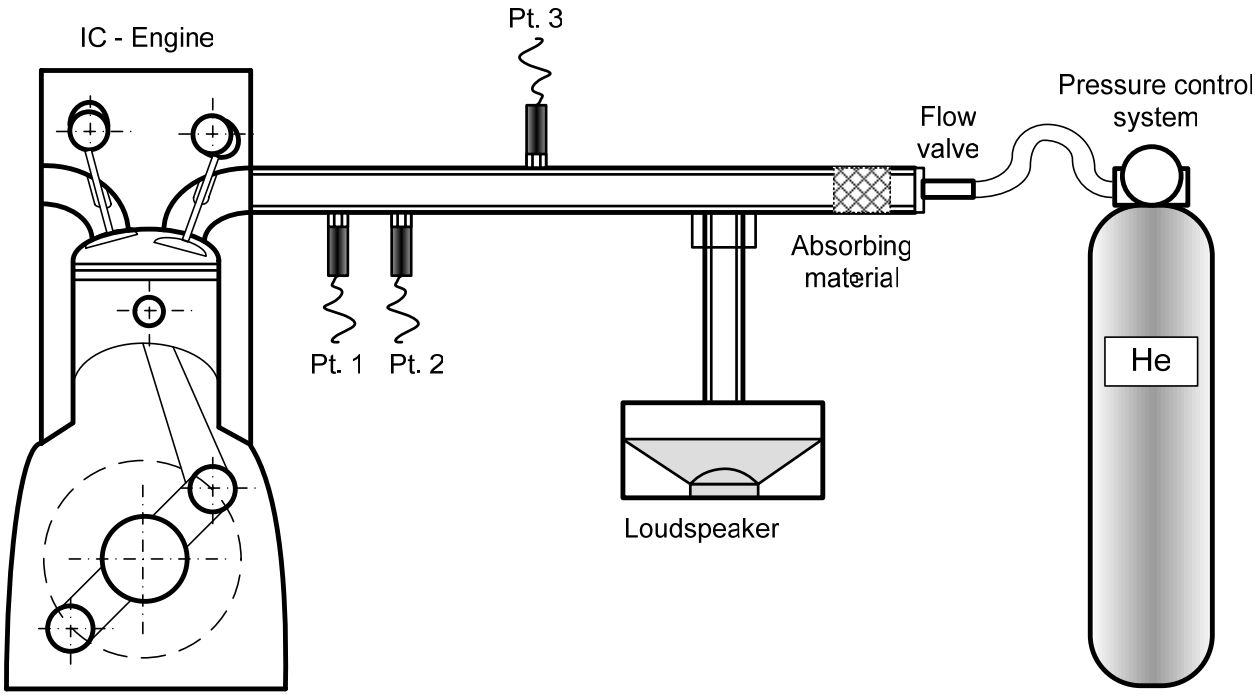

Fig. 2. Measurement set-up for exhaust port measurements

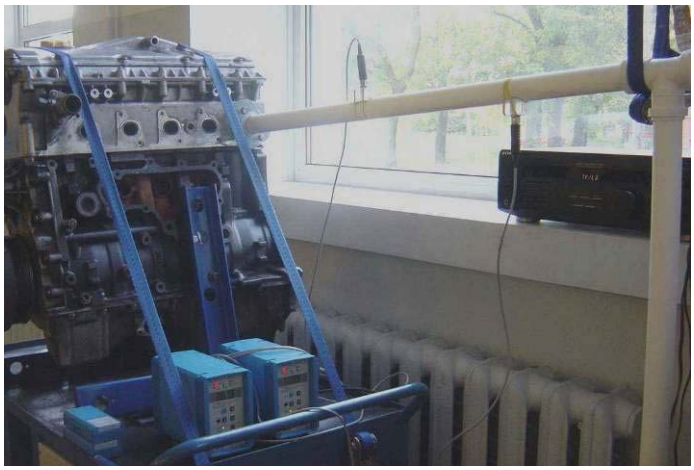

Fig. 3. A photo of plastic test-duct equipped with 2 piezo-transducers and mounted to diesel engine exhaust port during the reflection coefficient measurements

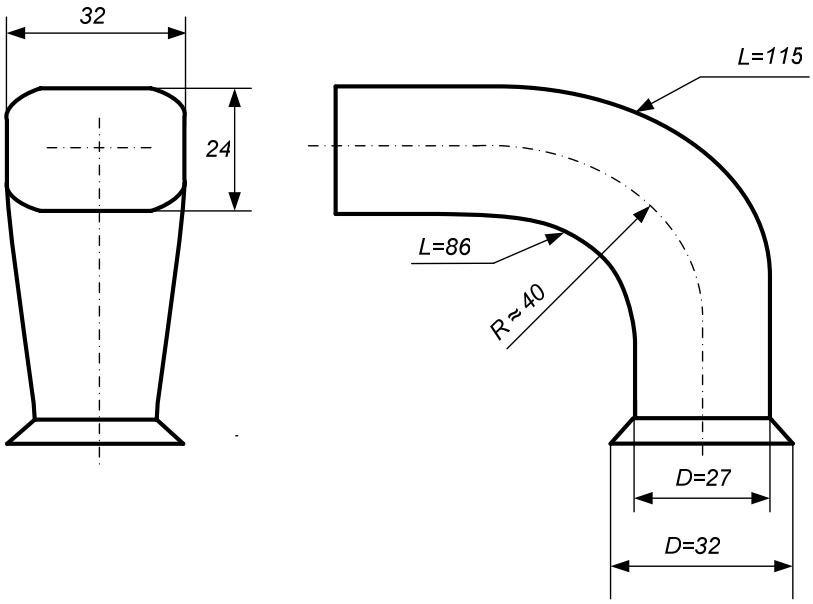

Fig. 4. The geometry of the diesel engine exhaust port. All dimensions are in mm.

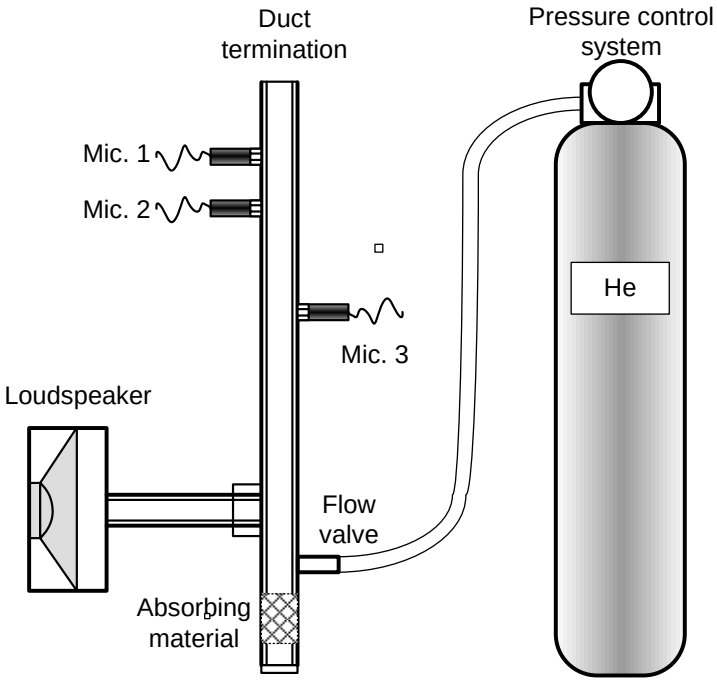

Fig. 5. Experimental set-up for duct termination reflection coefficient measurements.

Fig. 6. A photo of experimental set-up for duct termination reflection coefficient measurements.

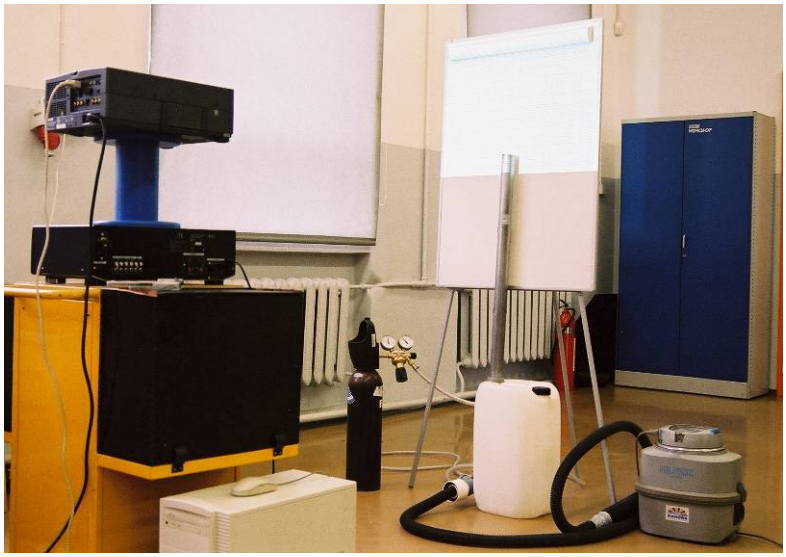

Fig. 7. A photo of experimental setup used during flow visualization experiments

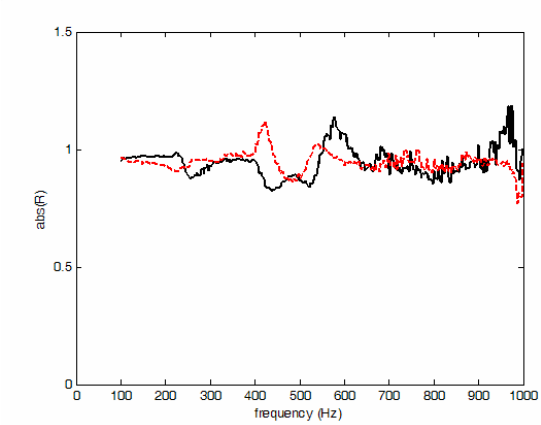

Fig. 8. The reflection coefficient (magnitude) of the engine exhaust port at TDC; air-filled duct (black full-line), helium-filled duct (red dashed-line)

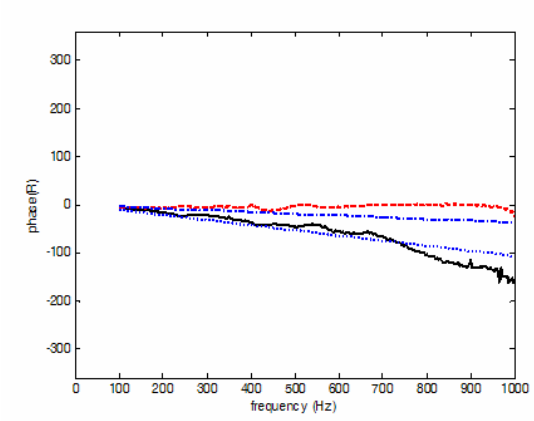

Fig. 9. The reflection coefficient (phase) of the engine exhaust port at TDC; air-filled duct (black full-line), helium-filled duct (red dashed-line)

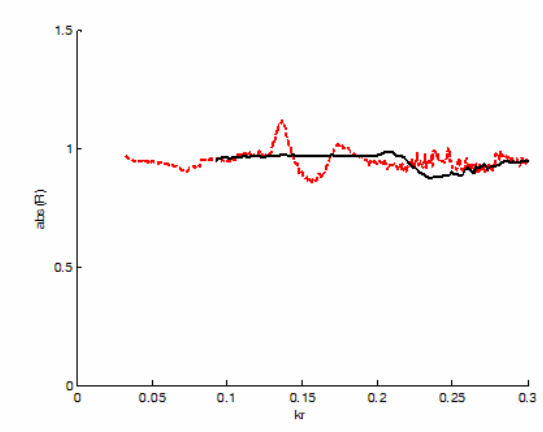

Fig. 10. The reflection coefficient (magnitude) of the engine exhaust port at TDC in Helmholz no. domain; air-filled duct (black full-line), helium-filled duct (red dashed-line)

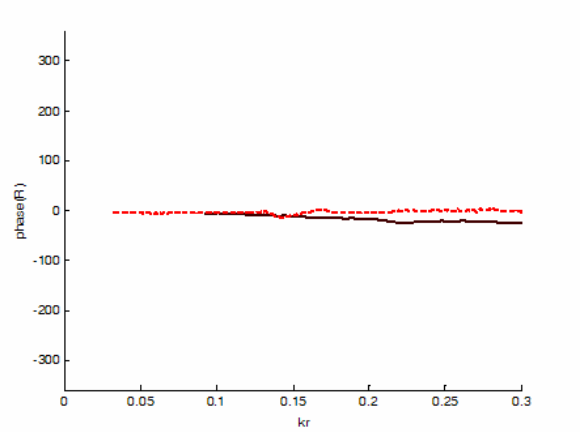

Fig. 11. The reflection coefficient (phase) of the engine exhaust port at TDC in Helmholz no. domain; air-filled duct (black full-line), helium-filled duct (red dashed-line)

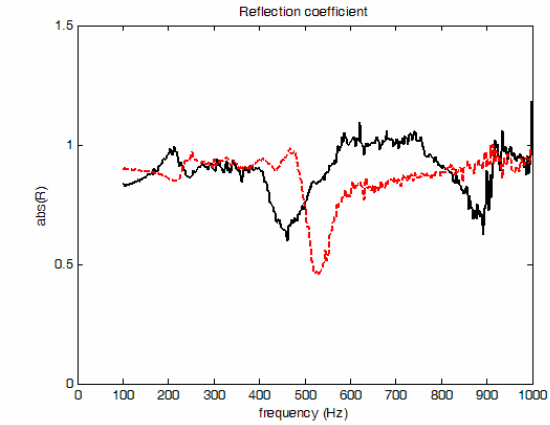

Fig. 12. The reflection coefficient (magnitude) of the engine exhaust port at BDC; air-filled duct (full-line), helium-filled duct (dashed-line)

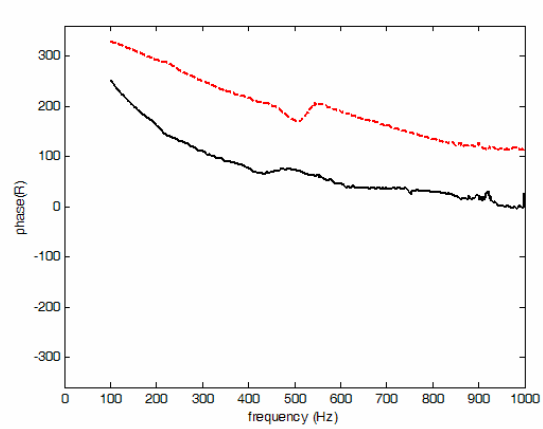

Fig. 13. The reflection coefficient (phase) of the engine exhaust port at BDC; air-filled duct (full-line), helium-filled duct (dashed-line)

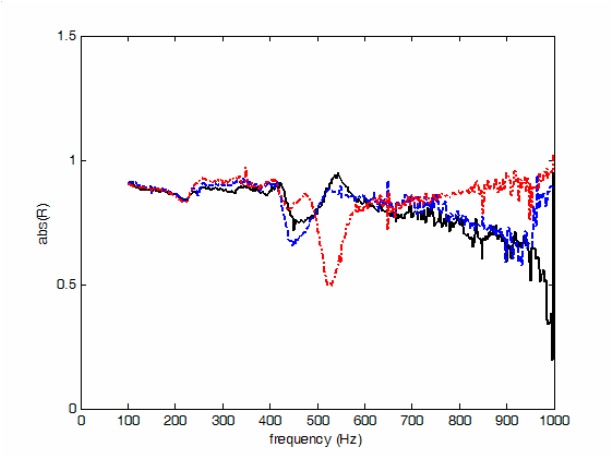

Fig. 14. The reflection coefficient (magnitude) of the engine exhaust port; helium-filled duct; BDC+30º (black full-line), BDC+60º (blue dotted-line), BDC+90º (red dash-dotted-line)

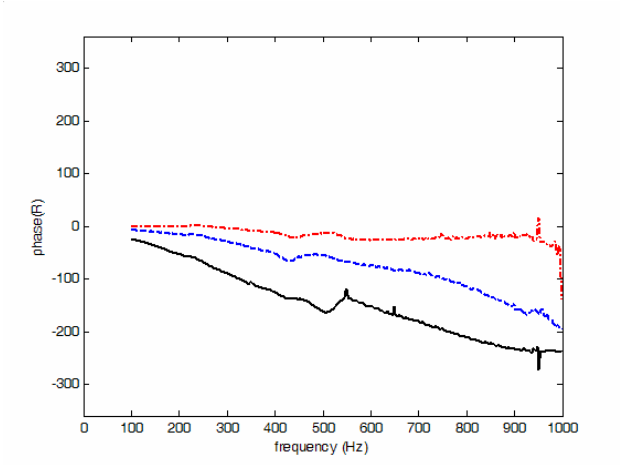

Fig. 15. The reflection coefficient (phase) of the engine exhaust port; helium-filled duct; BDC+30º (black full-line), BDC+60º (blue dotted-line), BDC+90º (red dash-dotted-line)

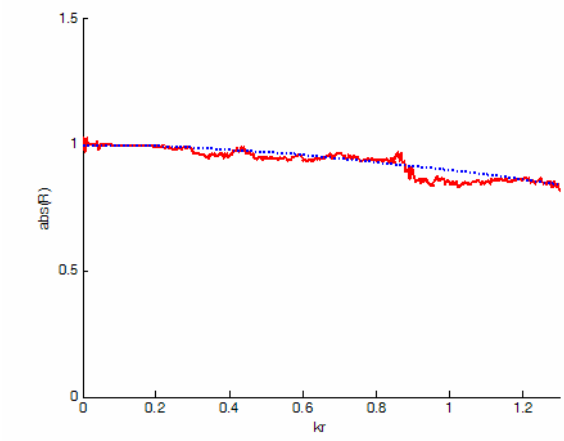

Fig. 16. The reflection coefficient (magnitude) of the open duct termination; air-filled duct, *t*=20°C; analytical result (Munt) (blue dotted-line), experimental result (red full-line)

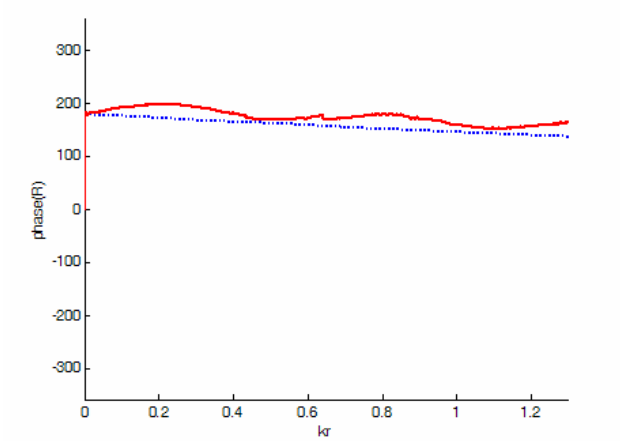

Fig. 17. The reflection coefficient (phase) of the open duct termination; air-filled duct, *t*=20°C; analytical result (Munt) (blue dotted-line), experimental result (red full-line)

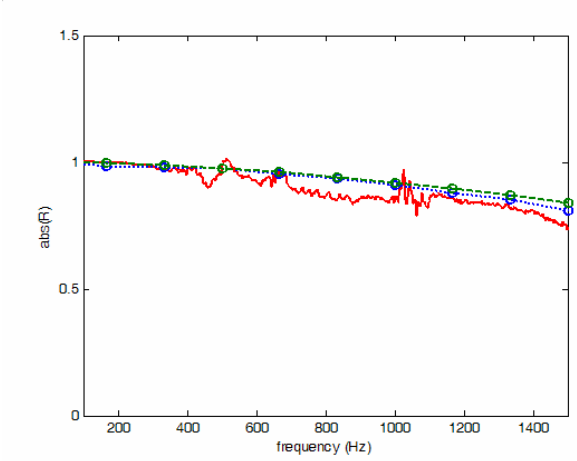

Fig. 18. The reflection coefficient (magnitude) of the open duct termination; experimental result, Helium, t=20°C (red full-line) analytical result, air at t=1065°C (Munt) (green dashed-line) analytical result, He at t=20°C (Munt) (blue dotted-line)

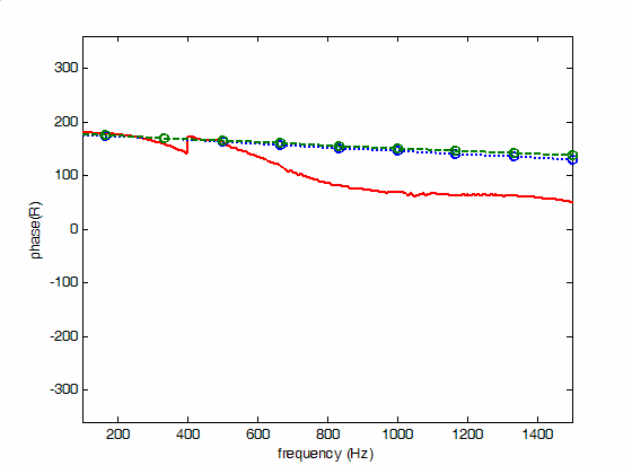

Fig. 19. The reflection coefficient (phase) of the open duct termination; experimental result, Helium, t=20°C (red full-line) analytical result, air at t=1065°C (Munt) (green dashed-line) analytical result, He at t=20°C (Munt) (blue dotted-line)

Fig. 20. Visualized flow of helium exhausting into air at t=20 ºC; U=0,3m/s

Fig. 21. Visualized flow of air at t=20 ºC exhausting into air at the same temperature; U=0,3m/s